

# **Further Studies of Denver Air Pollution**

By

N. Djordjevic, W. Ehrman, and G. Swanson

Principal Investigator: Elmar. R. Reiter

Technical Paper No. 105  
Department of Atmospheric Science  
Colorado State University  
Fort Collins, Colorado



**Department of  
Atmospheric Science**

Paper No. 105

FURTHER STUDIES OF DENVER  
AIR POLLUTION

by  
N. Djordjevic  
W. Ehrman  
G. Swanson

Principal Investigator: Elmar R. Reiter

This Report was Prepared with Support from  
Grant 5 ROI AP 00216-03 with the  
Department of Health, Education  
and Welfare

Department of Atmospheric Science  
Colorado State University  
Fort Collins, Colorado

December 1966

Atmospheric Science Paper No. 105

## TABLE OF CONTENTS

	<u>Pages</u>
Foreword	
by Elmar R. Reiter . . . . .	i - ii
Air Trajectories for Studying Denver Air Pollution	
by Nenad Djordjevic . . . . .	1-104
Data Processing Techniques Employed with Denver Air Pollution	
by William Ehrman. . . . .	105-108
Microscopical Analysis of Atmospheric Particulates Found in Denver Air Pollution	
by Glenda Swanson . . . . .	109-146

## FOREWORD

The Denver Air Pollution Study was authorized in November 1963. The first season of observations could not be started until the winter of 1964-1965. It was followed by a second observational season during the winter of 1965-1966.

Various unforeseen difficulties had to be overcome as the measurement program developed. So, for instance, it was necessary to develop a complete network of COH (coefficient of haze) samplers which, according to original plans, was supposed to be set up and operated by cooperating agencies. A Royco particle counter, acquired under Health, Education and Welfare funding, had to be adapted for field use. The large meteorological network, which was established in support of the air pollution study, required close supervision and a detailed maintenance schedule.

The present report constitutes the preliminary result of analysis work conducted on the large amount of meteorological and pollution data collected during the two pollution seasons mentioned above. Specific efforts were made to compare the behavior of air pollution patterns during certain episodes, as evident from the COH data, with the quasi-periodic wind regimes over the city of Denver. The phenomenon of the "heat island" was explored in a preliminary way by tracing constant level balloon trajectories, and by recording vertical temperature gradients in the lowest layers of the atmosphere by means of wiresondes. Even though it appears that under conditions of persisting inversions the "heat island" does not affect horizontal air trajectories to any great extent, more detailed measurements of three-dimensional air motions are desired. Especially for weather conditions in which inversions are briefly penetrated during the noon hours, the air trajectory behavior should be subject to additional investigation.

Microscopic analysis of filter samples of pollutants, described in the final part of this report, are still in a preliminary stage. From these analyses it appears that the identification of certain "characteristic" pollutants may be possible. It will be the task of additional measurements, in which pollution sample collection is closely coordinated with detailed meteorological observations, to obtain more definite indications of specific sources of pollutants, their relative abundance, and their diffusion over the metropolitan area of Denver.

In the author's opinion the following problem areas still remain to be challenged:

(a) What is the total "spectrum" of gaseous, liquid, and solid pollutants produced by various sources as a function of time?

(b) How do these pollutants disperse in the vicinity of the source, as well as over wide areas?

(c) How do the various gaseous, liquid, and solid pollutants interact with each other and with the atmosphere and its variable parameters such as moisture, pressure, temperature, radiation, and "natural" trace gases and aerosols?

(d) Detailed consideration of aerosol and pollution chemistry under varying atmospheric conditions is expected to yield "half-life" estimates of pollutants.

(e) A better understanding of the physical chemistry of pollutants may also yield improved methods of pollution control.

Although the present field study of air pollution in the Denver metropolitan area is not designed to answer these rather sophisticated--yet fundamental--questions, the data collected under this study will serve as basis of more refined research approaches.

Elmar R. Reiter, Acting Head  
Department of Atmospheric Science  
Colorado State University

# AIR TRAJECTORIES FOR STUDYING DENVER AIR POLLUTION

by  
Nenad Djordjevic

## ABSTRACT

During the 1964-1965 and 1965-1966 winter seasons, 32 days with air pollution were selected for study. The selection of days was made on the basis of an established criterion which is given in the text. From two-hourly wind fields a large sample of "quasi" horizontal air parcel trajectories were obtained using a kinematical method. Calculations of total and local change in the pollution following the trajectories were made. This allowed the determination of the horizontal advection of the pollutant. The term which represents the vertical advection is shown to be at least one order of magnitude smaller than the horizontal transport and was, therefore, neglected.

It was found that polluted air moved back and forth over the city in mountain and valley breezes during the days with air pollution; thus, the same contaminated air mass remained over Denver for a few days.

The main sources of pollutant were found to be located in the northeastern part of the Denver metropolitan area. The smaller sources which exist within the area could not be located by the presently applied method.

## CHAPTER I

### INTRODUCTION

The first study of air pollution in Denver was published by Scheneman (1957). He stressed the increasing seriousness of the air pollution problem in Denver for the near future. Since that time, measurements of the constituents of the pollutants were started at different places within the city, and the Colorado State Department of Health published a report in 1961 in order to mark "an important step in the battle to provide a clean and healthful environment for citizens of the Denver metropolitan area". This report showed that an air pollution problem already existed in 1961. A little later Riehl and Crow (1962) made a preliminary study of air pollution over Denver. They explored the methods "for a systematic approach leading to definitive computations explaining Denver pollution".

Shortly afterward, the Department of Atmospheric Science at Colorado State University conducted field measurements of the meteorological conditions accompanying Denver air pollution during two winter seasons (1964-1965 and 1965-1966). This report (thesis) is based on the data collected during this period, and it was completed under a contract between the U. S. Department of Health, Education and Welfare, Washington, D. C., and Colorado State University.

The weather conditions responsible for air pollution over the Denver metropolitan area in recent years are characterized by light winds and a stable stratification in the lower layer of the atmosphere (an inversion of temperature). The occurrence of this inversion is associated with broad scale weather features over the North American Continent. As can be seen from Fig. 1, the continental weather patterns during the period 6-10 December 1965 are characterized by a persistent anticyclone at 500 mb with light winds and a subsidence in the ridge located over the western states and along the eastern foothills of the Rocky Mountains. At the surface, a rather weak pressure

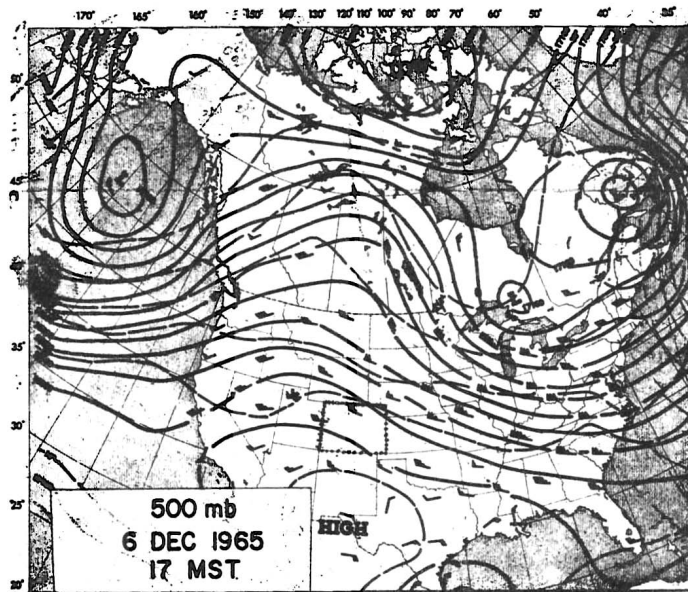
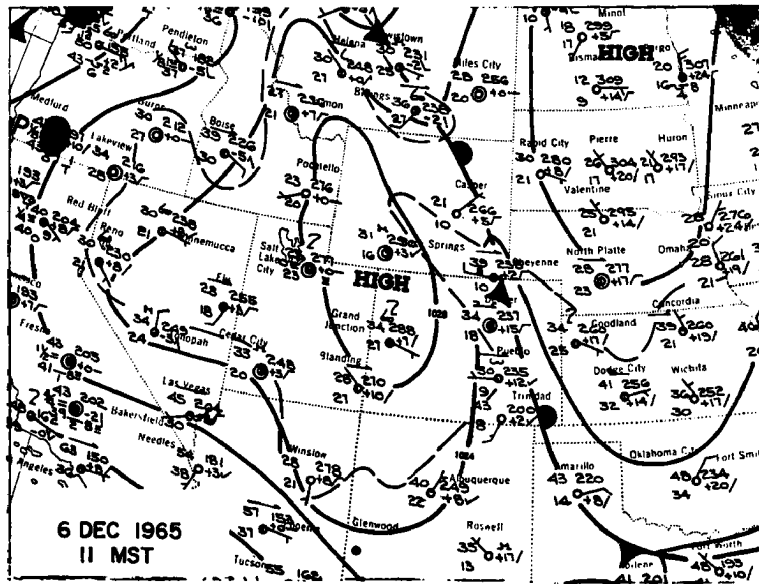


FIG. 1. Surface and 500 mb maps for 6-10 December 1965.



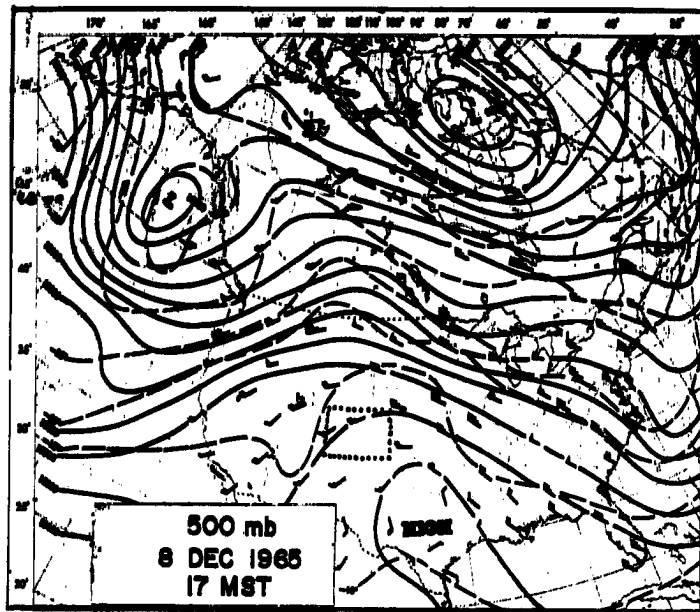
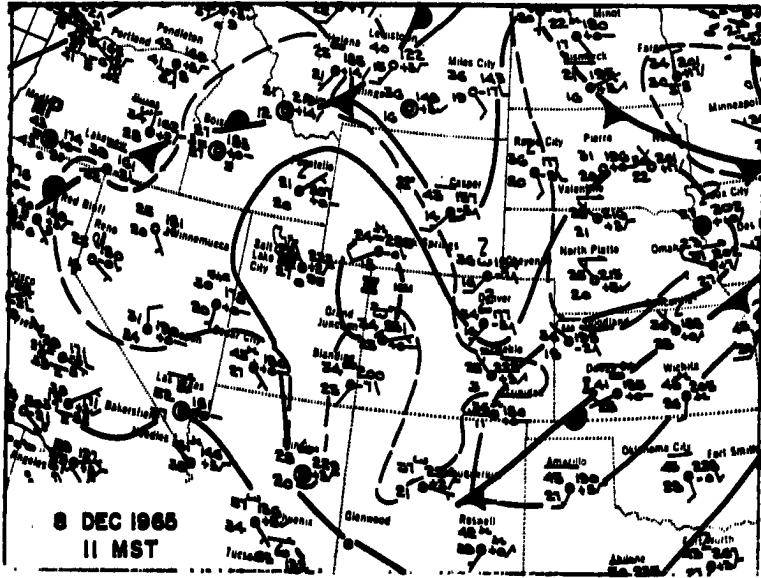


FIG. 1. Continued.

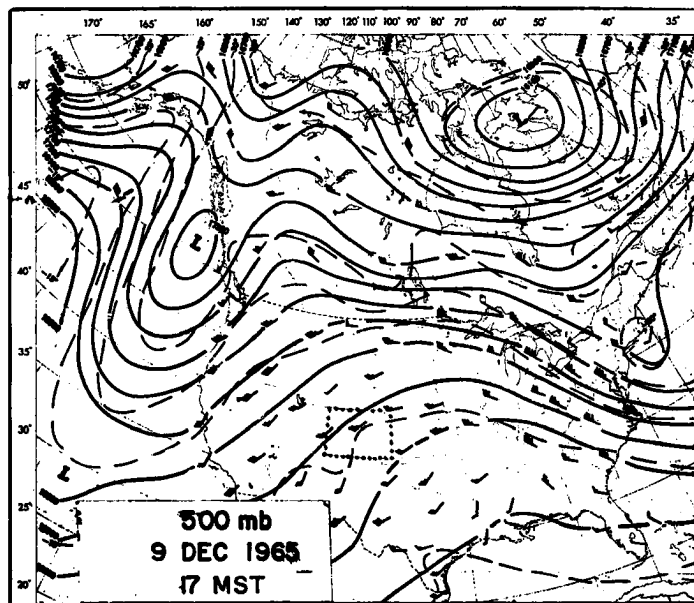
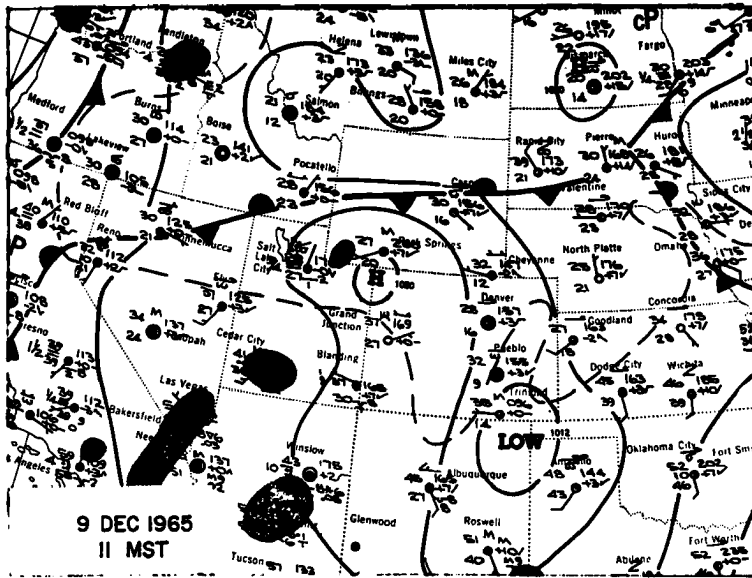


FIG. 1. Continued.

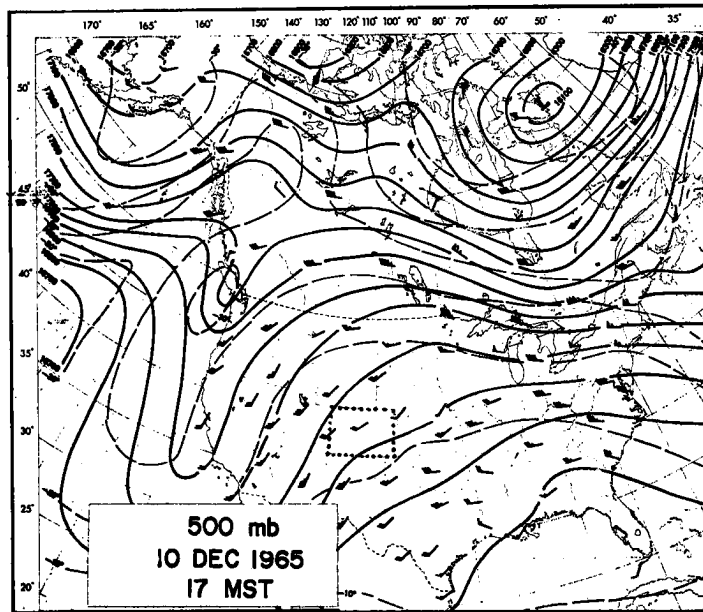
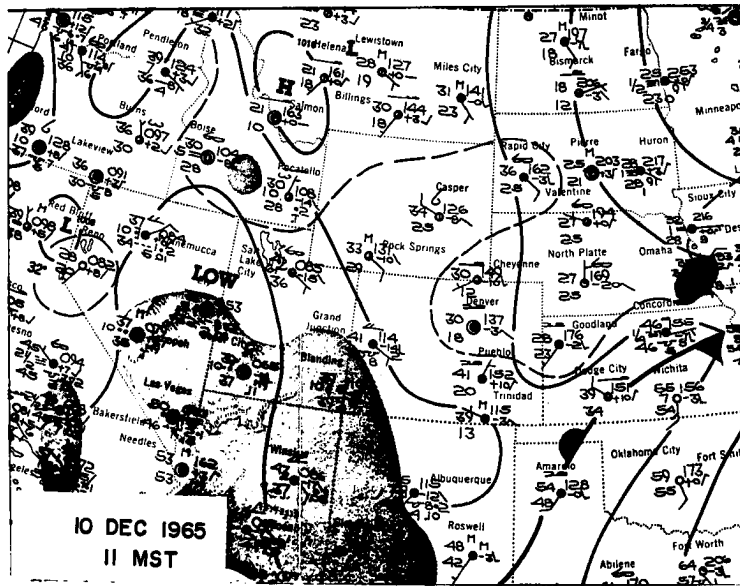


FIG. 1. Continued.

gradient does exist so that the surface wind field may undergo changes because of the local influence of terrain. Such well-developed and slowly moving anticyclones are characteristic for a broad scale weather pattern most likely to produce simultaneous occurrence of very low wind speed, pronounced stability, and fog over the continental United States for a few days, causing severe air pollution in many cities (Niemeier, 1960).

The influence of local topography in such weather situations on the wind regime in the lower layers of the atmosphere (up to about 2,000 feet) is pronounced. In mountain valleys, the phenomenon of a daily wind regime with upslope motion occurs during most of the daytime. During the night, a reversed flow down the valley takes place. It is not the purpose of this report to discuss the theory of mountain and valley winds which has already been given in a comprehensive form by Defant (1951). It will only be mentioned that such circulations are almost an everyday phenomenon over Denver on days with air pollution as will be seen later.

It is a well-known fact that the degree of air pollution depends on the amount of pollutants introduced and on the capability of the air to absorb and disperse this pollution. The latter in turn depends on the vertical structure and on the wind characteristics of the air mass (Gosline, et al., 1956).

The vertical structure of an air mass is described by the vertical temperature lapse rate. On the average, the lapse rate,  $\gamma$ , is about  $.6^{\circ}\text{C}/100$  meters. An air parcel displaced upward will change its temperature dry-adiabatically or pseudo-adiabatically, depending on whether the parcel is unsaturated or saturated with water vapor. Air stability is usually compared with the dry-adiabatic lapse rate  $\Gamma$  which is  $1^{\circ}\text{C}/100$  meters. Thus, at some height the parcel will be colder than its environment if  $\gamma < \Gamma$ , warmer if  $\gamma > \Gamma$ , and at the same

temperature as its environment if  $\gamma = \Gamma$ . These three values of  $\gamma$  characterize stable, unstable, and indifferent conditions, respectively.

When inversions are present, the temperature above a given place increases with height and  $\gamma < \Gamma$ . If the inversions are strong, as they sometimes are over Denver,  $\gamma$  may attain the value of  $-9^{\circ}\text{C}/100$  meters as will be seen later. Therefore, an air parcel displaced upward will always be colder than its environment, thus indicating stable conditions. Because of this, the possibility for a transport of the polluted air upward is limited.

The wind characteristics of an air mass important for a dispersion of the pollutants include wind speed and direction as well as the fluctuations of both around the mean values, the latter giving a measure of turbulence. Assuming that the sources of pollutants are constant, the greater the mean wind speed, the less concentrated will the pollutants be downstream from the source. Furthermore, the greater the fluctuations of instantaneous winds around the mean, the stronger the dispersion of pollutants. Neuberger et al. (1956) summarized the results of tentative statistical studies of the properties of turbulence and arrived at six major groups of characteristics from which only parts of two particularly relevant groups will be cited:

- (1) Turbulent energy is greater in unstable air, smaller in stable air;
- (2) Turbulent energy increases with increasing wind speed as well as with increasing vertical variations of the wind.

Thus, stability and low winds tend to prevent the dispersion of pollutants and may allow the concentration of contaminants to reach high values.

An illustrative description of how pollutants disperse under different stability conditions at the same wind speed is given in Fig. 2. As can be seen, the highest concentration in the plume can be expected in an inversion condition.

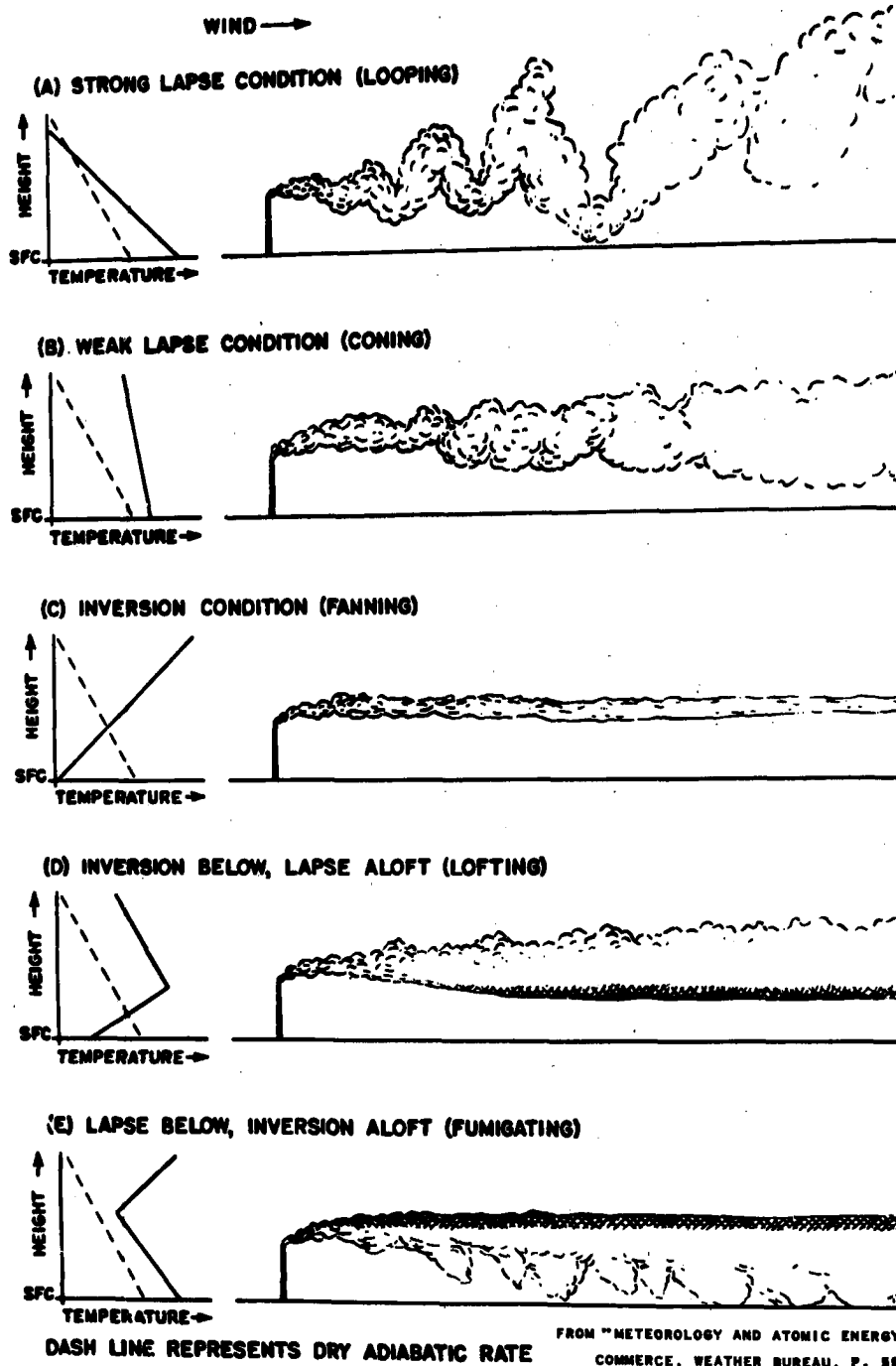


FIG. 2. Schematic representation of stack gas behavior under various conditions of vertical stability.

In an urban environment, the distribution of the pollution sources together with wind, stability, and topographic conditions may produce a very complicated distribution of pollutants. Furthermore, the height, the relative distance and the strength of sources, and the time variability of pollution emission, create exceedingly complex distributions of pollutants over certain observation points within a city. Neiberger (1961) in his theoretical study gave a schematic representation of the concentration variations of pollution at the earth's surface as a function of the distance from randomly sized and spaced elevated sources (Fig. 3). From this figure it follows that one may expect a gradual increase of the concentration downwind, up to the maximum at a certain distance from the first upwind source.

If this model is applied to the Denver area during the days with low wind speed and inversion of temperature, the highest concentration would be expected to be in the northern part of the city during the downslope flow and in the southern part during the upslope motion of the air.

A photograph taken from aircraft over Denver shows the polluted mass of air on such a day with inversion and low wind speed (Fig. 4).

### Purpose

The primary purpose of this study was to determine the main types of wind flow during the days with air pollution over the Denver metropolitan area. Air pollution was considered as a bulk property of air.

The secondary objective was to gain a knowledge on the sources of pollution and the trajectories of air motion over the Denver metropolitan area.

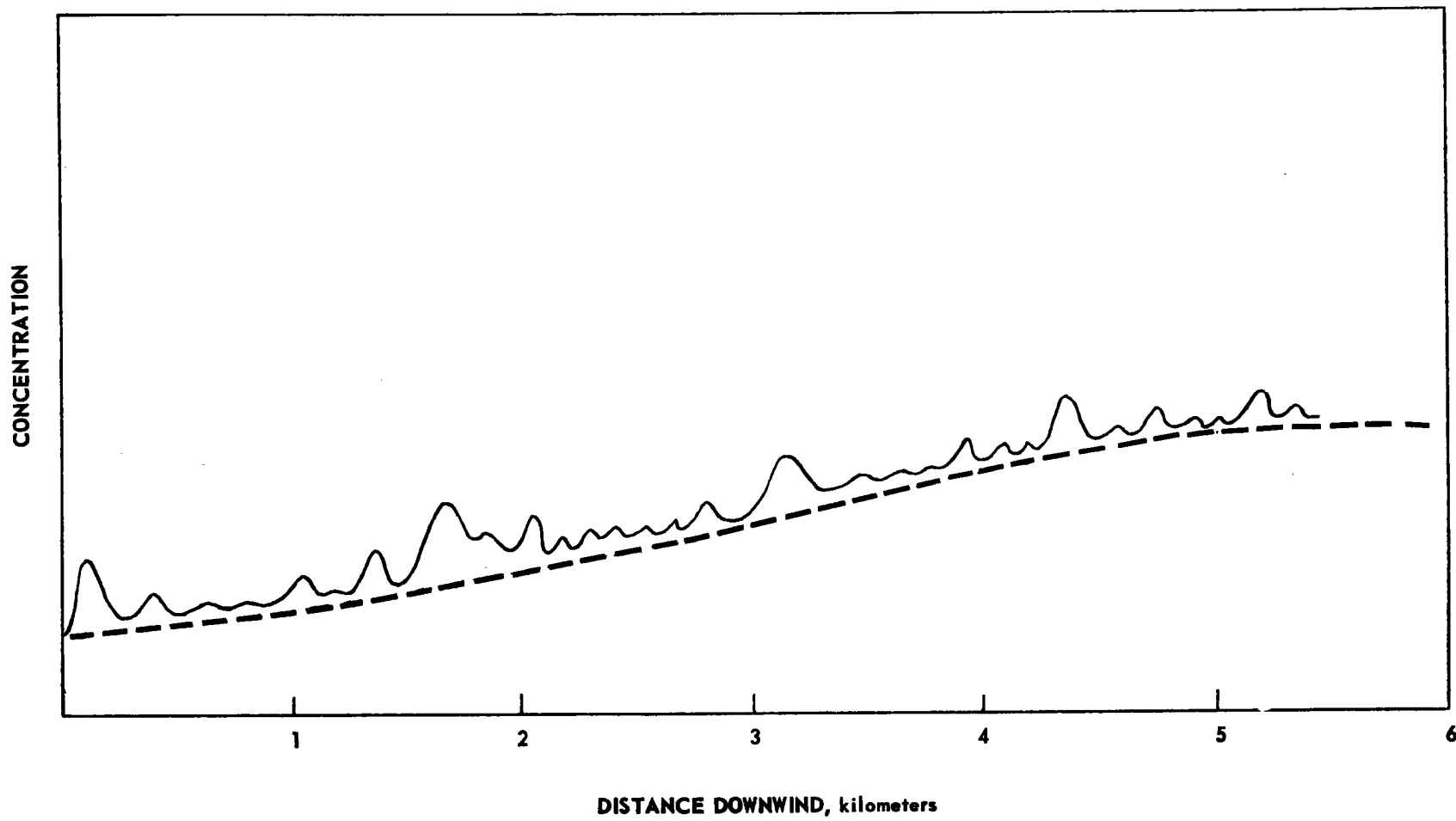


FIG. 3. Variation with distance of surface concentrations from randomly sized and spaced elevated sources (schematic).

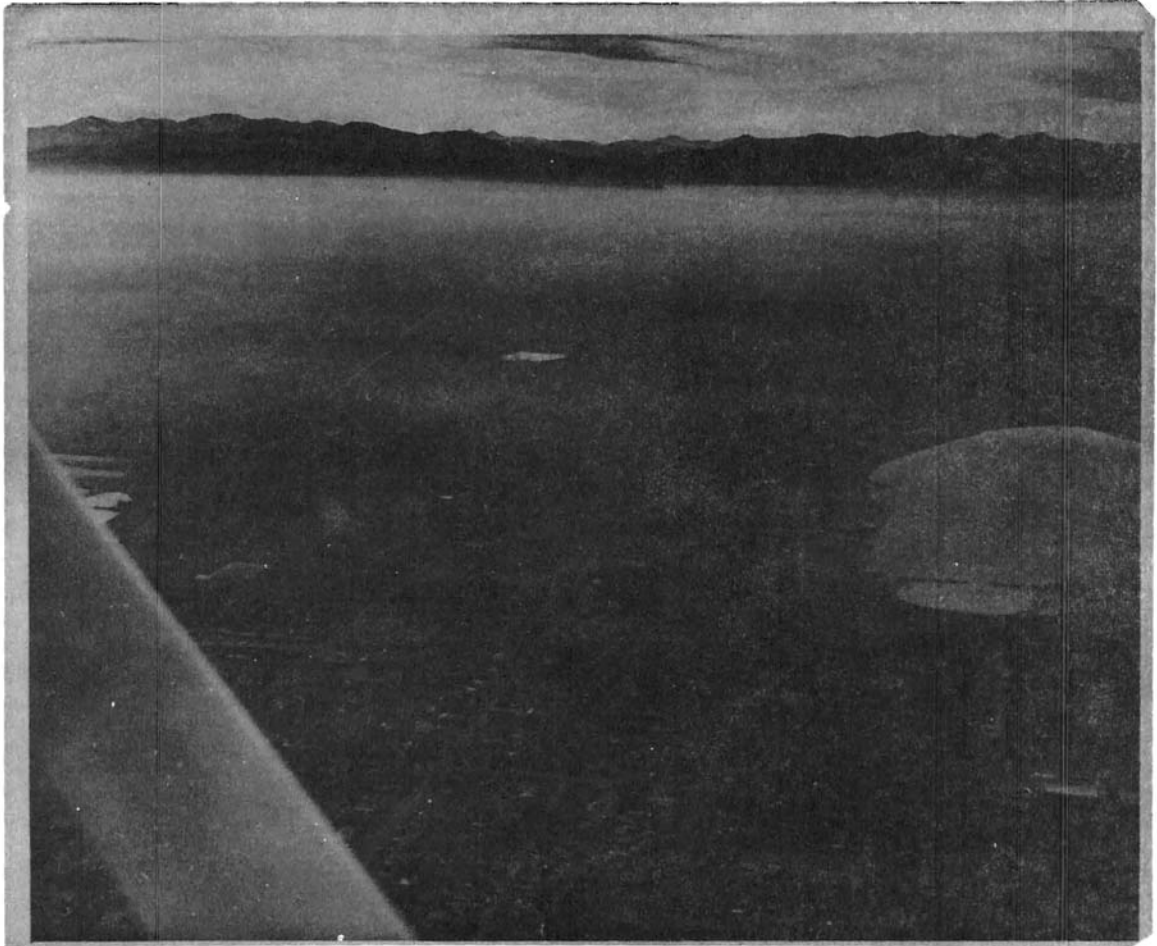


FIG. 4. Aerial photograph of air pollution over Denver taken on 6 December 1965 at 16 MST (Photograph by Charles Grover, Denver).

The third objective was to describe and explain the daily fluctuations of pollution as a function of meteorological conditions prevailing during the day. These goals are in accordance with previously mentioned work conducted in the Department of Atmospheric Science, Colorado State University (Riehl and Crow, 1962).

## CHAPTER II

### GENERAL FEATURES OF TERRAIN AND OBSERVATIONAL NETWORK

The metropolitan Denver area lies at the foothills east of the Rockies in the South Platte River Valley. The mountain peaks rise to about 8,000 feet above sea level to the west and to 6,000 to 7,000 feet to the southwest. The South Platte River flows from the southwest to the northeast through the heart of Denver which has an average altitude of about 5,250 feet. In Fig. 5 the approximate limits of the populated area and the contours of the terrain are given. Irregularities in the surface due to the different shapes and heights of buildings are not pronounced except in the downtown area. In general, the heights of buildings are between 20 to 30 feet. Some scattered high buildings can be found in other parts of the urban area, but it is supposed that their influence on the general flow patterns is limited to their near vicinity. It is estimated that pronounced irregularities due to buildings, which may affect natural conditions of flow, occupy less than one-tenth of the metropolitan area. Thus, it turns out that the city's topographical influence on the wind regime is not great. The thermal regime of the metropolitan area is not significant, as will be seen in the following paragraphs.

The meteorological network installed for the purpose of monitoring air pollution occurrences consisted of 17 principal stations at which wind direction and wind speed were recorded and, in most cases, air temperature. These observations of winds were supplemented by data from additional stations operated by the U. S. Weather Bureau at Stapleton Airport, by the U. S. Air Force at Lowry Air Force Base, etc. The number of additional stations varied from seven to three on days with air pollution. The location of all stations is given in Table I and in Fig. 5. It should be noted that the location and altitude of wind

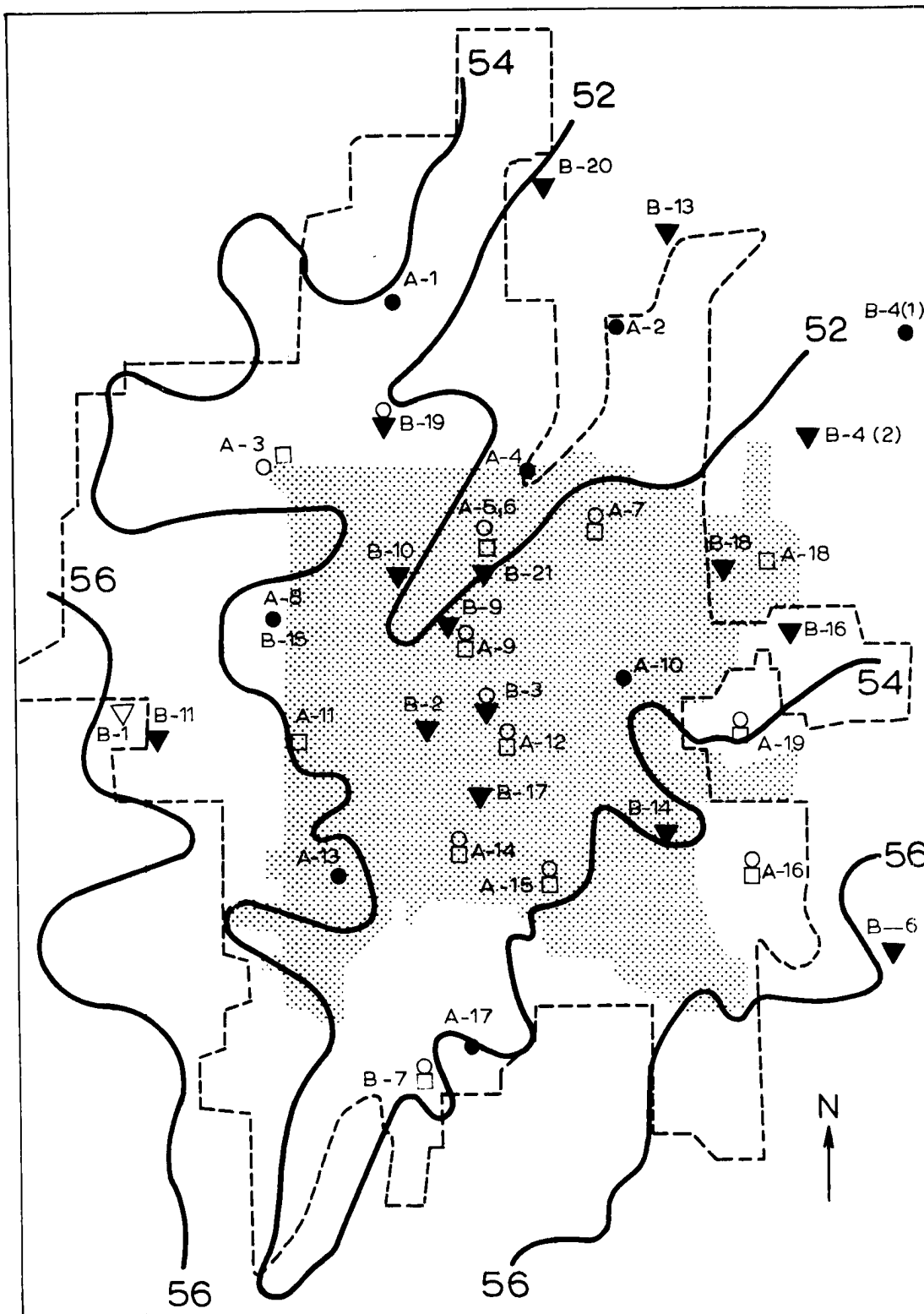


FIG. 5. The Denver metropolitan area (dashed line). Contours in hundreds feet (full lines); city limits (shaded area); symbols: ○ wind unit, □ temperature unit, ▽ sampling unit.

vanes were selected in accordance with recommendations from preliminary work (Riehl and Crow, 1962) in order to provide the most representative data.

The air sampling network utilized 22 Paper Tape Air Samplers (Mo. 23000, manufactured by Gelman Ins. Co., Ann Arbor). The locations of air samplers, as well as of the temperature and wind units, are given in Fig. 5. This network was designed to determine the general level of pollution over the whole city and to evaluate the distribution of pollution within the city for different weather situations.

The level of air pollution is expressed by a "coefficient of haze", or soiling index, COH. This unit was obtained by relative measurements of the intensities of light transmitted through clean paper,  $I_o$ , and through soiled paper,  $I$ . Hence, by definition

$$1 \text{ COH unit} = 100 \times \text{optical density (OD)}$$

where  $OD = \log \frac{I_o}{I}$ . The value of COH depends on the volume of air drawn through the filter paper. If  $V$  is the quantity of air sampled in units of 1000's of linear feet, it follows that:

$$V = \frac{\text{flow (ft}^3/\text{min)} \times \text{sampling time (min)}}{1000 \times \text{area of spot (ft}^2)}$$

In addition, the value of COH is normalized for  $V$ , thus:

$$COH = \frac{OD \times 100}{V} .$$

Adjectival ratings were used to determine the level of air pollution in accordance with the basic extensive measurements of smoke concentration prepared by the New Jersey State Department of Health (1958).

<u>Smoke Concentration</u>	<u>Adjectival Rating</u>
COH	
0.0-0.9	light
1.0-1.9	moderate
2.0-2.9	heavy
3.0-3.9	very heavy
> 4.0	extremely heavy

The sampling period was two hours at all stations. On some days with air pollution, supplementary observations were made by ground and aerial photography and by helicopter and wiresonde equipment taking temperature soundings, the results of which will be discussed in later sections. The RAOB reports from the U. S. Weather Bureau Station at Stapleton Airport were also used for every day with air pollution.

## CHAPTER III

### METHODOLOGY

#### Selection of Air Pollution Days

From COH observations, two-hourly maps of contamination were analyzed. The isolines of equal pollution were drawn for every 0.2 COH. Two examples of COH charts are given in Figs. 6 and 7. However, due to instrumental and operational difficulties, which are to be expected in a field experiment of such scope, it was not possible to obtain continuous measurements of COH at all stations during the two winter seasons. For that reason, the number of stations with usable measurements varied for the several observational times. For example, during 126 selected two-hourly episodes in the 1965-1966 winter season, the number of observations available from all stations was 2,033 instead of the maximum possible 2,268.

The criterion set-up for the selection of days with significant air pollution was rather subjective. It was partly based on the adjectival rating mentioned previously. Here the difficulty lies in the variability of pollution in time and space so that at some places the contamination may be high while at other places it may be negligible. Nonetheless, the air pollution problem over the Denver city area has to be considered regardless of the small COH values observed at stations in some parts of the city at a given time when pollution is significant elsewhere. Thus, in order to take into account the COH values over the whole area as well as those at any particular sampling place, a "compromise" criterion was established: Air pollution is present if the contamination at least at one station is equal to, or greater than, 1 COH and if the contamination at 50% or more of the remaining stations is greater than 0.5 COH.

It should be of interest to compare COH values for Denver and other cities. In Fig. 8 comparison is made between COH values





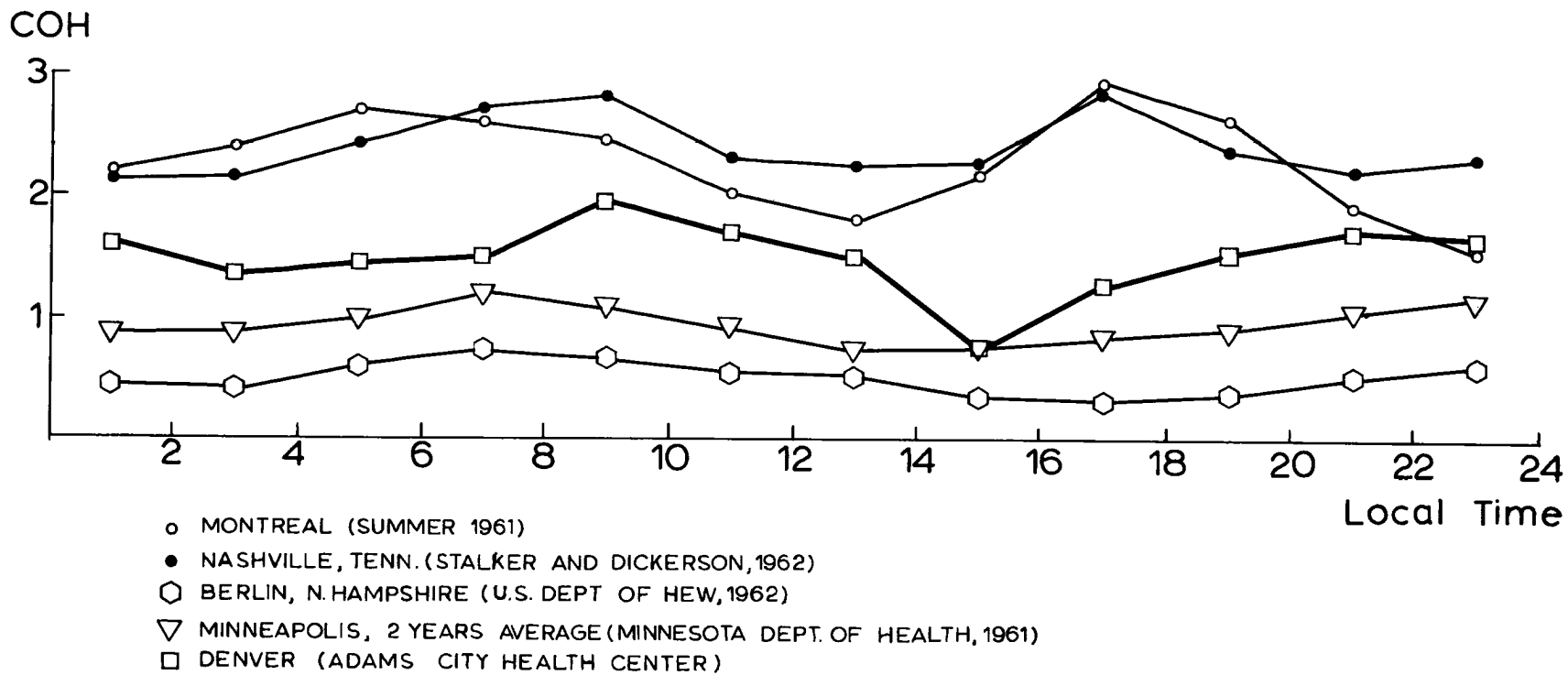


FIG. 8. Comparison of COH values in Denver with those in other cities.

measured during the air pollution days at the Adams City Health Center, Denver, during the 1964-1965 winter season with other cities. Averages for the other cities were obtained from daily measurements, not just from measurements during days with significant air pollution.

A basic difficulty in the comparison of COH data between one city and another is the assumption that the optical density of particles deposited on filter paper involves a linear relation to the volume of air filtered with constant area of deposit. Furthermore, the particulates suspended in an urban atmosphere are not of uniform size and the albedo of the deposit strongly depends on the size distribution of particulates (Katz et al., 1958). Sanderson and Katz (1963) concluded that "the simple linear relation between absorbance of smoke stain and the volume of air sampled, although often used, has limited value for comparison purposes". They suggested a standardization of the sampling time, air flow, and area of spot since only under such conditions a comparison between the measurements at different cities would be possible.

On the basis of established criteria, 32 days were selected for study of the Denver air pollution (Table II). The total duration of air pollution periods during the two winter seasons was 478 hours.

### The Wind Field

The two-hourly mean wind was calculated from the five-minute average values. Examples of the wind records, wind speed and direction, are given in Fig. 9. Maps of the two-hourly mean streamlines and isotachs were constructed from the wind values, applying a kinematical method (Petterssen, 1956). The wind velocity field is a vector field, given by wind direction and speed at every point in the space considered. If wind measurements are performed at several points, streamlines and isotachs may be constructed in order to obtain



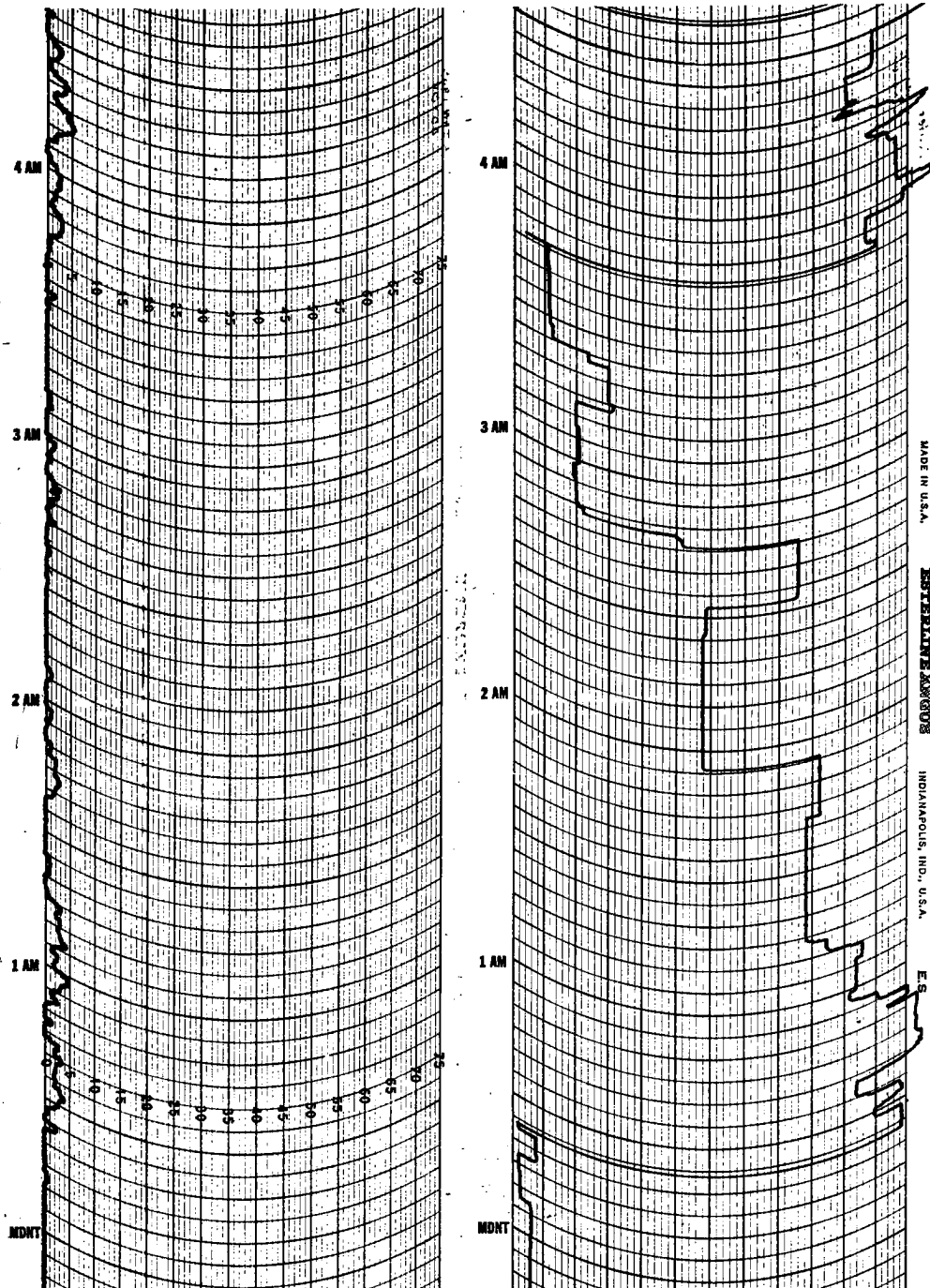


FIG. 9. Continued.

direction and speed of wind over an area. Evidently, the denser the observational network, the greater the accuracy in the construction of streamlines and isotachs, provided that "noise" produced by turbulence and instrument errors does not disturb the two-hourly mean values.

A streamline is defined as a line which at a given time is everywhere tangent to the wind vector. Thus, the equation of the streamline, written vectorially, is as follows:

$$d\vec{r} \times \vec{V} = 0 \quad (1)$$

or in the Cartesian coordinates;

$$dx: dy: dz = u: v: w \quad (2)$$

where  $d\vec{r}$  is a line element of the streamline;  $dx$ ,  $dy$ ,  $dz$  are its components in  $x$ ,  $y$ , and  $z$  directions, respectively; and  $\vec{V}$  is the velocity with components  $u$ ,  $v$ , and  $w$ .

In our case, the horizontal component of velocity,  $\vec{V}_h$  was measured. Then, the streamlines were constructed in such a way that at every observational point, Eqn. (1) was fulfilled.

The isotachs are by definition the lines of equal wind speed regardless of the direction of the wind. They can be readily analyzed from wind observation.

The two-hourly mean winds were obtained from wind records between two even hours. Thus, the streamline and isotach maps are valid for the middle, uneven hours. Examples of the wind field are given in Figs. 10 and 11.

### The Calculation of Horizontal Trajectories

A trajectory is defined as the path of an air parcel, satisfying the condition that the wind vector must be tangent to the trajectory at every moment of time. Since the streamlines at a given time are everywhere tangent to the wind vector too, the trajectories have to

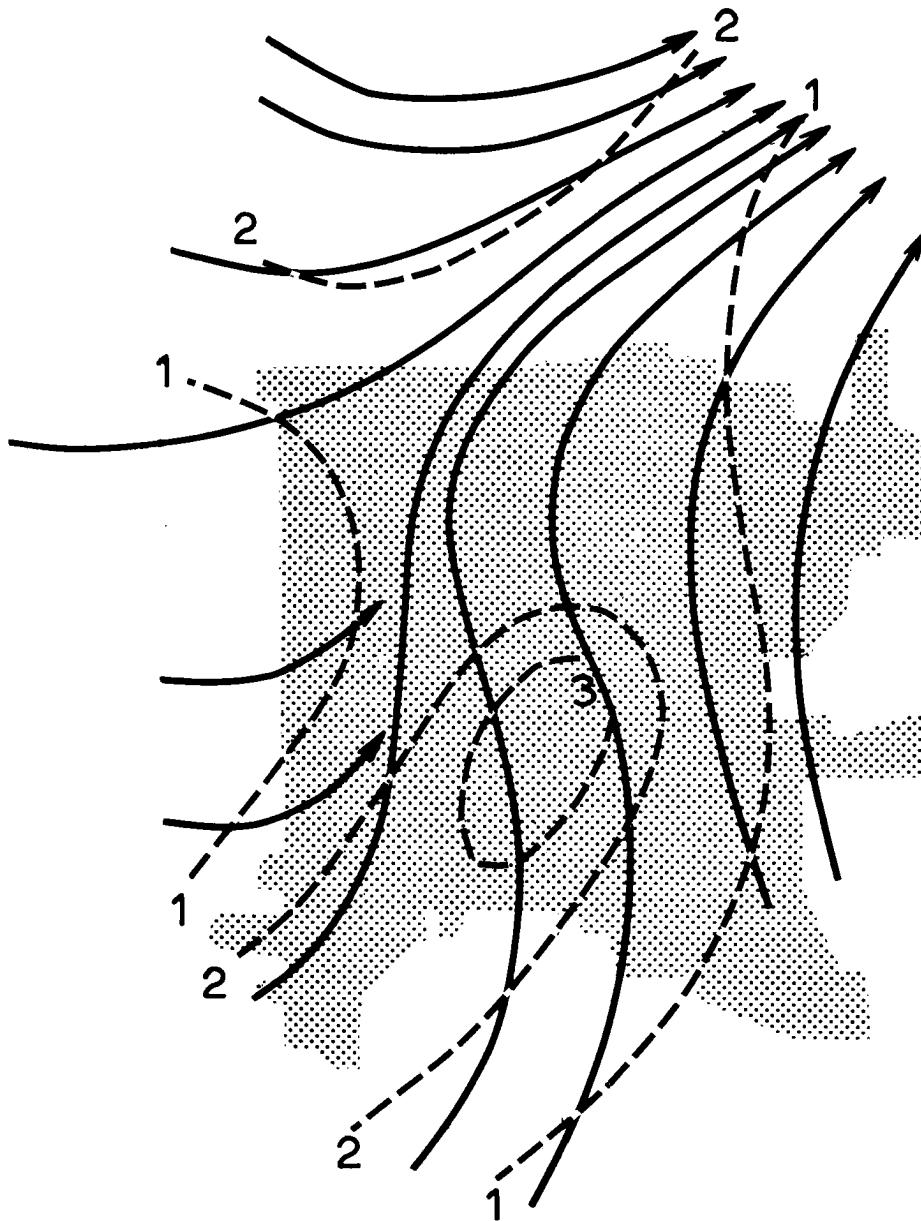


FIG. 10. Wind field on 10 December 1965 at 03 MST. Full lines are streamlines; dashed lines are isotachs (mph).

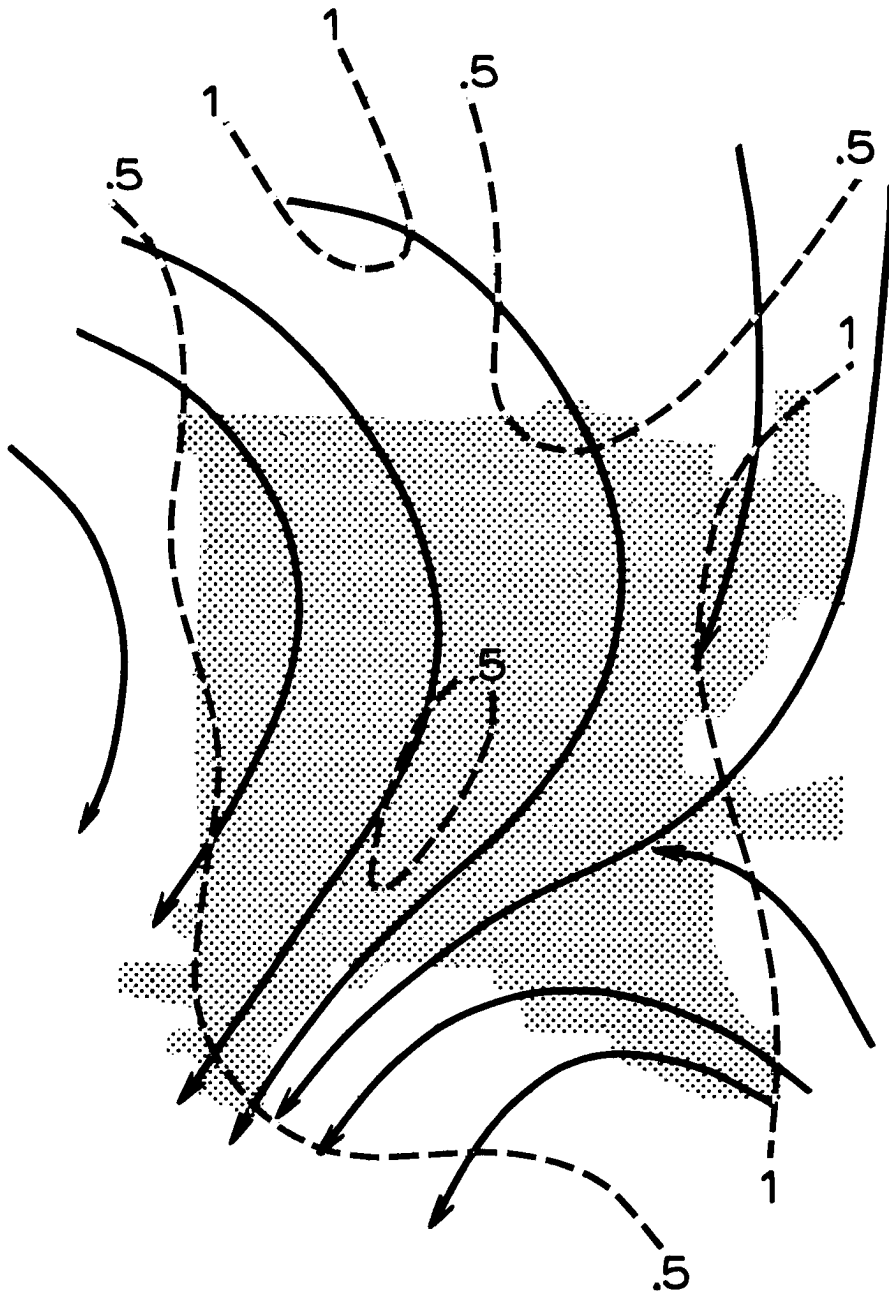


FIG. 11. Wind field on 16 December 1965 at 17 MST. Full lines are streamlines; dashed lines are isotachs (mph).

be tangent to the streamlines at the observation time for which the streamline pattern is analyzed. A coincidence between the streamlines and trajectories can occur only when the wind field remains stationary.

For the construction of horizontal trajectories, successive two-hourly maps of the horizontal wind field were used. A schematic representation of the method for trajectory calculation is given in Fig. 12. From above definitions of the trajectory and streamline, the resulting path of an air parcel, AB," has to be tangent to the streamline at time  $t_0 - \Delta t$ , and as time proceeds, must become tangent to the streamline at time  $t_0$ ; i. e., the air parcel should describe a curve between B" and A.

In our case, "horizontal trajectory" means a trajectory which is parallel to the terrain; it is actually a "quasi" horizontal trajectory, if one allows for terrain slope. However, for the sake of simplicity, it will be called "trajectory".

#### The Change of Contamination Along a Trajectory

The total change of COH along a trajectory may be obtained from COH charts at times  $t_0$  and  $t_0 - \Delta t$  as the difference in pollution between the ending and starting points (A and B"). This difference may be plotted in the middle of the trajectory if one assumes a linear change of the contamination of the air parcel with time along its trajectory.

This total COH change is equal to the local change during the time interval  $\Delta t$ , plus the advection term, or

$$\frac{dC}{dt} = \frac{\partial C}{\partial t} + \vec{V}_h \cdot \nabla C + w \frac{\partial C}{\partial z} \quad (3)$$

where  $\frac{dC}{dt}$  is the total change in COH,  $\frac{\partial C}{\partial t}$  is the local change in COH, and  $\vec{V}_h \cdot \nabla C$  the horizontal advection.  $\vec{V}_h$  represents the horizontal wind

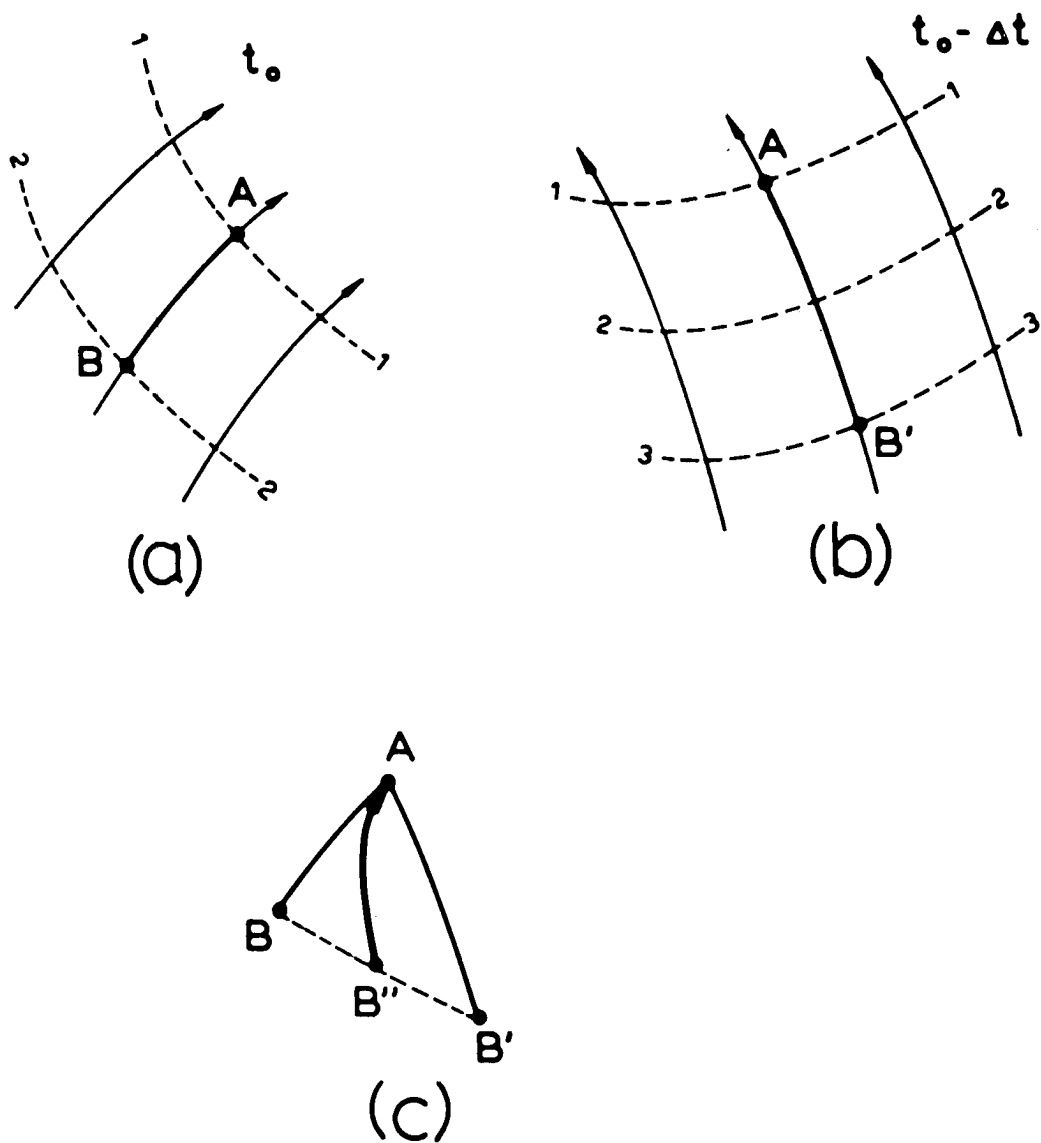


FIG. 12. Calculation of the air parcel trajectory (schematic). Thin full line: streamlines; dashed lines: isochrons; full line: trajectory.

vector and  $\nabla = \frac{\partial}{\partial x} \vec{i} + \frac{\partial}{\partial y} \vec{j}$  expresses the horizontal gradient operator. The third term on the right side of Eqn. (3),  $w \frac{\partial C}{\partial z}$ , allows for the possibility that an air parcel may experience a vertical displacement during its path between B'' and A; this term is referred to as vertical advection; its value will be estimated in the following chapter.

### Estimate of Vertical Velocities

In order to obtain an estimate of the vertical velocity field, the most straightforward method is a kinematical one. From wind observations, streamline and isotach charts can be constructed and wind velocity and direction can be determined at any point, though grid points with constant distance are used (Petterssen, 1956). At each grid point, the wind is divided into u and v components. Then the divergence may be obtained as a difference in u and in v at two successive grid points. When the divergence is computed, the vertical velocity can be obtained with the help of the continuity equation, assuming a constant density, or

$$w = - \int_0^z \text{div } \vec{V}_h dz , \quad (4)$$

where  $\vec{V}_h$  is the horizontal wind vector and z is the height.

The calculation of w from Eqn. (4) requires high accuracy in the wind observations. A small error in measuring wind direction and speed will produce a significant error in the divergence. If one wants to determine the divergence with an accuracy of 10%, the wind has to be measured within 1%. Clearly, such precise wind measurements are not possible with the present standard equipment at a weather station (Thomson, 1961). Therefore, the application of Eqn. (4) in synoptic analysis is limited.

In our case, the error in the divergence was reduced due to the high density of the observation stations and by use of two-hourly mean winds.

The studied area is 180 square miles with 17 principal wind recording stations, a density of approximately one station per ten square miles. This station density is at least 250 times greater than that of the standard meteorological network. In determining this station density, the auxiliary stations were not included because their number varied from time to time. However, data from the U. S. Weather Bureau Station at Stapleton Airport and from Lowry Air Force Base were available at all times during the 1964-1965 and 1965-1966 winter seasons. If these two stations are included, the density of the observational network further increases and provides for an even higher accuracy in the analysis of the wind fields and in the divergence calculations.

It was mentioned previously that the two-hourly mean wind was calculated from the five-minute average value. It is assumed that use of the five-minute period will provide a fairly good estimate of the average wind speed and direction. Examples of wind records from two stations are shown in Fig. 9. At low wind speed, which is common over the Denver city area on days with air pollution, it was possible to determine the five-minute average wind without difficulty. The average values of the two-hourly u and v components (Table III) were small at both sites (Kunsmiller Junior High School and Adams County Health Center), ranging from almost zero to 2.8 miles/hour or 0-1.4 meters/sec (roughly 1 meter/sec = 2 miles/hour). It turns out that the largest difference in u or v components between adjacent grid points is  $\pm 2-3$  meters/sec. Thus, the divergence has an order of magnitude  $10^{-4} \text{ sec}^{-1}$ , or

$$\frac{\Delta u}{\Delta x} + \frac{\Delta v}{\Delta y} \sim 10^{-4}$$

where  $\Delta x = \Delta y = 3 \text{ miles} \sim 5.5 \cdot 10^3 \text{ meters}$  ( $\Delta x$  and  $\Delta y$  are grid distances). By integration of Eqn. (4) from  $z = 0$  to  $z = 10$  (the average height above ground of the wind vane), and by taking into account  $w = 0$  at  $z = 0$  and that  $\text{div } \vec{V}_h \sim 10^{-4} \text{ sec}^{-1}$ , one obtains the order of magnitude of the vertical component of velocity, or

$$w \sim 10^{-3} \text{ meters/sec} .$$

The five-minute average values may fluctuate around two-hourly means in a wide range. In this case, the two-hourly mean wind will have a large probable error,  $r$ . The latter can be calculated by the following formula (Panofsky and Brier, 1958):

$$r = 0.6745 \sqrt{\frac{\sum (u_i - \bar{u})^2}{n - 1}} \quad (5)$$

where  $u_i$  are the five-minute averages from which  $\bar{u}$ , the two-hourly mean is calculated and  $n$  is the sample size, in this case 24. The same formula is valid for the  $v$ -component.

The probable error,  $r$ , is valid for a Gaussian distribution which can be accepted as a fairly good approximation for the wind variations (Pasquill, 1962). The calculation of  $r$  for the wind records shown in Fig. 9 is given in Table IV. For low wind speeds ( $< 1/2 \text{ mps}$ ), the probable error in the two-hourly mean can be more than twice as great as the error in the mean wind itself for the  $u$ -component and 30 times as great as the error in the mean wind for the  $v$ -component since the latter usually is much weaker than the former. It turns out that the mean itself does not exceed 1 meter/sec even with a large probable error in the two-hourly mean wind. At higher values for the two-hourly mean (3 miles/hour), the highest value for the probable error is approximately 50% of the mean itself so that the true mean lies between 4.5 and 1.5 miles/hour (Table IV, Kunsmiller Junior High School). Consequently, in the worst possible combination the

differences in the u or v component do not exceed 5 meters/sec. Thus, the divergence and w may have maximum values of the order of  $10^{-3}$  and  $10^{-2}$ , respectively. However, the value for w was never higher than  $3 \cdot 10^{-3}$  meters at any point during the 1964-1965 winter season. This corresponds to a vertical displacement of the air particles of 20 meters in two hours. An example of this vertical displacement is given in Fig. 13 on the 3 February 1965, 02-04 MST. As can be seen, this displacement does not exceed 13 meters for two hours.

In proof of the normal distribution for the five-minute averages, the following formula is applied (Conrad, 1950):

$$\sqrt{\frac{\sum (u_i - \bar{u})^2}{n - 1}} = \sqrt{\frac{\pi}{2}} \times \frac{\sum (u_i - \bar{u})}{n} \quad (6)$$

The result given in Table IV shows an absolute difference in the standard deviation calculated from data (Table III) and with the help of formula (6). Only in one case the difference between right and left side of Eqn. (6) is as large as .21. This is an effect of the extremely large number of five-minute averages with zero values. In this case the two-hourly mean depends on the extremes.

#### Estimate of the Horizontal and Vertical Advection

The order of magnitude of the horizontal and vertical advection can be estimated from the values of  $\vec{V}_h$ , w,  $\nabla C$ , and  $\frac{\partial C}{\partial z}$ . The magnitude of the vertical velocity, w, has been discussed in detail before. It was found to be  $w \sim 10^{-3}$  meters/sec. Furthermore, it was shown that the two-hourly mean wind is light; its value varies from between zero and three meters per second, taking into account the probable error. This is a common range of the horizontal wind speed as can be seen from the two examples of the wind field shown in Figs. 10 and 11.

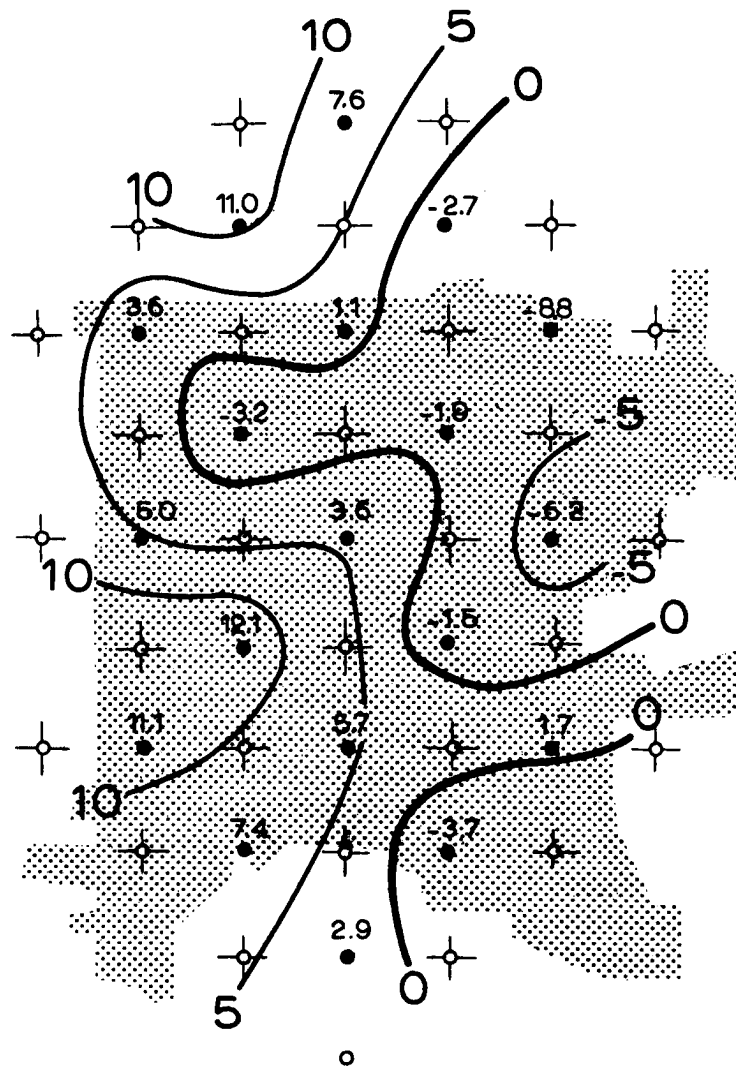


FIG. 13. Two-hourly vertical displacement of air in meters on the 3 February 1965, 02-04 MST. Grid points--circles.

The horizontal and vertical gradients of COH may be estimated from the charts of contamination and from the observations of COH at two different levels. In order to compare the horizontal and vertical gradients of COH, measurements of COH in the vertical and in the horizontal directions had to be performed simultaneously.

The vertical gradient,  $\frac{\partial C}{\partial z}$ , was calculated from observations performed in Denver at Signal Broadcast Production, Inc., 1601 Arapahoe Street, at an elevation of 324 feet above the ground, and at the CSU Field Office, 23rd and Broadway Streets, at 12 feet above the ground. The horizontal distance between these two observational sites is .7 miles. For this calculation, the period between 10 MST on 8 December to 10 MST on 9 December 1965 was chosen. From the COH chart for the same period,  $\nabla C$  was calculated from grid points three miles apart; however, only those points at which the analysis was certain were taken into account (see Fig. 6 for analysis and grid). From 12 charts, 107 values were taken or an average of nine points per chart. In this manner, a better value for  $\nabla C$  over the whole is obtained than could be from two points only. The calculation is given in Table V, and the results are shown in Fig. 14. The difference between two gradients is evident:  $\frac{\partial C}{\partial z}$  is at least one order of magnitude higher than the corresponding value for  $\nabla C$  at any time of day even though it never reached  $10^{-1}$ .

Consequently, since  $V \sim 10^0$ ,  $w \sim 10^{-3}$ ,  $\nabla C \sim 10^{-4}$ , and  $\frac{\partial C}{\partial z} \sim 10^{-2}$ , the value of the horizontal advection is at least one order of magnitude higher than the value of the vertical one, or

$$\vec{V}_h \cdot \nabla C \sim 0 (10^{-4}), \quad w \frac{\partial C}{\partial z} \sim 0 (10^{-5}).$$

For that reason, it is assumed that the horizontal wind is responsible for the transport of polluted air over the city and that, therefore, the third term on the right side of Eqn. (3) can be neglected.

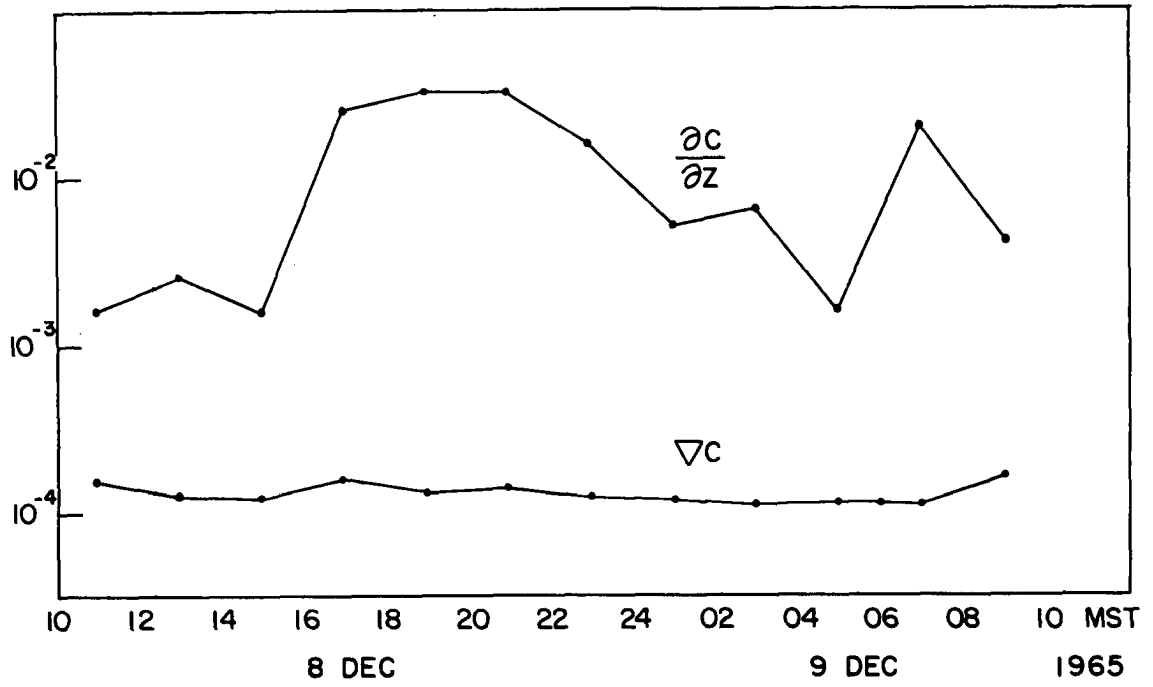


FIG. 14. The horizontal and vertical gradient of COH.

### The Errors in the Trajectory Calculations

Regardless of the small value of the vertical velocity calculated from the wind field, an air parcel may be affected by the temperature field and the vertical wind profile. For example, high temperatures at low levels of the atmosphere will produce an upward motion of the air parcel due to the difference between the density of the air parcel and that of its environment. The vertical acceleration of the air parcel is proportional to the difference in temperature between the air parcel and its environment, assuming that the pressure of the air parcel and its environment are the same.

Over Denver, the surface temperature field shows the effect of the well-known phenomenon of "the city heat island". That is, the difference in temperature between the downtown area and the suburbs may reach as much as  $10^{\circ}\text{F}$ . Such a difference can generate vertical motion over the "heat island" which may affect the horizontal trajectory.

The Denver RAOB reports show the presence of a strong inversion in the lower layer ( $\sim 1500$  feet) of the atmosphere which is in excess of at least twice the horizontal temperature difference. An example of the Denver RAOB report is given in Fig. 15 for 7 December 1965 at 05 MST. The temperature field for this day (Fig. 16) shows "the city heat island" over the downtown area with a temperature of  $46^{\circ}\text{F}$ . If the average height of buildings in downtown Denver is assumed to be 100 feet, an air parcel will attain the same temperature as in the free atmosphere at 90 feet above roof level, under the assumption that the temperature of the air parcel decreases with height dry-adiabatically. This vertical distance is negligible in comparison with the horizontal one which an air parcel traveled during two hours. Furthermore, the temperature at Kunsmiller Junior High School is  $48^{\circ}\text{F}$  at the elevation 5,535 feet above m. s. l. The same temperature in the free atmosphere over Stapleton Field, according to the RAOB report, occurs at

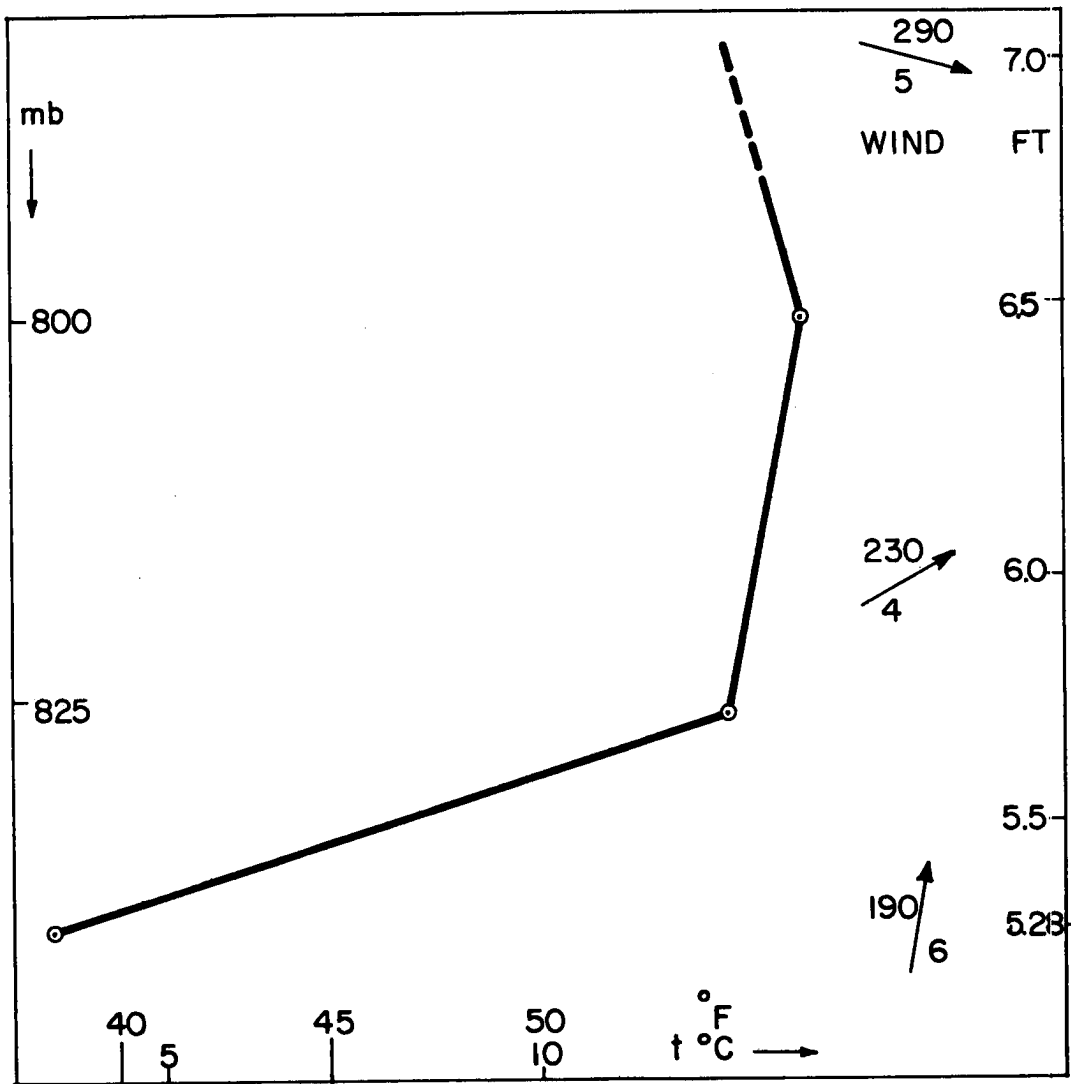


FIG. 15. Denver RAOB report on the 7 December 1965, 05 MST.

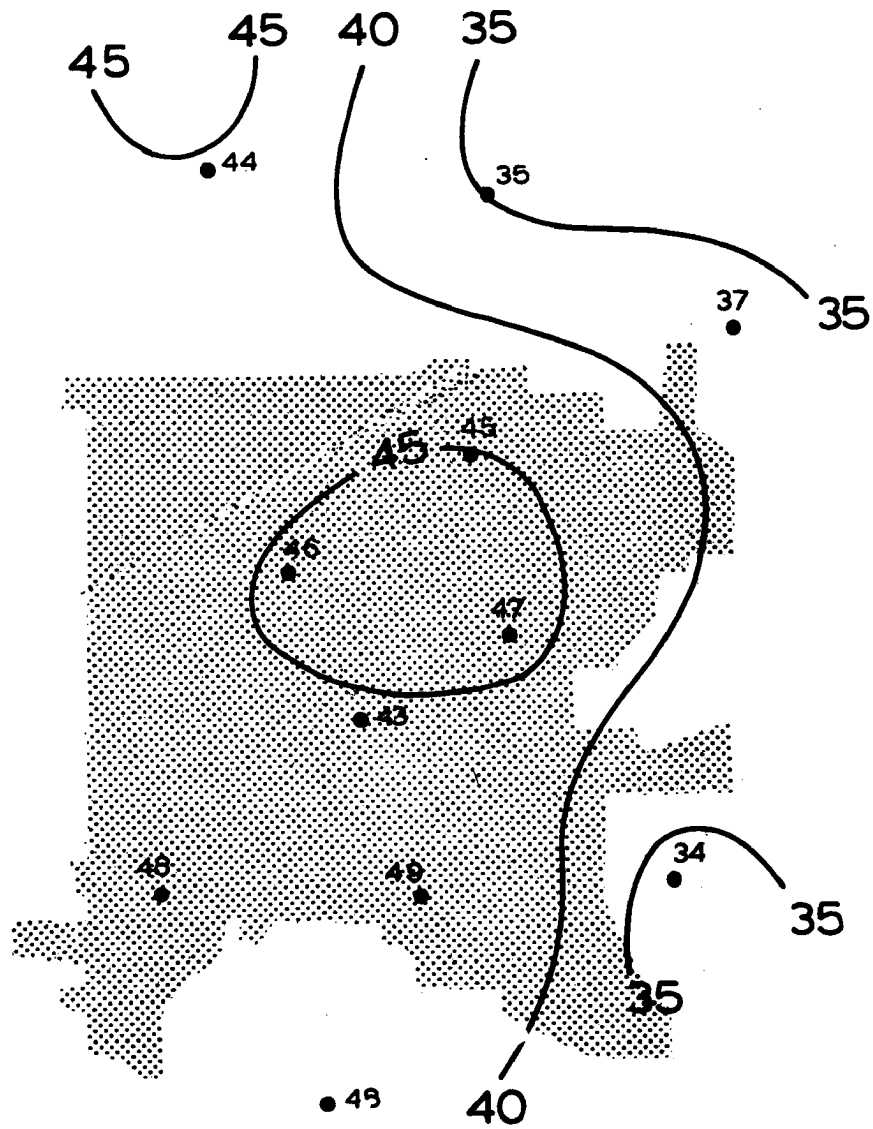


FIG. 16. Temperature field on the 7 December 1965, 05 MST.

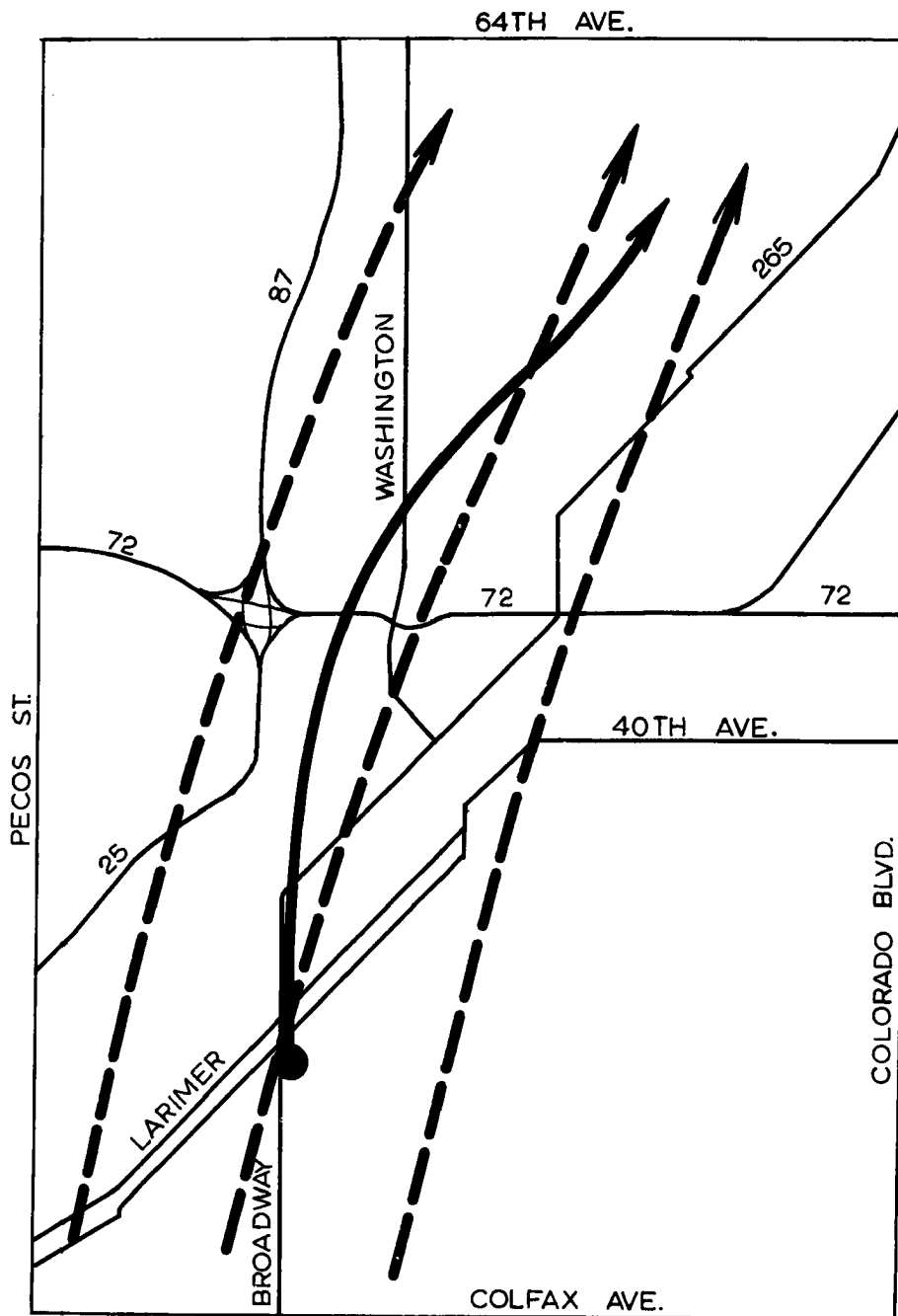


FIG. 18. The path of tethered balloon (full line) and streamlines (dashed lines) for the flight performed during the night of 13 January 1966.

## CHAPTER IV

### ANALYSIS

#### Soiling Index

For the ten sampling sites, which had a large number of observations during the 1964-1965 and 1965-1966 winter air pollution seasons, the daily course of two-hourly average COH values is given in Fig. 19. The average values are plotted at the midpoint of the sampling period.

In the northern part of the city (the stations: State Game, Fish, and Parks Department, Northridge Lumber Company, Adams City Health Center, Denver Sewage Treatment Plant and Wheatridge Sanitation District), the maximum COH occurs at nine o'clock in the morning and the minimum in the middle of the afternoon. Secondary extremes occur at nine o'clock in the evening (maximum) and in the early morning (minimum).

The daily course of contamination is a function of both the rate of emission and meteorological conditions. The morning peak may be ascribed to increasing business activity at this time of day. The occurrence of the primary minimum in the afternoon, between one o'clock and three o'clock, can be attributed to the warming of the lowest layer of the atmosphere due to solar heating which increases the vertical mixing. The displacement of the maximum to the afternoon at the Signal Broadcast Productions, Inc., in the downtown area at 324 feet above the ground, may also be related to the increasing of vertical mixing. Such an explanation for the afternoon minimum is suggested by Riehl and Crow (1961). However, another possibility exists: The afternoon minimum may be due to both the warming of the lowest layer of the atmosphere and the prevailing wind at this time of the day. The latter may bring cleaner air into the region and in this manner decrease pollution. The

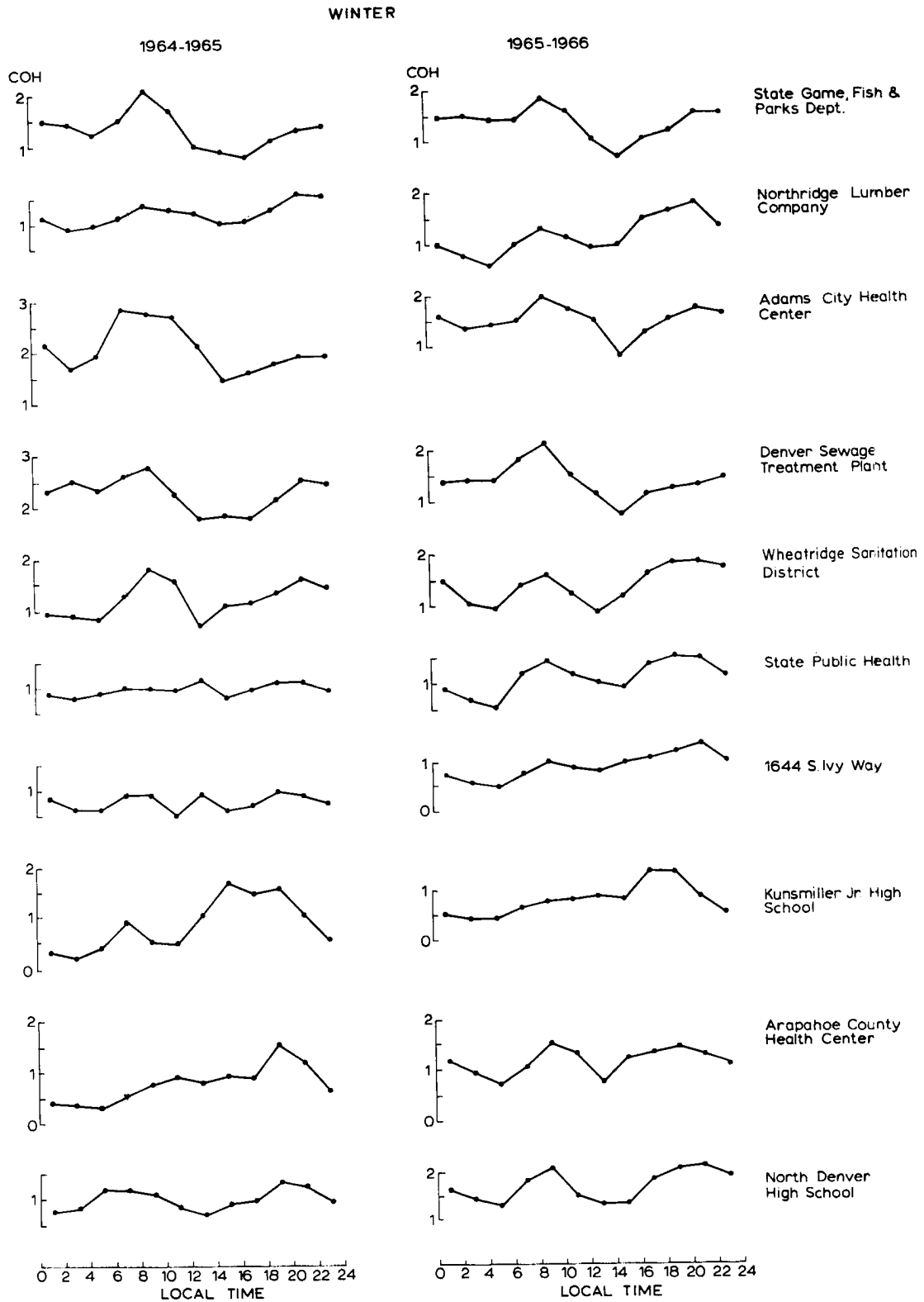


FIG. 19. The daily course of COH during the days with air pollution in the 1964-1965 and 1965-1966 winter seasons.

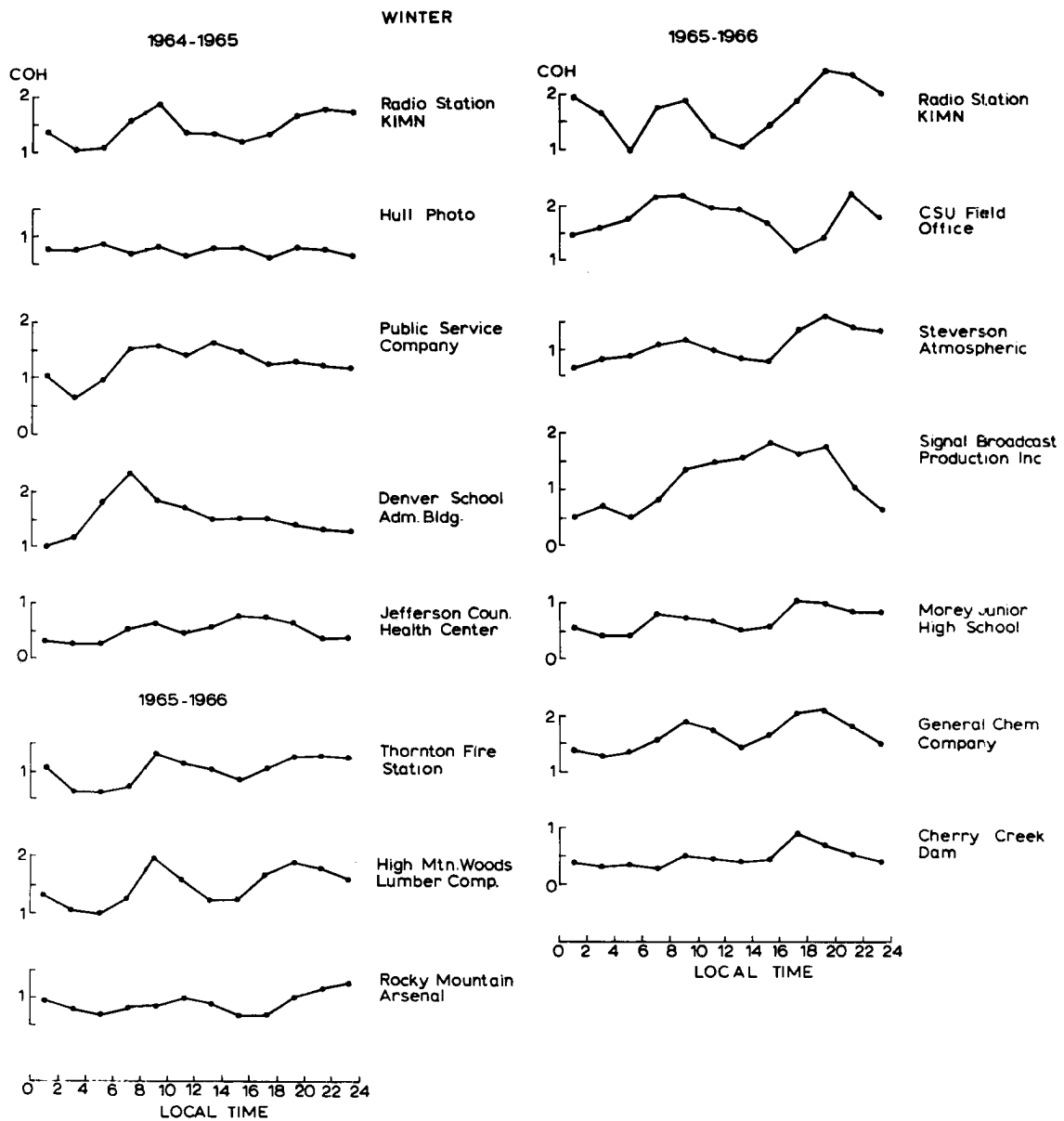


FIG. 19. Continued.

morning peak is generally ascribed to "fumigation"<sup>1</sup> (Hewson, 1961), which depends on the vertical stability of air (see Fig. 2). However, one would not expect the occurrence of fumigation under inversion conditions in the lowest layer of the atmosphere, but rather a "fanning"<sup>2</sup> (Gosline et al., 1956).

The two stations in the southern part of the city, Kunsmiller Junior High School and Arapahoe Health Center, show the steady increasing of pollution from the morning to the afternoon with a maximum between three o'clock and seven o'clock, which is most pronounced at the first station. Thus, these stations show a daily course opposite to that of the stations in the northern part of the city. The cause for this diurnal change will be explained later.

It is a fairly good assumption that the strength of sources responsible for the contamination of air over the Denver area was not different in the two winter seasons. Since the daily course of COH has the same characteristics in both air pollution seasons, one may conclude that the same factors are responsible for the similar daily course of contamination in different parts of the city. This will be studied in the following pages.

The charts of mean COH values are given in Figs. 20 and 21. For the majority of the stations, the mean values were obtained from large samples and these means may be accepted as very close to the real level of the average contamination during study days with air pollution. As can be seen, the city area with heaviest pollution lies along the South Platte River Valley.

---

<sup>1</sup>The phenomenon referred to as "fumigation" occurs during a transition from smooth to turbulent flow. Generally, it is caused by heating of the lower layer of the atmosphere from the ground.

<sup>2</sup>"Fanning" is another characteristic shape of plume when an inversion is present. A "fanning plume" has a very small extent in the vertical direction and due to slight shifts in wind direction, the plume meanders downwind in the shallow layer.

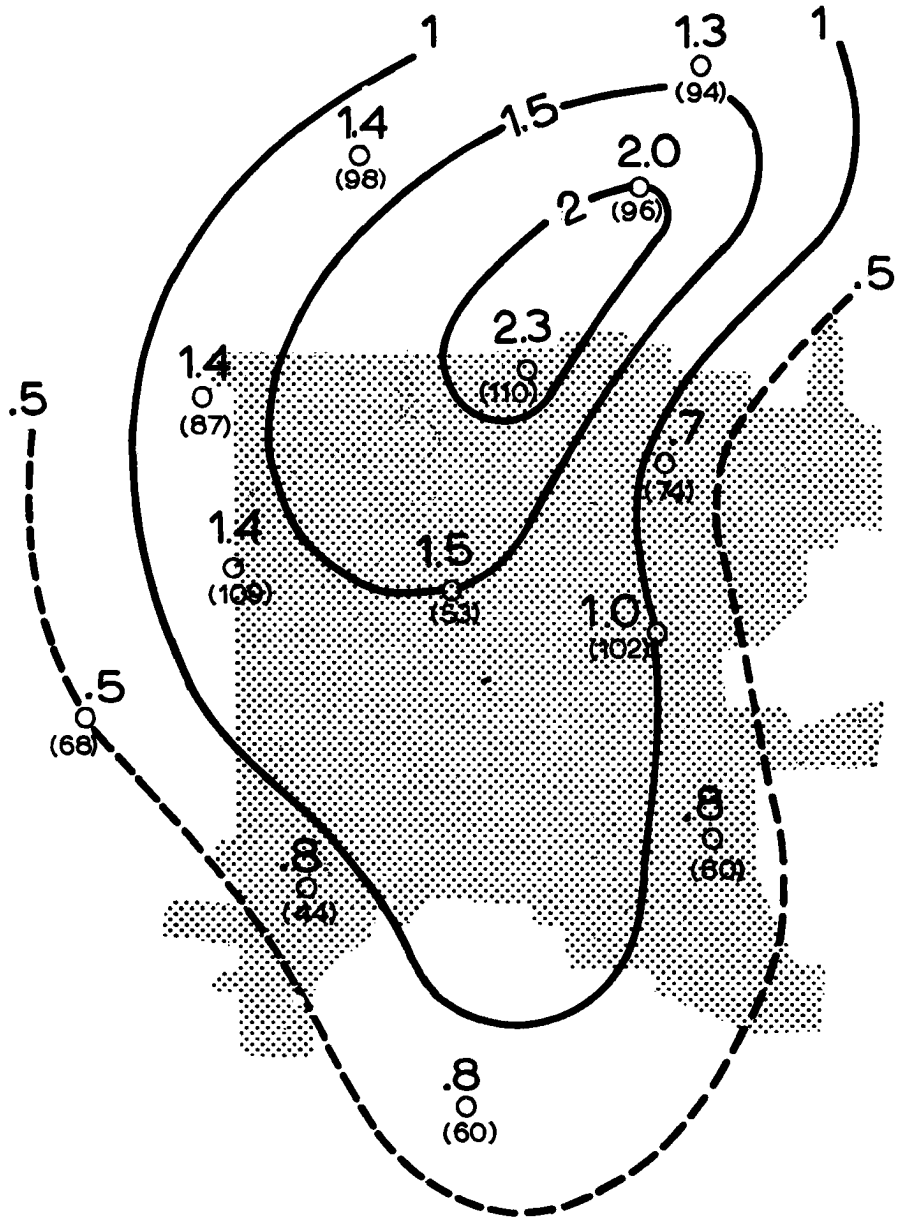


FIG. 20. The mean values of COH during the 1964-1965 air pollution season. Number of observations are given in parentheses; region with insufficient number of observations are indicated by dashed lines.

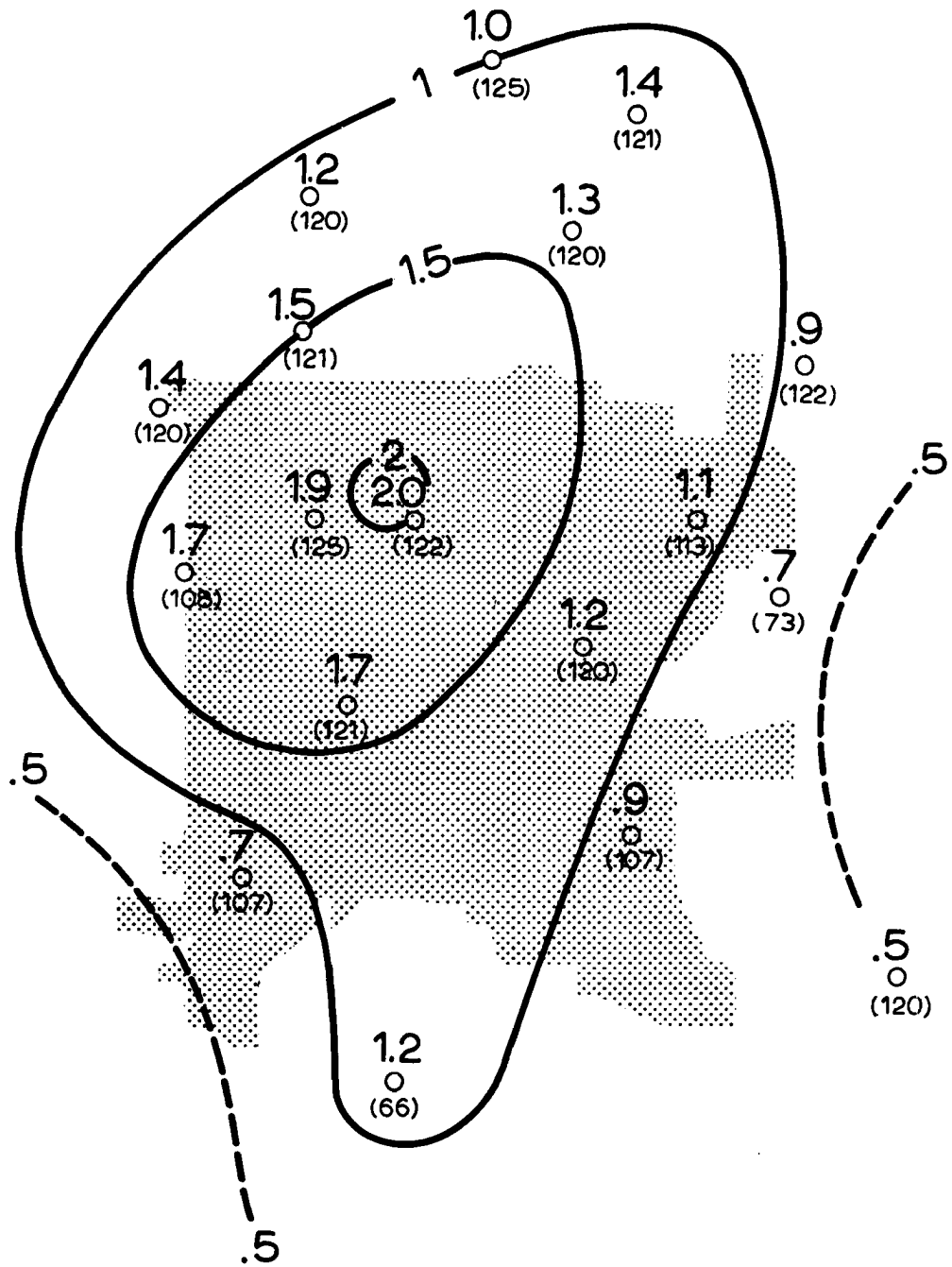


FIG. 21. The mean values of COH during the 1965-1966 air pollution season. For explanation, see Fig. 20.

### The Wind Field

For the two air pollution seasons, the flow patterns over the Denver area may be divided into four major groups:

(1) S-SW winds, downslope motion, drainage wind down the Platte River Valley;

(2) N-NE winds, upslope motion, also along the river valley with some deflection along mountain sides;

(3) A combination of (1) and (2) with a convergence line which moves over Denver. This type of flow is associated with very light winds or almost calm conditions. It occurs during the turning of S-SW to N-NE flow, and vice versa. Its duration is usually from two to four hours. For the sake of simplicity, this flow will be called N-S;

(4) SE winds, observed in only 14 cases.

The occurrence of the S-SW type of flow makes up 56% (133 cases) of the whole sample period, while N-NE makes up 27% (65 cases). Thus, these two flow patterns provide a sufficiently large sample for a study of the motion of pollutants. Clearly, the center of attention should be N-NE and S-SW situations. An attempt was also made to study the N-S type, but the result was not satisfactory due to the very light winds and the calm conditions at the majority of the stations. Uncertainties in the streamlines, as well as in the isotach analyses, are unavoidable under these conditions. Moreover, the position of the convergence line is questionable. The small number of cases with N-S flow, only 11% or 27 cases during the whole sample period, does not permit one to draw any statistically meaningful conclusions. For the same reason, the SE flow has not been considered either.

The analyses show that the downslope (S-SW) flow usually begins between seven o'clock and ten o'clock in the evening and lasts until noon the next day, after which time the flow changes to

N-NE type. This reversal of the wind flow will be studied in the following section.

An example of the two-hourly average streamlines and isotachs in S-SW flow is shown in Fig. 10. As can be seen, the influence of topography on the wind field is very well marked. The streamlines strictly follow the shape of the terrain; the small hill in the northeastern part of the Denver metropolitan area, and the tributary valleys on the west and east of the South Platte River (Layden Creek, Turkey Creek, Cherry Creek, etc.) have a well-defined influence on the direction of flow. As was shown previously, the wind speeds are light over the whole area.

The influence of the terrain on the N-NE (Fig. 11) type of flow is almost the same. Thus, the topographic features around Denver strongly determine the wind direction and speed when the general weather situation is characterized by very light winds aloft and subsidence. The strong inversion may persist for several days during which the wind flow has a direction in the night and morning hours (S-SW) opposite from the one in the afternoon (N-NE). In such weather situations, the movement of a polluted air mass is very slow along the South Platte River Valley, and one may expect that the pollution is not transported very far away from the city limits. Gifford (1953), in his study of low-level air trajectories using zero-lift balloons, has shown that under inversion conditions the balloon paths obeyed downslope motion and were closely parallel to the terrain. Neiberger (1961) studied the change of the hydrocarbon and CO concentrations along an air parcel trajectory over Los Angeles and found a good agreement between the amounts of cumulative contamination along a trajectory and the observed value measured at the end point of the same trajectory.

Relation Between COH, Wind Flow, and Inversion

It was mentioned earlier that the most polluted area of Denver lies along the South Platte River Valley. Also, it was stressed that the daily course of COH in the southern part of the city is opposite from the one in the northern part of the city. In order to explain the daily course of COH and to show the reversal of wind flow (from S-SW to N-NE) during the days with air pollution over Denver as well as to establish some relation between the wind regime and the temperature stratification of air with the distribution of pollution along the South Platte River Valley, the following method of analysis was used. First, the whole metropolitan area was divided into equal squares with sides of three miles each (Fig. 22). Then, two-hourly COH values were computed, employing a weighting method, for the squares numbered 3, 6, 10, 14, and 18. These squares lie along the river valley. For the same squares, the two-hourly mean winds were determined in the central point of each square, and from these, the mean wind along the valley was computed. Both, the two-hourly COH values and the mean wind, were plotted together with the RAOB reports from the U. S. Weather Bureau Station at Stapleton Airport for all days with air pollution. The lapse rate,  $\gamma$ , was calculated for the lowest layer of the atmosphere, up to the first characteristic point on the temperature curve ( $\gamma$  was expressed in  $^{\circ}\text{C}/100$  meters). In addition, the upper winds at 6,000 and 7,000 feet above m. s. l. were plotted at the approximately corresponding heights of 200 and 550 meters above the ground, respectively. The surface mean wind along the river valley was plotted at the middle point of the time interval. The result is given in Fig. 23. From this figure, one may conclude that the reversal of the wind flow along the South Platte River Valley was a frequent occurrence during the days with air pollution over Denver. As was mentioned in the preceding section, N-NE flow generally occurs during the afternoon. Winds

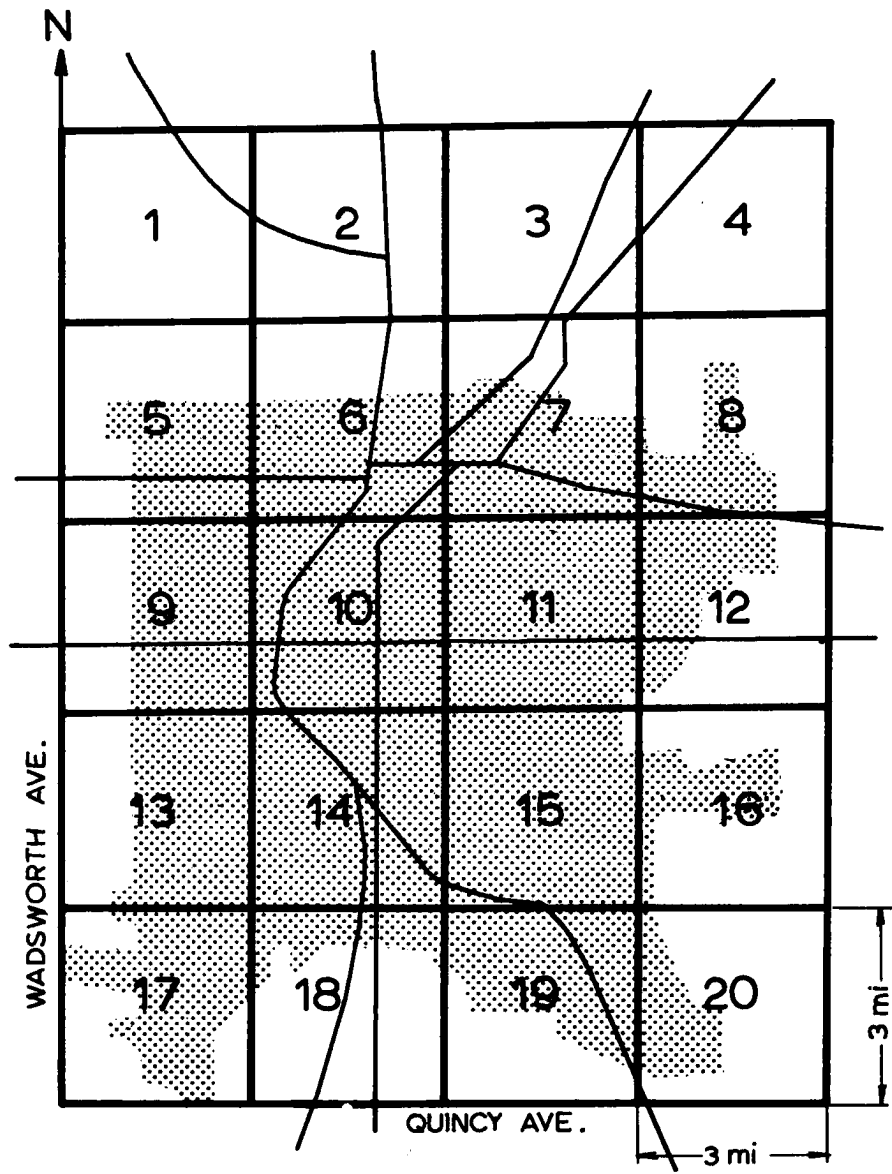


FIG. 22. "Squares" for the computation of mean wind and mean COH. Main traffic routes are indicated by thin lines.

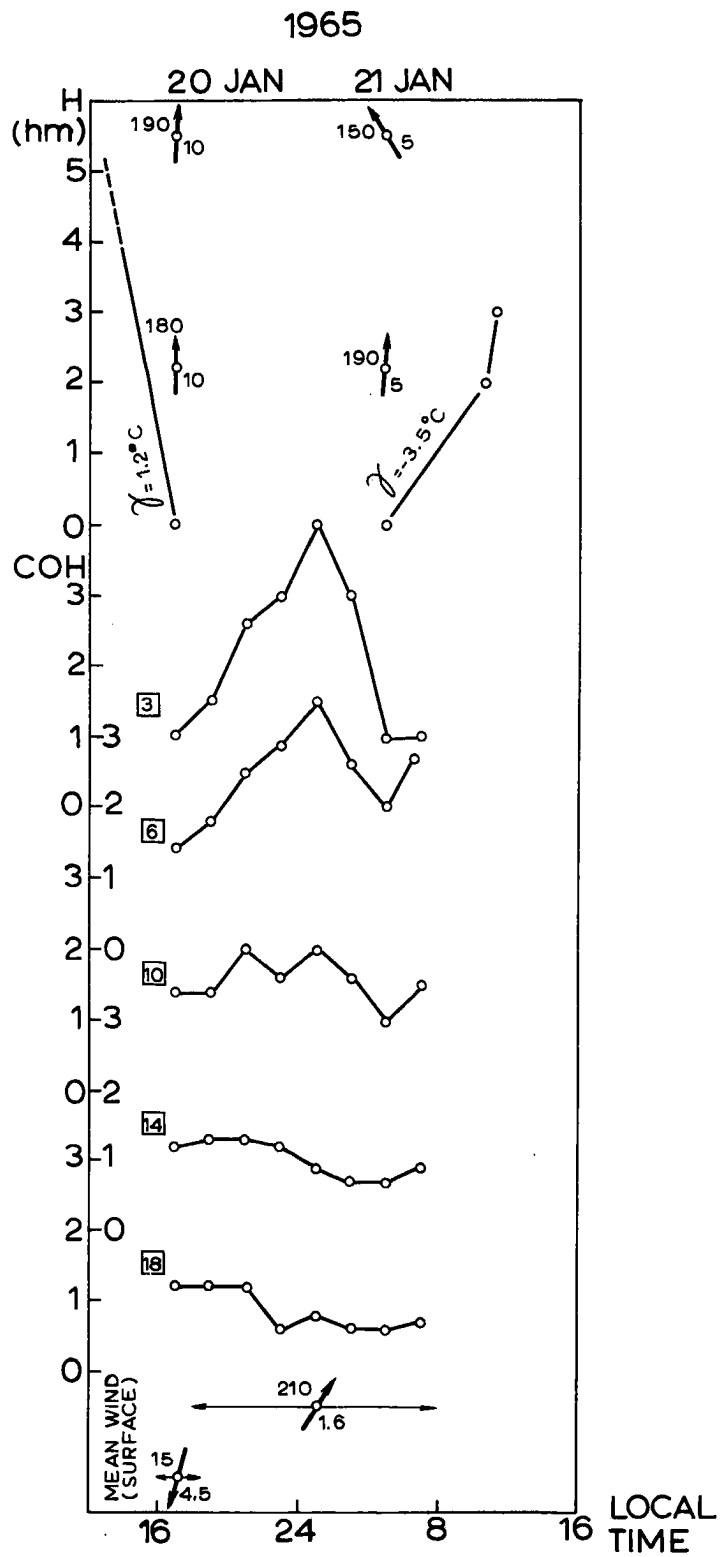


FIG. 23. Mean COH values, average surface winds along the South Platte River Valley, and Denver RAOB reports. "H" is height in hundreds of meters.

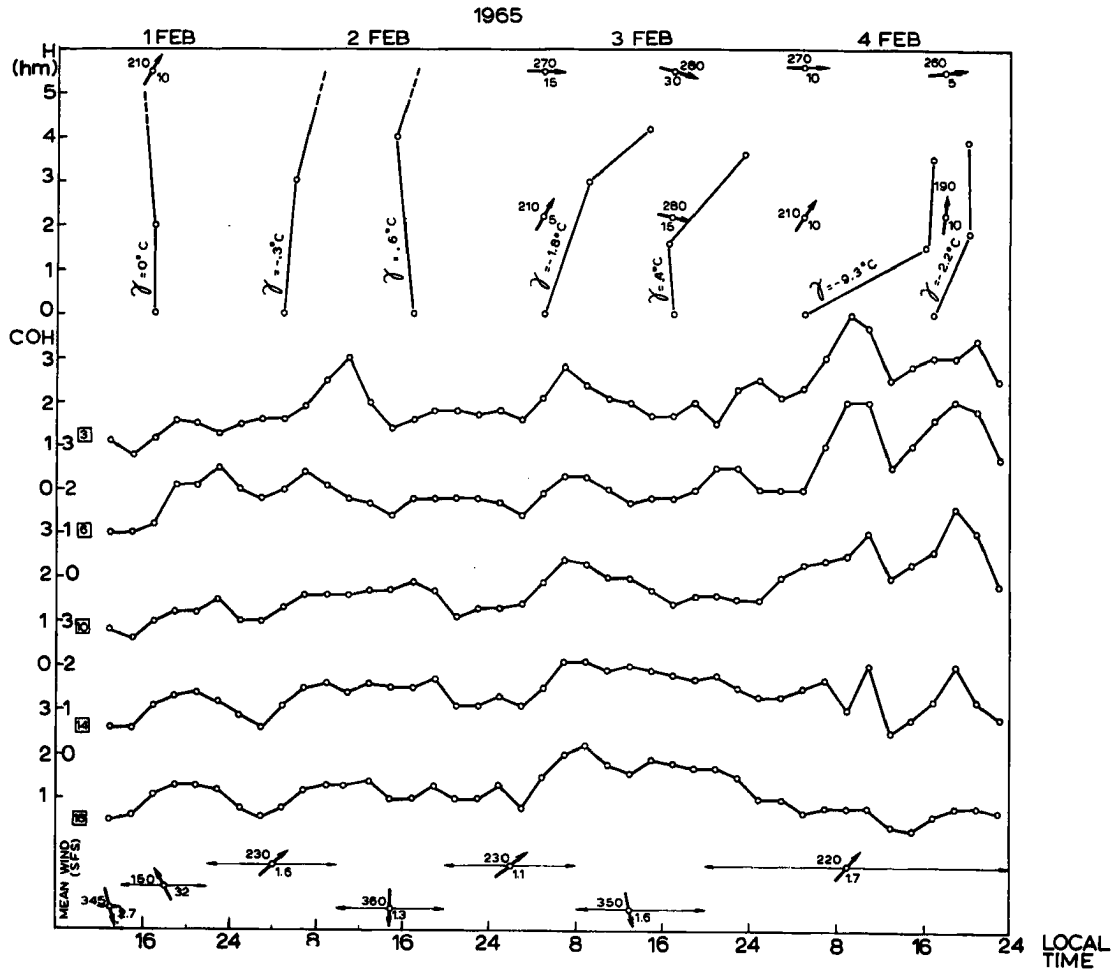


FIG. 23. Continued.

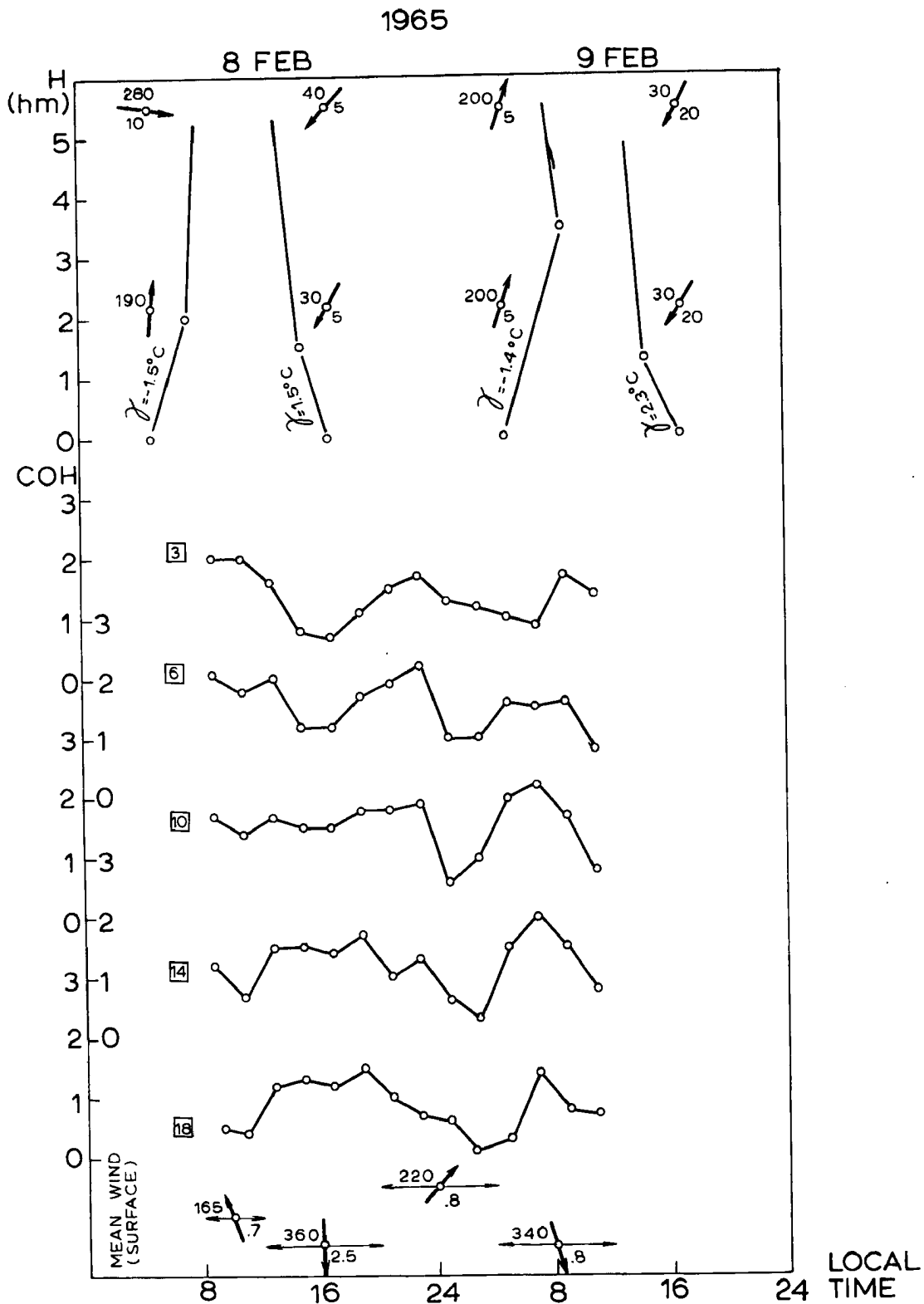


FIG. 23. Continued.



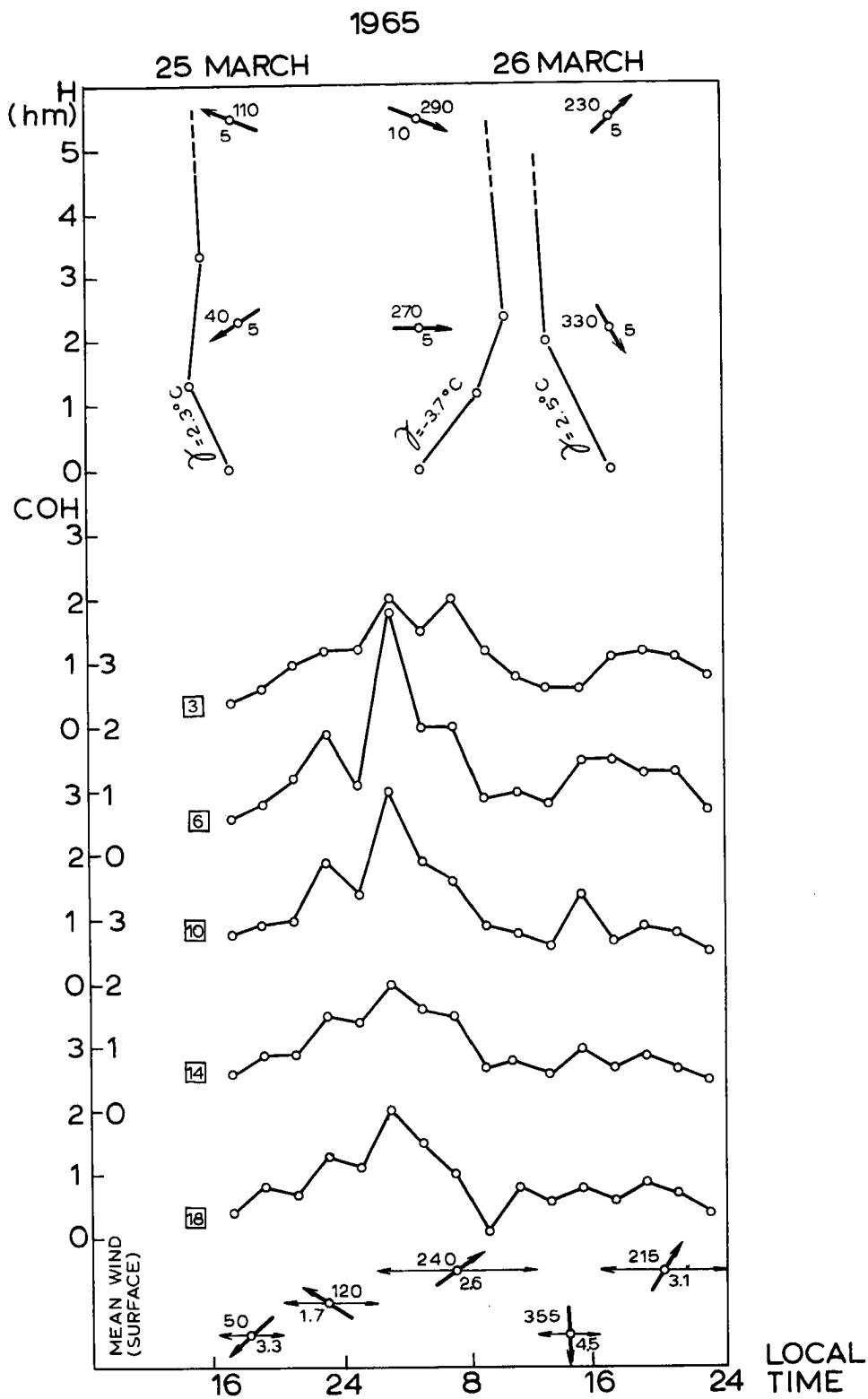


FIG. 23. Continued.

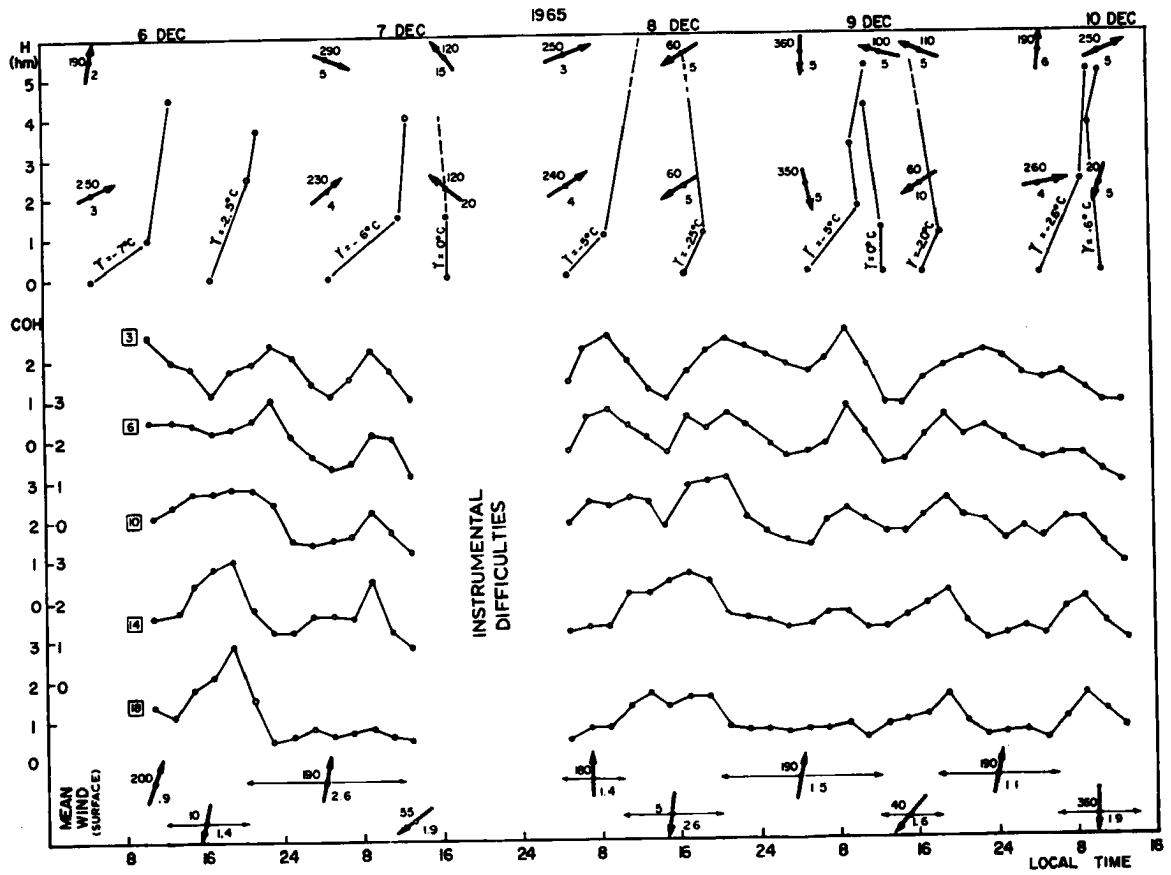


FIG. 25. Continued.

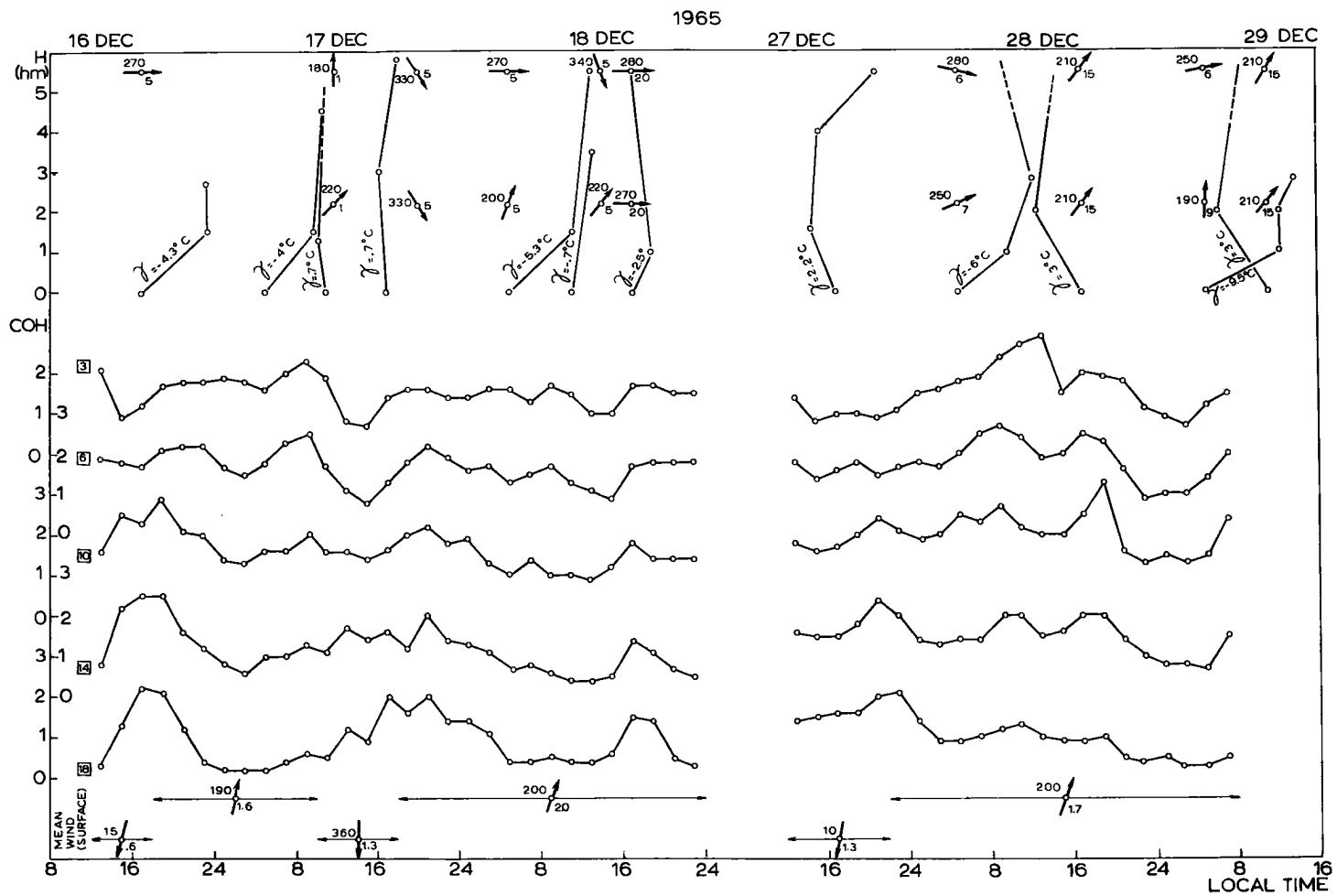


FIG. 23. Continued.

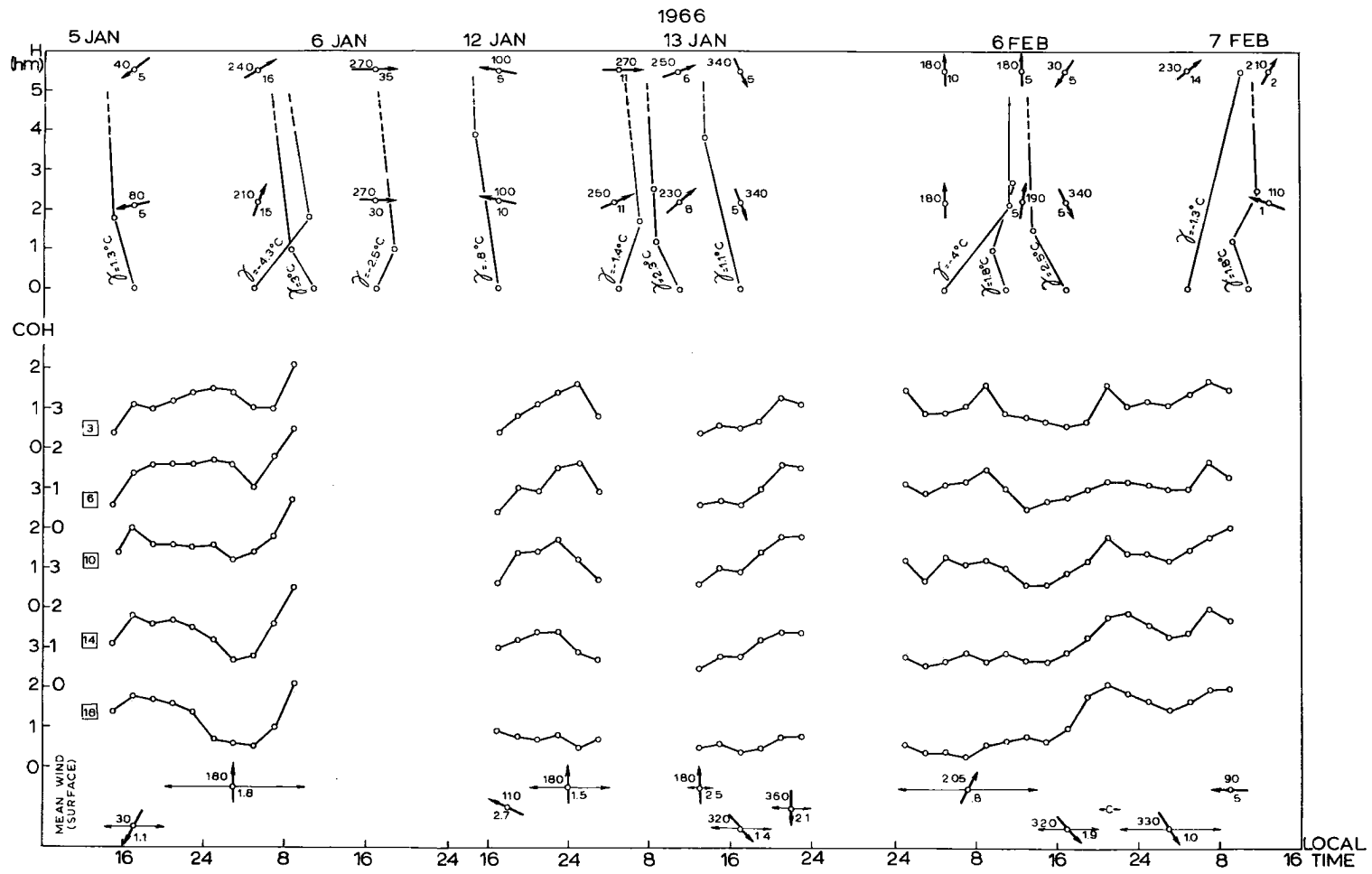


FIG. 23. Continued.

reversed to S-SW in the early evening, and this flow lasted until noon of the next day. During certain days, the reversal of flow did not occur as, for example, on the 18, 28, and 29 of December 1965. During these days, the RAOB reports showed increasing wind speeds at 6,000 and 7,000 feet (15 to 20 knots), indicating that the daily wind regime did undergo changes under the influence of the large scale weather pattern which caused a strengthening of the pressure gradient and an increase of the wind. Furthermore, the non-appearance of the daily reversal in the wind flow during these three days was associated with the break in the air pollution episode. Wind speed at the surface increased until eleven o'clock on 18 December 1965 when the wind reached almost 10 mph. The same phenomenon occurred on the morning of 29 December 1965. In both cases, inversions of the temperature existed. Thus, increasing wind speeds at the surface and in the lower layer of the atmosphere are sufficient to alleviate or terminate air pollution situations over Denver.

The vertical temperature profiles taken from the RAOB reports showed a presence of the temperature inversion during the night and morning. The strength of the inversion, as well as its depth, varied during the day. Morning lapse rates attained values to  $-9^{\circ}\text{C}/100$  meters, with the most frequent value of about  $-5^{\circ}\text{C}/100$  meters. In some cases, the temperature inversion was broken in the lowest layer of the atmosphere during the daytime and the lapse rate reached a positive value (see, for example, Fig. 23). When such a situation of a weakening or breaking inversion occurred, the air pollution period was not necessarily ended. On occasions even an increase of COH appeared in the southern part of the city in the afternoon, as was the case on 17 December 1965, typical for many other days. In these cases, the wind speeds at the surface as well as at 220 and 550 meters above the ground

were rather small, less than 5 knots. Thus, the breaking or weakening of the inversion was not by itself sufficient to end air pollution over Denver.

It was mentioned earlier that two stations in the southern part of the city (Kunsmiller Junior High School and Arapahoe Health Center) show, on the average, a steady increase in pollution from morning to afternoon with the maximum reached at sunset. It is possible to relate the occurrence of COH extremes in the different parts of the city to the prevailing winds and to the height of the inversion layer. It can be seen from Fig. 23 that the onset of N-NE flow is associated with decreasing COH values in the northernmost part of the city (squares 3 and 6). By afternoon, either the depth of the lowest inversion layer increased or the inversion shifted to some height above the ground. In both cases, the pollution layer extended to the height of 200 to 300 meters above the ground, and the occurrence of "fanning" or "fumigation" at the highest elevation above the ground was common (see Fig. 2). Stronger pollution will be found in the areas with higher elevations. In Denver these are the southern parts of the city. Thus, the transport of polluted air in N-NE flow during the afternoon and the change of the temperature profile during the daytime were responsible for the occurrence of COH maxima in the late afternoon in the southern section of the city.

In Fig. 24 the mean COH values for the northern and for the southern areas of the city (squares 3 and 6, 14 and 18, respectively) are given with respect to the prevailing flow during different times of the day for December 6 to 10 and December 16 to 18, 1965. As can be seen from this figure, COH mean values during S-SW flow show increases in the northern part of the city and decreases in the southern part. An opposite COH course was associated with N-NE flow. On the basis of Fig. 23, one may safely conclude that the

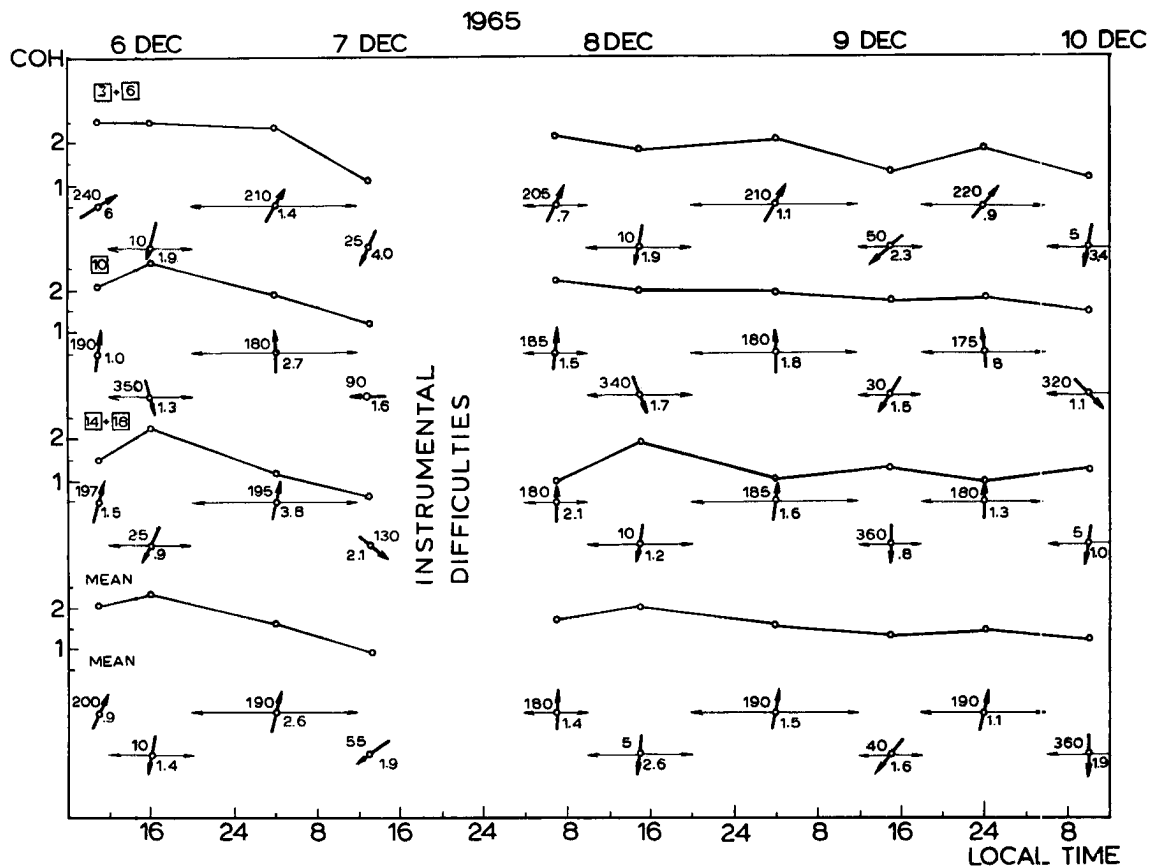


FIG. 24. Mean COH values for the northern and the southern parts of the city (squares number 3 and 6, 14 and 18, respectively), and the average surface winds along the South Platte River Valley during 6 to 10 December and 16 to 18 December 1965.

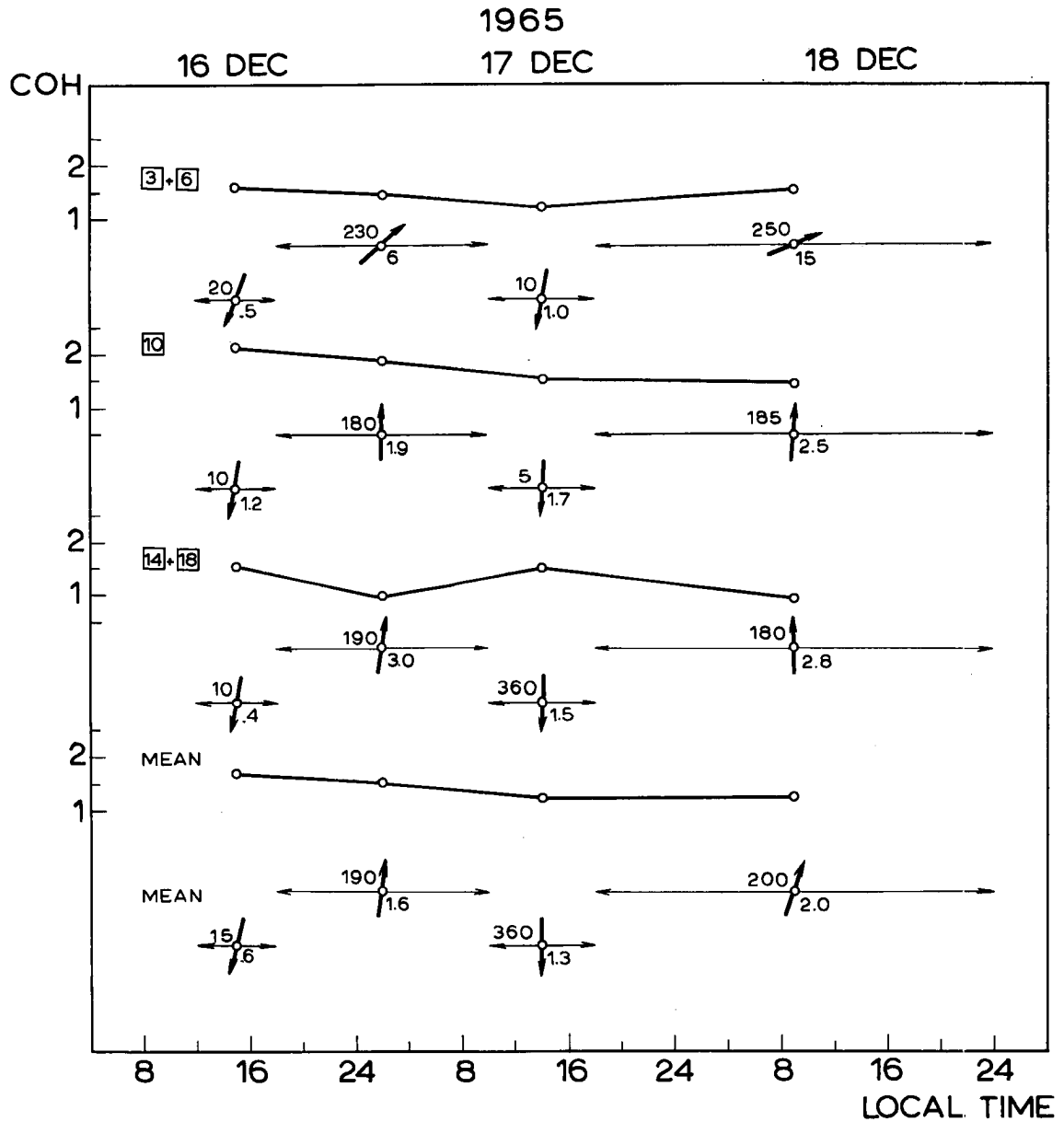


FIG. 24. Continued.

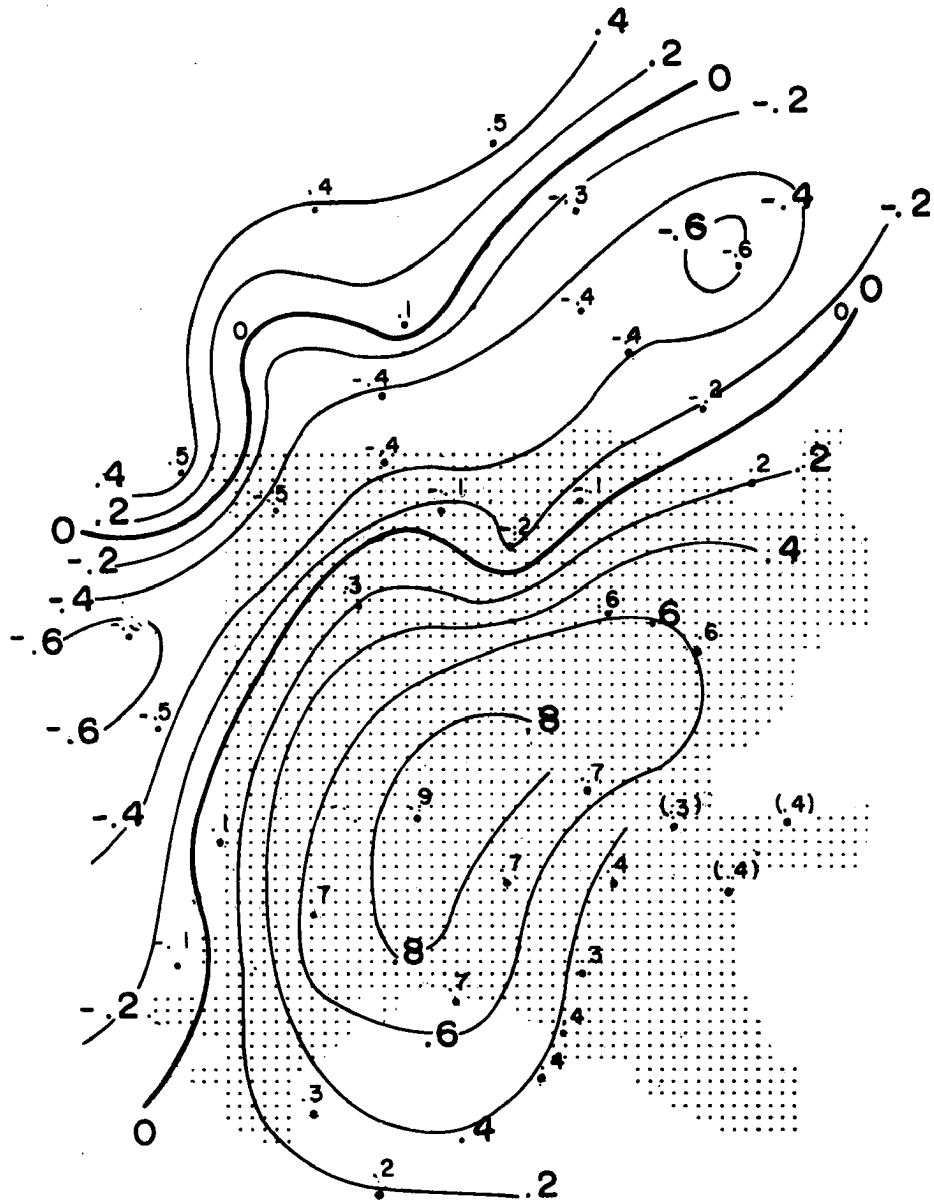


FIG. 26. The total change of COH along air parcel trajectories on 10 December 1965, 01-03 MST.

one cannot conclude that the city area is the main source of air pollution because the local change of COH,  $\frac{\partial C}{\partial t}$ , is included in the total one,  $\frac{dC}{dt}$ . From Eqn. (3), after neglecting the vertical advection, it follows that

$$\frac{dC}{dt} - \frac{\partial C}{\partial t} = \vec{V} \cdot \nabla C . \quad (7)$$

The local change has to be subtracted from  $\frac{dC}{dt}$  in order to obtain a horizontal advection. A map of  $\frac{\partial C}{\partial t}$  is given in Fig. 27; it was obtained by subtracting the corresponding maps of COH. The final step is a subtraction of two fields,  $\frac{dC}{dt} - \frac{\partial C}{\partial t}$ , (Figs. 26 and 27), and the result is shown in Fig. 28. As can be seen, the area with negative advection lies along the South Platte River in the northeastern part of the metropolitan area. This means that the local change, or the production of the pollutant in this area, is stronger than its transport by flow into this area. Such a conclusion is drawn on the basis of only one episode with S-SW flow. To find whether this conclusion holds on the average, all S-SW situations have to be studied. This will be discussed in the following pages.

During the N-NE flow, the trajectories of the air parcels show an opposite transport of pollution (Fig. 29). Corresponding maps of the local and total COH change and advection are given in Figs. 30, 31, and 32. The difference in the advection between S-SW and N-NE wind patterns is evident (compare Figs. 28 and 32). During N-NE flow the advection is positive in the northern part of the city, but in the southwestern and southeastern parts, it is negative. It will be seen later that such a distribution of advection during N-NE flow is valid on the average and not only for this specific case. For the moment it shall be stressed that a pronounced difference exists in the values of advection over the city during these two types of wind flow.

In the case when the flow changes from S-SW to N-NE, the resulting wind patterns and their corresponding trajectories show

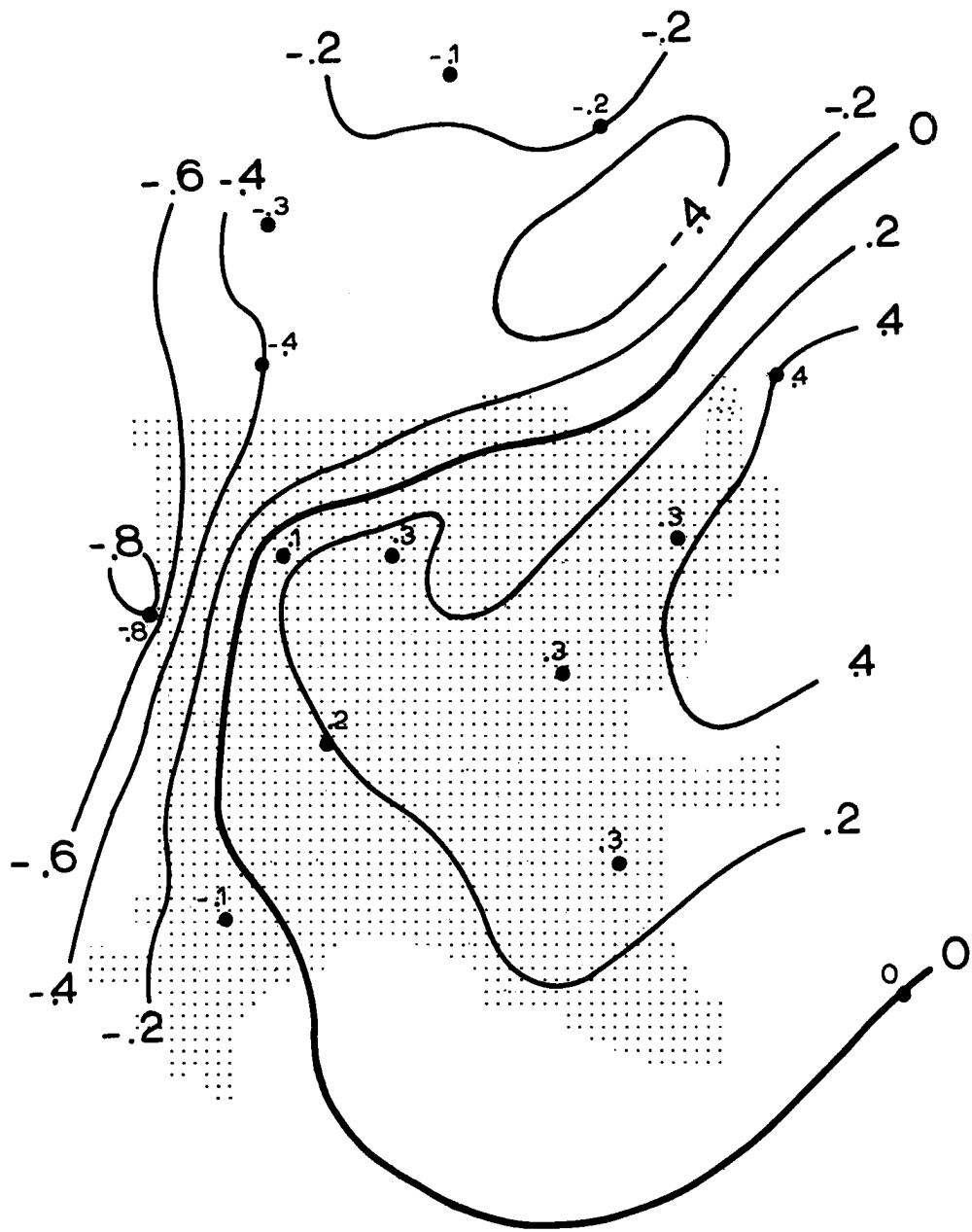


FIG. 27. The local change of COH,  $-\frac{\partial C}{\partial t}$ , on 10 December 1965, 01-03 MST.

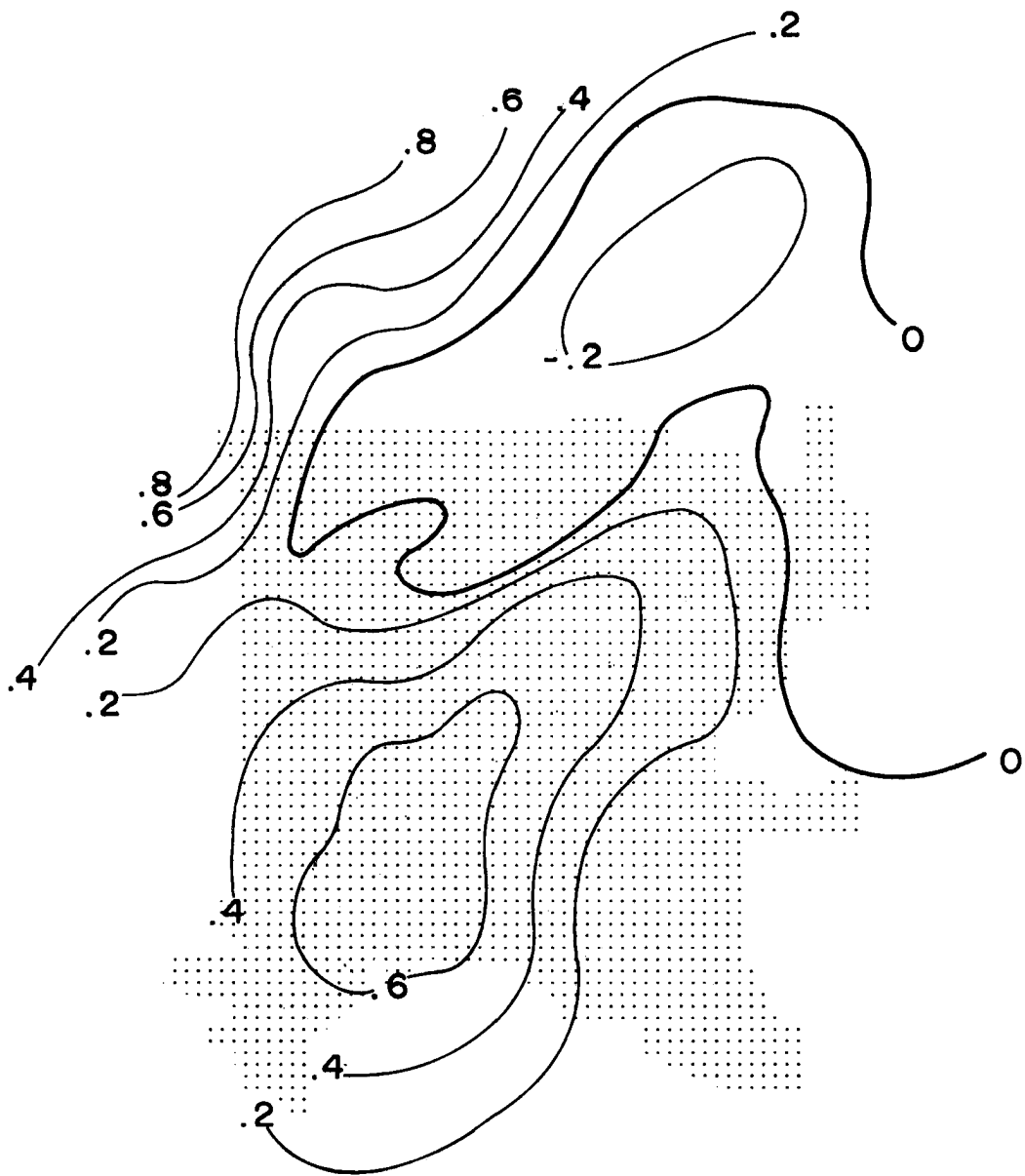


FIG. 28. Distribution of COH advection,  $\bar{V} \cdot \nabla C$ , on 10 December 1965, 01-03 MST.

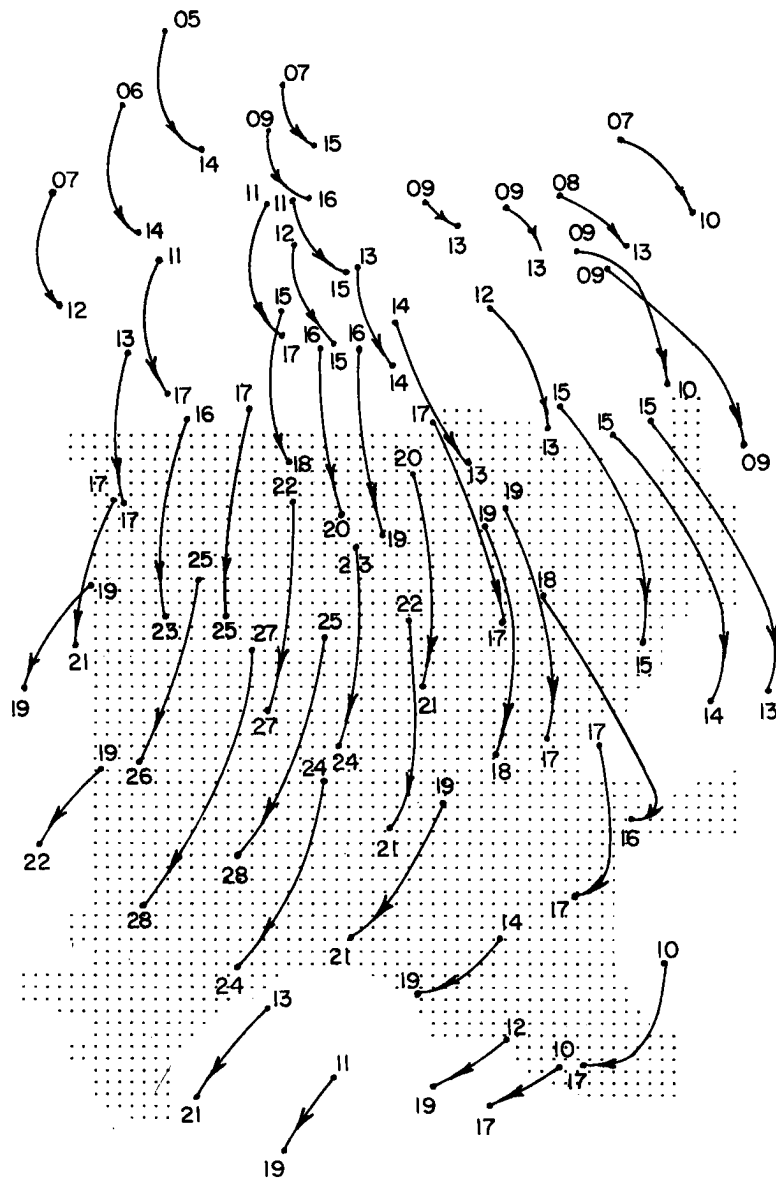


FIG. 29. The trajectories of air parcels over Denver during N-NE flow on 16 December 1965, 15-17 MST.

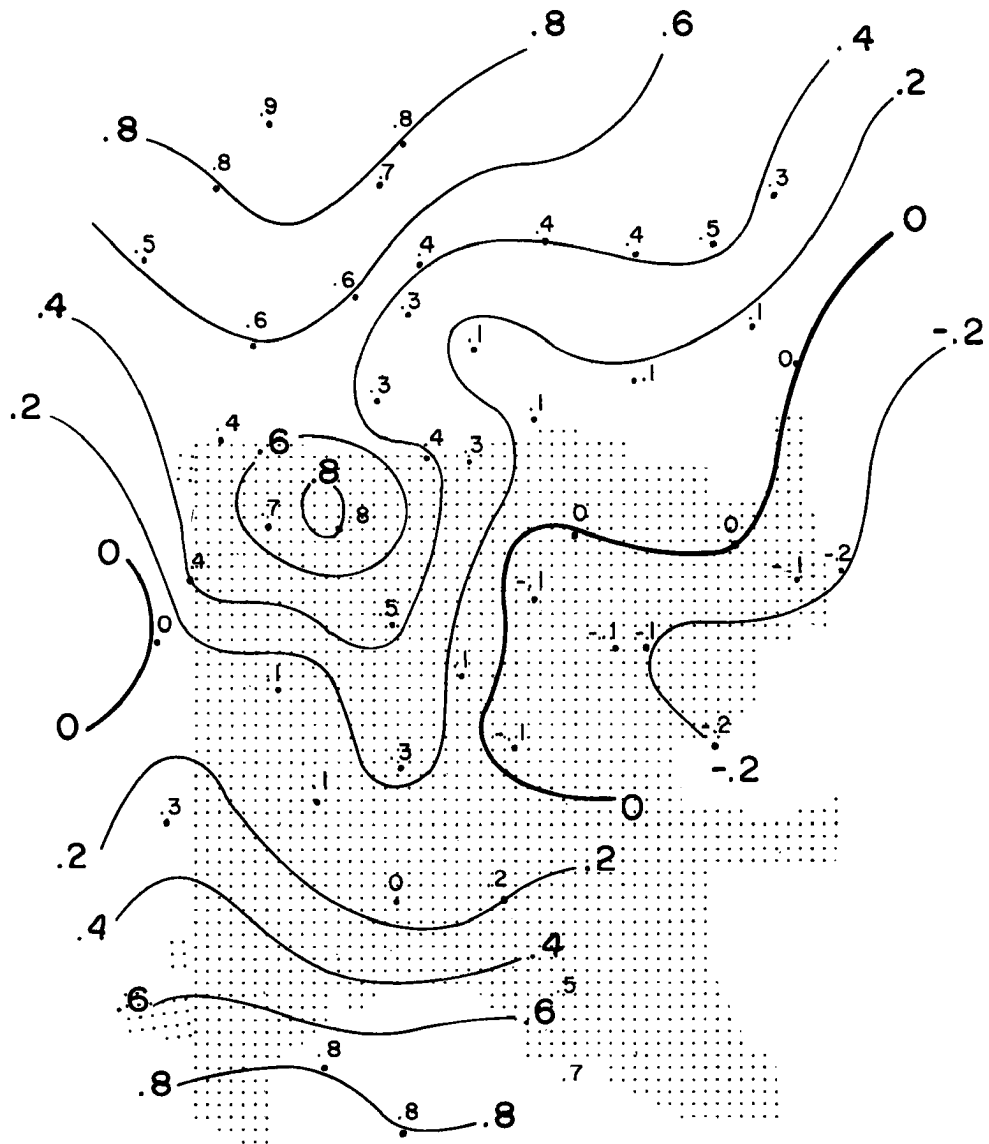


FIG. 30. The total change of COH along air parcel trajectories on 16 December 1965, 15-17 MST.

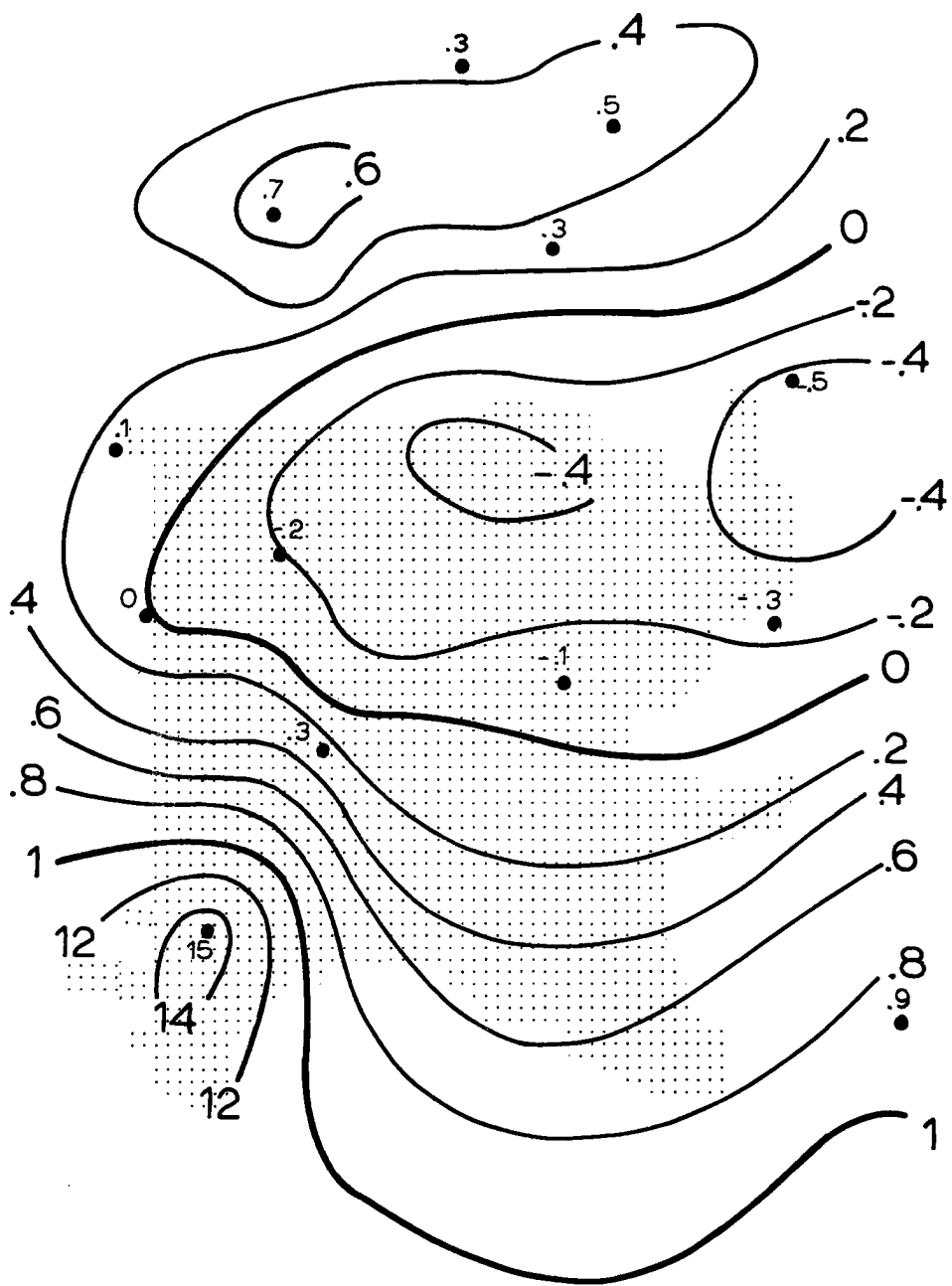


FIG. 31. The local change of COH,  $\frac{\partial C}{\partial t}$ , on 16 December 1965, 15-17 MST.



pronounced changes in the advection over different parts of the city. Examples are given in Figs. 33, 34, and 35 for 8 December 1965. At 09 MST the wind field (Fig. 33) had a pronounced S-SW direction, and its flow was very similar to that in the previous example (Fig. 10). The trajectories strictly followed streamlines indicating a stationary wind field, and an advection map ( $\vec{V} \cdot \nabla C$ ) showed in general the same distribution of positive and negative regions, as was shown in the above mentioned case. At 11 MST the majority of stations experienced a reversal of wind direction from S-SW to N-NE (Fig. 34). The corresponding trajectories (obtained from two successive wind fields at 09 and at 11 MST) show that the air parcels turned over the city from the north to the south. Net advection was rather weak over the entire city area because the air parcels reversed their track. Complete reversal of the wind occurred at 13 MST at all stations except two in the southernmost part of the area. At this hour, the paths of the air parcels were oriented to the south, and the corresponding advection was opposite to that at 09 MST (compare Fig. 35 to Fig. 33).

It was mentioned earlier that an increase in wind speed is sufficient to end severe air pollution over Denver. When such an increase occurs and it is followed by the breaking up of the inversion, the polluted air disperses very rapidly in both the horizontal and vertical directions. An example of such dispersal of air pollution over Denver is given for 10 December 1965. On the morning of this day (09 MST), the wind was light and the COH values at the majority of stations were higher than 1 (Fig. 36). The trajectories were very similar to those given in the previous examples with N-NE flow. However, from that time until noon the surface wind increased, and at 13 MST on that same day, it reached 6 mph at one station in the northern part of the city (Fig. 37). Now the COH values were less than one except for two stations in the southeastern part of the city. On this morning the inversion had been

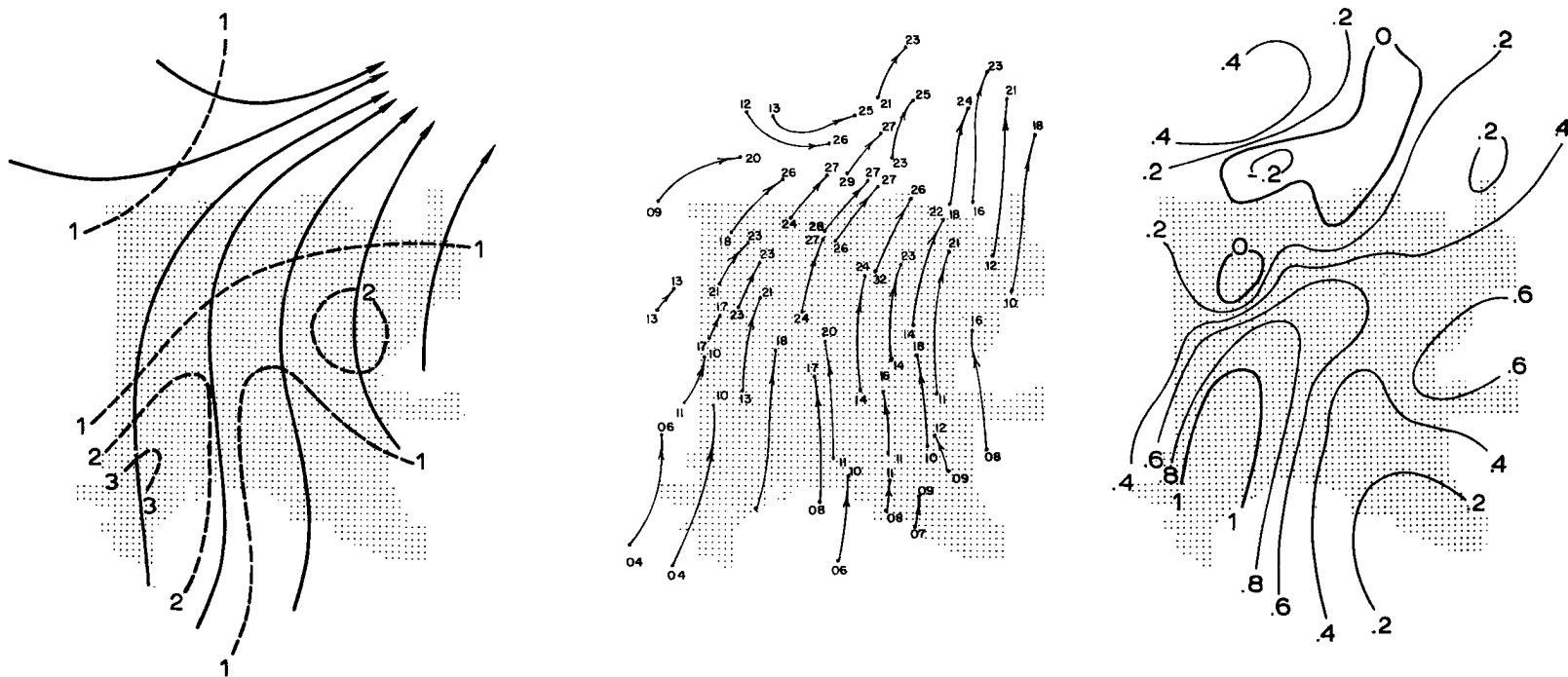


FIG. 33. Wind field on 8 December 1965, 09 MST. Full lines are streamlines; dashed lines are isotachs (mph). The trajectories of air parcels and the chart of COH advection,  $\bar{V} \cdot \nabla C$ , on the same day, 07-09 MST.

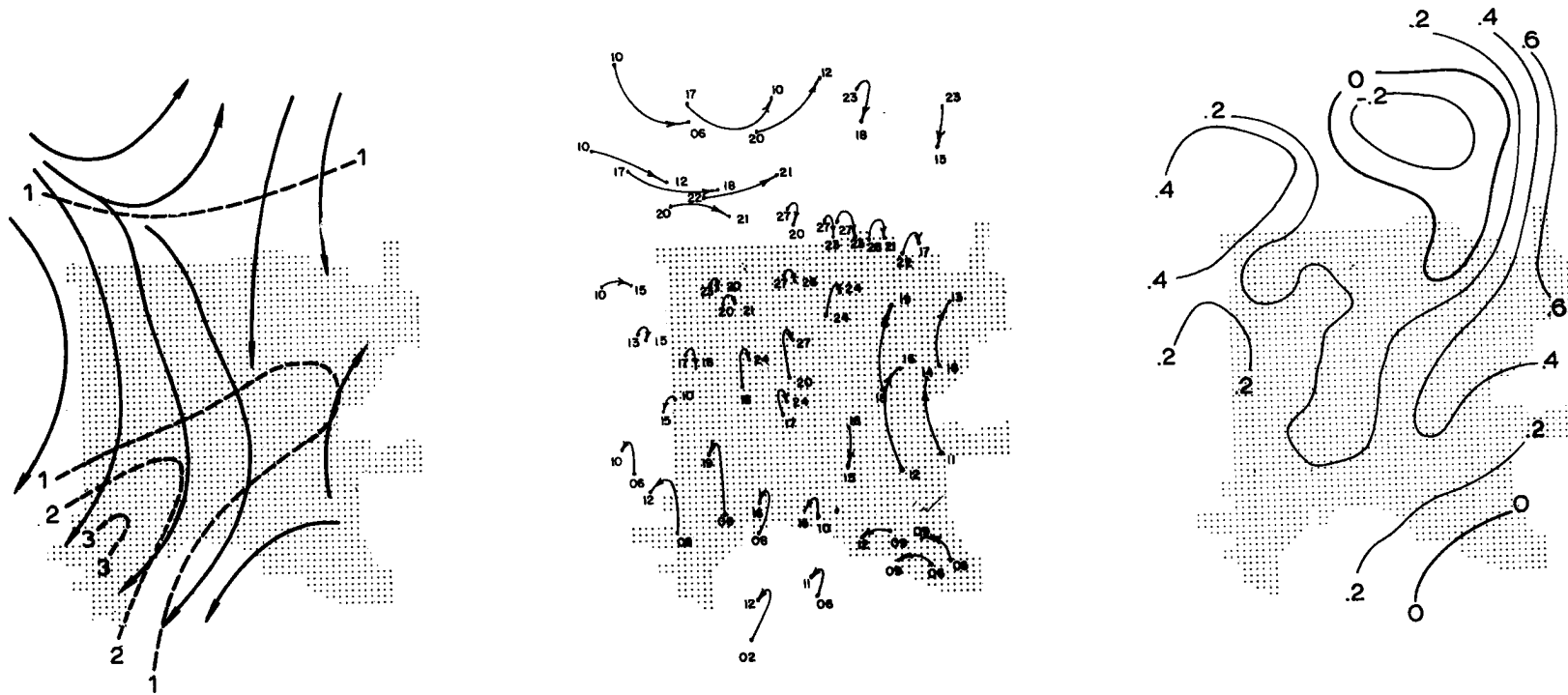


FIG. 34. Wind field on 8 December 1965, 11 MST. Full lines are streamlines; dashed lines are isotachs (mph). The trajectories of air parcels and the chart of COH advection,  $\bar{V} \cdot \nabla C$ , on the same day, 09-11 MST.

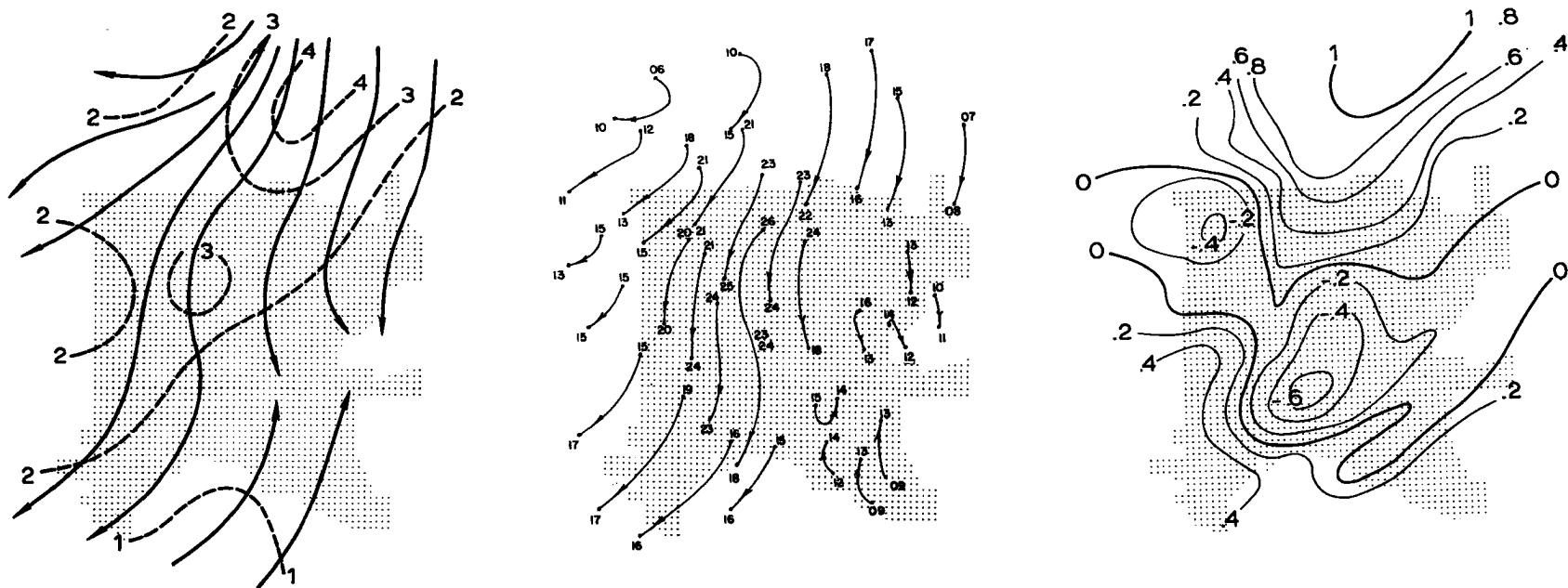


FIG. 35. Wind field on 8 December 1965, 13 MST. Full lines are streamlines; dashed lines are isotachs (mph). The trajectories of air parcels and the chart of COH advection,  $\nabla \cdot \nabla C$ , on the same day, 11-13 MST.

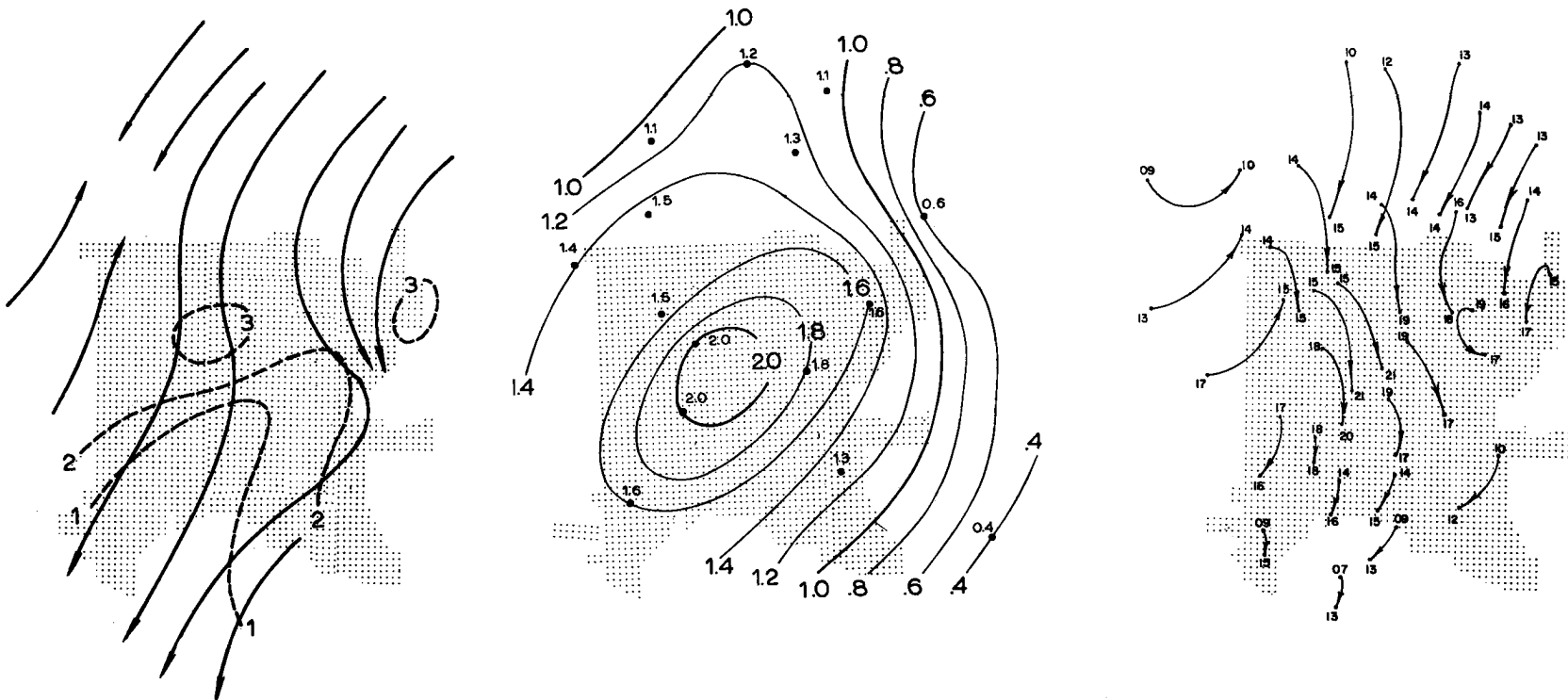


FIG. 36. Wind field on 10 December 1965, 09 MST. Full lines are streamlines; dashed lines are isotachs (mph). COH chart at 09 MST, and the trajectories of air parcels on the same day, 07-09 MST.

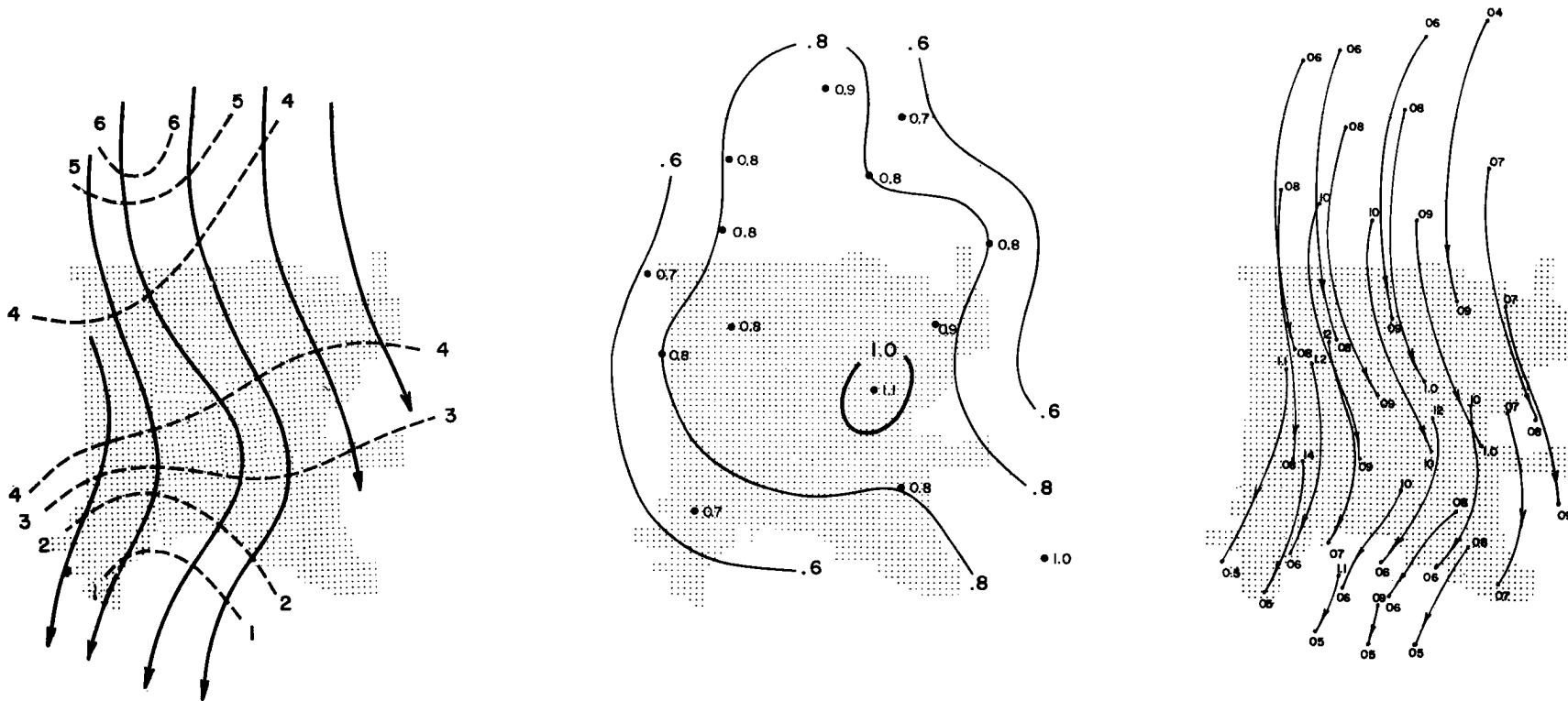


FIG. 37. Wind field on 10 December 1965, 13 MST. Full lines are streamlines; dashed lines are isotachs (mph). COH chart at 13 MST; and the trajectories of air parcels on the same day, 11-13 MST.

230 meters thick with  $\gamma = -2.6^{\circ}\text{C}$ , as may be seen from Fig. 23. Before 11 MST, warming had destroyed the inversion and it had caused free mixing of the air in the vertical. This mixing, together with an increase in surface wind, exported the polluted mass from the city. By noon, the two-hour air parcel trajectories over the city (Fig. 37) had become rather long, indicating the fast movement of air and the dispersion of pollution.

CHAPTER V  
SUMMARY OF RESULTS

In order to evaluate the average advection during the S-SW and N-NE flow patterns, the whole metropolitan area was divided into equal squares with sides of three miles each (Fig. 22). Employing a weighting method, the values of advection were computed. The average values of advection for all S-SW and all N-NE flows were plotted in the center of the corresponding squares. It should be emphasized that the minus sign indicates the region of sources, and the positive sign indicates the transport of polluted air. The average maps show which factor--the advection or the sources--contributed more to the level of pollution in the various parts of the city.

The average of horizontal COH advection during downslope S-SW flow is given in Fig. 38. The maximum of positive advection is found in the southwestern part of the area as it was in the previous examples for S-SW flow (square numbers 13 and 14). In the northeastern part of the city during S-SW flow, one would expect the highest rate of advection since an air parcel passing over the city becomes more and more contaminated from numerous sources located along its route. In spite of this fact, contamination from the local sources on the average exceeds the effect of advection by more than a factor of 10. The frequencies of advected COH for all squares during S-SW flow are given in Table VI.

The values in square numbers 7 and 8 are rather small indicating that the contributions of advection and of local sources to the pollution in this part of the city are the same. In other city regions the average advection in S-SW flow exceeds the influence of local sources by at least five times (Table VI).

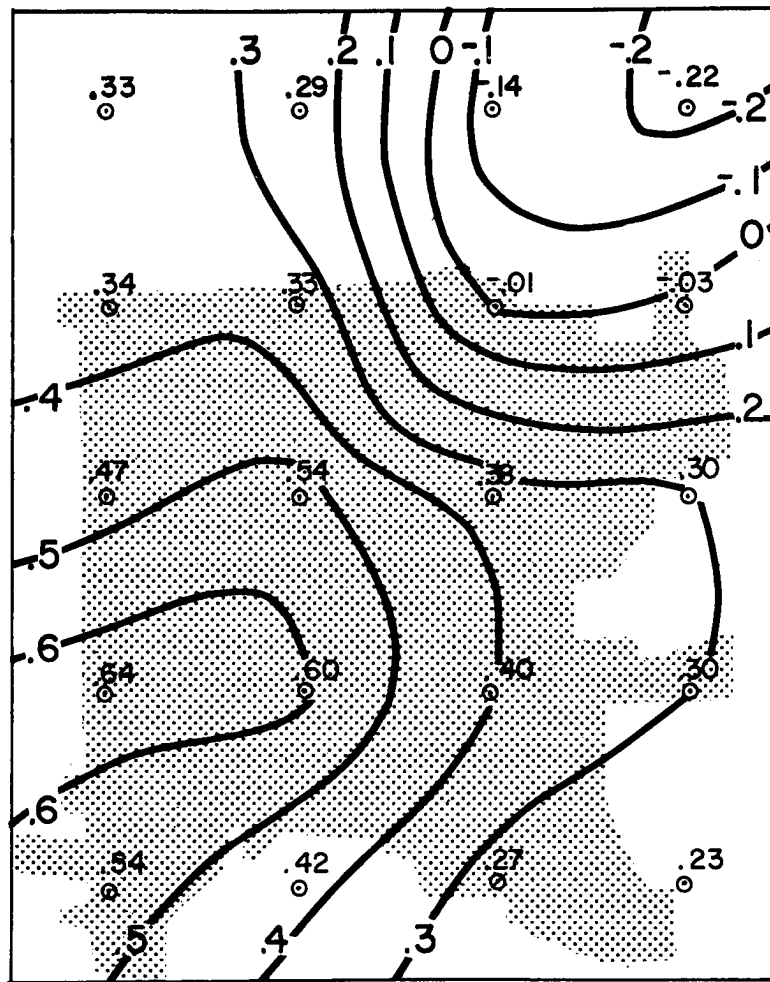


FIG. 38. The average values of COH advection during all cases of S-SW flow.

During N-NE flow a distribution of the average advection occurs over the city opposite to the one observed during a S-SW situation (Fig. 39). In the northeastern part of the metropolitan area, the advection on the average contributed to the contamination more than the local sources do (Table VII, square numbers 1 to 4 and 6 to 8). In the southern part of the city, the influence of the local sources is a little greater on the level of pollution than that of advection. Such values of advection in these two areas are in agreement with the previous examples for N-NE flow. In other squares the average advection is small. It indicates the high rate of alternation between the transport of pollution from adjacent areas and its introduction from local sources.

Such distributions of the average advection during S-SW and N-NE wind patterns require explanations. In the northeastern part of the metropolitan area, along the South Platte River, the alternation of positive and negative advection occurs in connection with the change of flow patterns. Positive values of advection occur during N-NE flow and may be ascribed to the insufficient dilution of polluted air outside the limits of the metropolitan area or to the additional increment of pollution taking place outside the area. However, the N-NE flow prevails during the afternoon when the minimum of COH occurs at stations located in the same region (see Fig. 19). Thus, a cleaner air is brought into the area and causes a decrease of pollution. In spite of such a coincidence, the transport of the polluted matter outward is greater than the local change of COH during the same time as can be seen from Table VIII. This implies that the emission rate of polluted matter into the atmosphere in the northeastern part of the metropolitan area is smaller during the afternoon.

In the southwestern part of the city, the daily maximum of COH occurs during the afternoon when the N-NE flow is prevailing

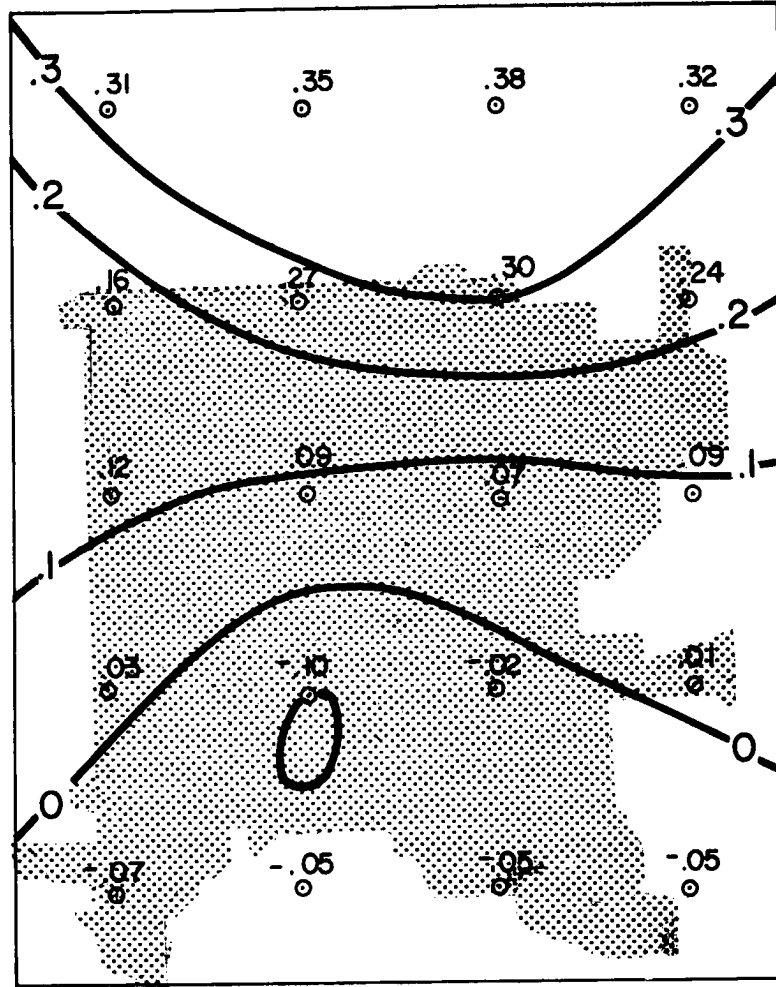


FIG. 39. The average values of COH advection during all cases of N-NE flow.

(see Fig. 19). At the same time, the average value of the advection has a negative sign; i. e., the emission rate of pollutants within the area exceeds the transport of pollutants into it, although the difference between the two is small. Thus, the occurrence of the daily maximum during the afternoon may be attributed to the sources within the area as well as to the advection of pollutants from the adjacent regions.

## CHAPTER VI

### CONCLUSIONS

The horizontal trajectories of the air parcels provide useful information of the movement of the polluted mass over the metropolitan area. A local circulation pattern with a pronounced daily variation exists over Denver during days with air pollution and the influence of the topography on the wind field is dominant. The dispersion of pollutants is reduced due to the light winds and the temperature inversion in the lower layer of the atmosphere.

The daily course of COH has different characteristics in the northern and in the southern parts of the metropolitan area. It depends on the business activity and on the circulation pattern during different times of the day.

The polluted mass of the air follows the horizontal wind field, and it moves along the South Platte River Valley. An air parcel becomes more and more polluted during its progress over the city, but the main increase to its pollution is obtained in the northeastern part of the metropolitan area.

### ACKNOWLEDGEMENTS

The author wishes to acknowledge the guidance and suggestions by Professor Herbert Riehl and Professor Elmar Reiter. He also benefited from discussions with Dr. William Marlatt.

The author wishes to express his appreciation to Mrs. Kosara Markovic and Miss Brana Ckonjevic who drafted the diagrams and to Mrs. Sandra Olson who typed the manuscript.

Valuable computational assistance was obtained through the computer facility at the National Center for Atmospheric Research in Boulder.

TABLE I  
LOCATION OF STATION

Name of Organization	Altitude	
	Ground	Wind Vane
A-1 Northridge Lumber Co. 7900 North Federal Boulevard	5380'	5400'
A-2 Adams City Health Center 4301 East 72nd Avenue	5110'	5135'
A-3 Wheatridge Sanitation District 4900 Marshall	5300'	5315'
A-4 Denver Sewage Treatment Plant 52nd and Downing	5140'	5215'
A-5 Yellow Cab Company 3455 Ringsby Court	5160'	5400'
A-6 Yellow Cab Company 3455 Ringsby Court	5160'	5300' 5200'
A-7 Barteldes Seed Company 3770 East 40th Avenue	5270'	5300'
A-8 Jefferson High School 2305 Pierce Street	5350'	5380'
A-9 Denver School Administration Building 414 14th Street	5225'	5300'
A-10 State Public Health 4210 East 11th Avenue	5310'	5390'
A-11 Hested Store Company 185 South Sheridan Boulevard	5400'	5450'
A-12 Byers Junior High School 150 South Pearl	5285'	5315'

Table I Continued

Name of Organization	Altitude	
	Ground	Wind Vane
A-13 Kunsmiller Junior High School 2250 South Quitman	5460'	5535'
A-14 Overland Golf Course South Santa Fe Drive and W. Jewell Ave.	5250'	5280'
A-15 Denver Research Institute 2050 East Iliff Avenue	5375'	5440'
A-16 Cherry Creek Water and Sanitation District 8501 East Iliff Avenue	5942'	5480'
A-17 Arapahoe County Health Center 4857 South Broadway	5405'	5435'
A-18 U. S. Weather Bureau Stapleton International Airport	5283'	5303'
A-19 Lowry Air Force Base 24th Weather Sqdn.	5385'	5393'
A-20 Buckley Field (Buckley Ang. Base) 140th PAC Ftr. Wg. Weather Section	5660'	5678'
B-1 Federal Center 6th and Kipling	5585'	5660'
B-2 General Chemical Company 1271 West Bayaud	5210'	5280'
B-3 Radio Station KLZ 131 Speer Boulevard	5220'	5280'
B-4(1) Rocky Mountain Arsenal Fire Department Station #1	5265'	5300'

Table I Continued

Name of Organization	Altitude	
	Ground	Wind Vane
B-4(2) Rocky Mountain Arsenal South Gate, W. 56th and Havana	5260'	5310'
B-5 U. S. Weather Bureau 19th and Stout Street (Downtown)	5220'	5300'
B-6 Cherry Creek Dam 3311 South Parker Road	5645'	5660'
B-7 Public Service Co. - Bellview Ser. Center 1800 West Bellview (Bellview at Windermere)		
B-9 Signal Broadcast Production, Inc. 1601 Arapahoe (D and F Tower)	5212'	5536'
B-10 North Denver High School 2960 North Speer Boulevard	5320'	5400'
B-11 Jefferson County Health Center 260 South Kipling	5595'	5615'
B-13 State Game, Fish and Parks Department Irondale Road	5085'	5090'
B-14 Donald N. Livingston 1644 South Ivy Way	5460'	5460'

Table I Continued

	Name of Organization	Altitude	
		Ground	Wind Vane
B-15	Radio Station KIMN 5350 West 20th Avenue	5315'	5340'
B-16	Morey Junior High School 840 East 14th Avenue	5350'	5405'
B-17	Shwayder Brothers 1050 South Broadway	5265'	5300'
B-18	Steverson Atmospheric, Inc. 36th and Syracuse - Stapleton International Airport	5300'	5300'
B-19	Hugh M. Woods Company 5700 North Federal Boulevard	5210'	5220'
B-20	Thornton Fire Station 9471 Dorothy Boulevard	5260'	5272'
B-21	CSU Field Office 23rd and Broadway Streets	5208'	5220'

TABLE II

Days With Air Pollution  
in Denver

Winter

1964-1965	1965-1966
January 20-22	December 6-10
February 1-4	December 16-18
February 8-9	December 27-29
February 16-19	January 5-6
March 25-26	January 12-13
	February 6-7

Table III

Station: Adams City Health Center (u and v components mph)

3 February 1965

Time	Direct'n	Spd.	$u_i$	$u_i - \bar{u}$	$(u_i - \bar{u})^2$	$v_i$	$v_i - \bar{v}$	$(v_i - \bar{v})^2$	Time	Direct'n	Spd.	$u_i$	$u_i - \bar{u}$	$(u_i - \bar{u})^2$	$v_i$	$v_i - \bar{v}$	$(v_i - \bar{v})^2$
0005	0	0	0	-.65	.423	0	-.58	.336	0205	0	0	0	-.25	.063	0	-.01	0
10	0	0	0	-.65	.423	0	-.58	.336	10	0	0	0	-.25	.063	0	-.01	0
15	0	0	0	-.65	.423	0	-.58	.336	15	0	0	0	-.25	.063	0	-.01	0
20	0	0	0	-.65	.423	0	-.58	.336	20	0	0	0	-.25	.063	0	-.01	0
25	0	0	0	-.65	.423	0	-.58	.336	25	0	0	0	-.25	.063	0	-.01	0
30	258	1	.96	.31	.096	.20	-.38	.144	30	0	0	0	-.25	.063	0	-.01	0
35	252	3	2.85	2.20	4.840	.94	-.36	.130	35	0	0	0	-.25	.063	0	-.01	0
40	240	2	1.74	1.09	1.188	1.00	.42	.176	40	0	0	0	-.25	.063	0	-.01	0
45	282	2	1.96	1.31	1.716	-.40	-.98	.960	45	0	0	0	-.25	.063	0	-.01	0
50	0	0	0	.65	.423	0	-.58	.336	50	30	1	.36	.11	.012	-.87	-.88	.774
55	270	1	1.00	.35	.123	0	-.58	.336	55	0	0	0	-.25	.063	0	-.01	0
0100	228	4	2.97	2.32	5.382	2.58	2.00	4.000	0300	330	1	.36	.11	.012	-.87	-.88	.774
05	222	2	1.33	.68	.463	1.49	.91	.828	05	0	0	0	-.25	.063	0	-.01	0
10	222	3	2.01	1.36	1.850	2.23	1.65	2.722	10	0	0	0	-.25	.063	0	-.01	0
15	192	3	.68	-.02	0	2.93	2.35	5.522	15	0	0	0	-.25	.063	0	-.01	0
20	0	0	0	-.65	.423	0	-.58	.336	20	0	0	0	-.25	.063	0	-.01	0
25	0	0	0	-.65	.423	0	-.58	.336	25	0	0	0	-.25	.063	0	-.01	0
30	0	0	0	-.65	.423	0	-.58	.336	30	0	0	0	-.25	.063	0	-.01	0
35	0	0	0	-.65	.423	0	-.58	.336	35	0	0	0	-.25	.063	0	-.01	0
40	0	0	0	-.65	.423	0	-.58	.336	40	0	0	0	-.25	.063	0	-.01	0
45	180	2	0	-.65	.423	2.00	1.42	2.016	45	0	0	0	-.25	.063	0	-.01	0
50	186	1	.20	-.45	.203	.96	.38	.144	50	234	3	2.42	2.17	4.709	1.77	1.76	3.098
55	0	0	0	-.65	.423	0	-.58	.336	55	234	1	.81	.56	.314	.43	.42	.176
0200	0	0	0	-.65	.423	0	-.58	.336	0400	276	2	1.89	1.74	3.028	-.21	-.22	.048
Total			15 65	17.19	21.743	13.93	18.97	21.343	Total			5.94	19.44	9.272	.25	4.351	4.870

1031

Table III

continued

Station: Kunsmiller Jr. High School

3 February 1965

Time	Direct'n	Spd.	$u_i$	$u_i - \bar{u}$	$(u_i - \bar{u})^2$	$v_i$	$v_i - \bar{v}$	$(v_i - \bar{v})^2$	Time	Direct'n	Spd.	$u_i$	$u_i - \bar{u}$	$(u_i - \bar{u})^2$	$v_i$	$v_i - \bar{v}$	$(v_i - \bar{v})^2$
0005	270	1	1.00	.45	.20	0	-2.82	7.95	0205	210	7	3.55	1.87	3.50	6.06	5.12	26.21
10	264	2	1.99	1.44	2.07	.21	-2.61	6.81	10	192	10	1.90	.22	.05	9.81	8.87	76.68
15	216	2	1.18	.63	.40	1.62	-1.20	1.44	15	198	7	2.19	.51	.03	6.65	5.71	32.60
20	228	3	2.23	1.68	2.82	2.01	-.81	.66	20	180	10	0	-1.68	2.82	10.00	9.06	82.08
25	240	1	.87	.32	.10	.50	-2.32	5.38	25	174	7	-.71	-2.39	5.71	6.95	6.01	36.12
30	228	4	2.98	2.43	5.90	2.68	-.14	.02	30	240	3	2.60	.92	.85	1.50	.56	.31
35	198	2	.69	.14	.02	1.90	-.92	.65	35	150	4	-2.00	3.68	13.54	3.46	2.52	6.35
40	180	1	0	-.55	.30	1.00	-1.82	3.31	40	180	3	0	-1.68	2.82	3.00	2.06	4.24
45	210	5	2.55	2.00	4.00	4.33	1.51	2.28	45	180	3	0	-1.68	2.82	3.00	2.06	4.24
50	222	3	2.02	1.47	2.16	2.23	-.59	.35	50	30	3	-1.50	-3.18	10.11	-2.60	-3.54	12.53
55	132	3	-2.23	-2.78	7.73	2.05	-.77	.59	55	270	1	1.00	-.68	.46	0	-.94	.88
0100	180	3	0	-.55	.30	3.00	.18	.03	0300	240	1	.87	-.81	.66	.50	.44	.19
05	66	2	-1.83	-2.38	5.66	-.81	-3.63	13.20	05	210	3	1.50	-.18	.03	2.60	1.66	2.76
10	60	2	-1.72	-2.28	5.20	-1.00	-3.83	14.67	10	330	4	2.00	.32	.10	-3.46	-4.40	19.36
15	138	4	-2.67	-3.22	10.37	2.97	.15	.02	15	324	3	1.76	.08	.06	-2.43	-3.37	11.36
20	150	4	-2.00	2.55	6.50	3.46	.64	.41	20	318	6	4.02	2.34	5.48	-4.46	-5.40	29.16
25	180	4	0	-.55	.30	4.00	1.18	1.39	25	312	4	2.98	1.30	1.69	-2.68	-3.62	13.10
30	180	4	0	-.55	.30	4.00	1.18	1.39	30	318	1	.67	-1.01	1.02	-.74	-1.68	2.82
35	174	6	-.67	-1.22	1.49	5.97	3.15	9.92	35	294	4	3.65	1.97	3.88	-1.69	-2.63	6.92
40	198	5	1.55	1.00	1.00	4.75	1.93	3.73	40	288	7	6.65	4.98	24.80	-2.14	-3.08	9.49
45	180	5	0	-.55	.30	5.00	2.18	4.75	45	282	4	.84	-.84	.71	-3.91	-4.84	23.43
50	240	4	3.46	2.91	8.47	2.00	-.82	.67	50	300	5	4.33	2.65	7.02	-2.50	-3.44	11.83
55	168	7	-1.35	-1.90	3.61	6.87	4.05	16.40	55	312	4	2.98	1.30	1.69	-2.68	-3.62	13.10
0200	210	10	5.02	4.47	19.98	8.65	5.83	33.99	0400	330	2	1.00	-.68	.46	-1.73	-2.67	7.13
Total			13.06	138.02	89.18	67.59	144.04	130.21	Total			40.29	136.94	90.11	22.51	187.30	433.00

TABLE IV\*

The Probable Error in u and V and Check for a  
Gaussian Distribution of the Five-Minute  
Average Wind (Sampling Time 2 Hours)  
3 February 1965

<u>Station</u>	<u>Time (hours)</u>	<u>u</u>	$\frac{+r}{-}u$	<u>v</u>	$\frac{+r}{-}v$	Check Difference**	
Adams City	00-02	.65	.60	.58	.65	.00	.05
Health Center	02-04	.25	.43	.01	.31	.14	.02
Kunsmiller Jr.	00-02	.55	1.33	2.82	1.57	.01	.03
High School	02-04	1.68	1.34	2.92	.94	.03	.21

\* Data From Table III.

\*\* Given in absolute value (see formula 6 on page 33 ).

Table V

The Estimation of the Horizontal and Vertical Gradients of COH ( $\Delta x = \Delta y = 3$  miles)

8 December 1965

Time	10-12			12-16			16-16			16-18			18-20			20-22			22-24			24-02		
	I	II	III	I	II	III	I	II	III	I	II	III	I	II	III	I	II	III	I	II	III	I	II	III
Point																								
1																								
2	.2	1.6	2.70	.3	.5	.34	.0	.3	.09	.8	1.3	2.33	.2	.8	.68	.8	.4	.80	.6	.7	.85	.5	1.1	1.46
3	.6	.8	1.00	.7	.6	.81	.6	.4	.52	.5	.6	.61	.8	.7	1.13	.8	.8	.64	.2	.8	.68	.1	.5	.26
4	1.1	.0	1.21				.6	.3	.45	1.0	.3	1.09				.5	.3	.34	.4	.3	.25			
5										.6	.1	.37												
6	.5	.3	.34	0.2	.7	.53	.1	.2	.05	.2	.2	.08	.0	.9	.81	.3	1.5	2.34	.6	1.1	1.57	.6	.6	.72
7	1.2	.3	1.53	1.0	.6	1.36	.8	.2	.68	.7	.5	.74	1.0	.6	1.36	.7	.4	.65	.3	.4	.25			
8	1.2	.0	1.44																					
9										1.1	.3	1.30												
10	.5	.0	.25	.6	.3	.45	.7	.9	1.30	.4	.3	.25	.2	.2	.08	.4	.6	.52	.3	.6	.45	.3	.3	.18
11	1.0	.4	1.16	.6	.4	.52	.9	.0	.81	1.4	.8	2.70	.7	.2	.53	.2	.9	.85	.6	.3	.45	.3	.2	.13
12																								
13																								
14	.3	.6	.45	.7	.3	.58	.8	.6	.84	.1	1.0	1.01	.4	1.1	1.37	.2	1.4	2.00	.4	.9	.97	.3	.9	.90
15	.4	.6	.52	.3	.4	.25	.4	.5	.41	.7	1.3	2.18	.1	.7	.50	.3	.8	.73	.3	.4	.25	.1	.3	.10
16																								
E			10.60			4.84			5.15			12.66			6.46			8.88			5.72			3.75
Mean			1.06			.605			.57			1.145			.807			.876			.65			.536
$\nabla C$ in $10^{-4}$			1.85			1.40			1.36			1.93			1.59			1.68			1.45			1.32

9 December 1965

Time	02-04			04-06			06-08			08-10			Vertical COH Gradient $\Delta Z = 312$ ft. $\sim$ 100 meters
	I	II	III	I	II	III	I	II	III	I	II	III	
Point													
1													
2	1.0	.3	1.09	.8	.5	.89	.4	.5	.41	.1	1.9	3.62	
3	.2	.7	.53	.8	.8	.64	.3	.5	.34	.9	1.3	2.50	
4	.6	.2	.40	.6	.1	.37	.5	.3	.34	1.0	.5	1.25	
5													
6	.4	1.1	1.37	.7	.8	1.15	.3	.2	.13	.6	.1	.37	8-9 Dec. $\Delta C$
7	.3	.4	.25		.7	.49	.5	.1	.26	.7	.8	1.13	10-12 .2
8													12-14 .4
9													14-16 .2
10	.4	.2	.20	.5		.25	.6	.5	.61	.2	.6	.40	16-18 1.4
11	.6		.36	.4	.2	.20	.5	.2	.29	.6	.2	.40	18-20 1.5
12													20-22 1.5
13													22-24 1.2
14	.3	.9	.90		.6	.36		1.2	1.44	.4	1.1	1.37	24-02 .7
15	.1	.3	.10	.4	.1	.17	.3	.6	.45	.2	.5	.29	02-04 .8
16													04-06 .4
E			5.20			4.52			4.27			11.33	06-08 1.3
Mean			.477			.503			.475			1.26	08-10 .6
C in $10^{-4}$			1.24			1.28			1.24			2.02	Mean 8 5 $10^{-3}$ COH/meter

$I = \Delta Cx$   
 $II = \Delta Cy$   
 $III = (\Delta Cx)^2 + (\Delta Cy)^2$

Table VI

The Frequencies of COH Advection,  $V_h \Delta C$ , During S-SW Flow

Class $V_h \Delta C$	Center $C_i$	Squa re																					
		1		2		3		4		5		6		7		8		9		10			
		$f_i$	$f_i C_i$	$f_i$	$f_i C_i$	$f_i$	$f_i C_i$	$f_i$	$f_i C_i$	$f_i$	$f_i C_i$	$f_i$	$f_i C_i$	$f_i$	$f_i C_i$	$f_i$	$f_i C_i$	$f_i$	$f_i C_i$	$f_i$	$f_i C_i$		
>3	3.2																			1	3.2		
2.5-3	2.7											2	4.4	1	2.2					1	2.2	1	2.2
2-2.5	2.2									1	2.2	3	5.7	1	1.9							4	7.6
1.8-2.0	1.9	2	3.8	1	1.9					1	1.9	2	1.7	1	1.7								
1.6-1.8	1.7			1	1.7					2	3.4	1	1.5							3	4.5	5	7.5
1.4-1.6	1.5	1	1.5		1.5			1	1.5	3	4.5	2	2.6	1	1.3	2	2.6			3	3.9	3	3.9
1.2-1.4	1.3	3	3.9	1	1.3	1	1.3			3	3.9	6	6.6	1	1.1	2	2.2			8	8.8	8	8.8
1.0-1.2	1.1	4	4.4	6	6.6	3	3.3	1	1.1	3	3.3	12	10.8	6	5.4	4	3.6			10	9.0	10	9.0
.8-1.0	.9	8	7.2	12	10.6	1	.9	2	1.8	6	5.4	9	6.3	3	2.1	10	7.0			10	7.0	16	11.2
.6-.8	.7	10	7.0	7	4.9			6	4.2	10	7.0	7	3.5	8	4.0	12	6.0			17	8.5	18	9.0
.4-.6	.5	14	7.0	23	11.5	5	2.5	3	1.5	19	9.0	20	6.0	20	6.0	15	4.5			50	15.0	29	8.7
.2-.4	.3	37	11.1	22	6.6	9	2.7	14	4.2	25	7.5	32	3.2	20	2.0	18	1.8			20	2.0	22	2.2
0-.2	.1	29	2.9	21	2.1	26	2.6	19	1.9	29	2.9	20	2.0	22	2.2	26	2.6			5	.5	14	1.4
-0-.2	-.1	13	1.3	17	1.7	32	3.2	29	2.9	20	2.0	11	3.3	18	5.4	22	6.6			4	1.2	2	.6
-.2-.4	-.3	7	2.1	15	4.5	30	9.0	26	7.8	8	2.4	5	2.5	18	9.0	12	6.0						
-.4-.6	-.5	5	1.5	5	2.5	11	5.5	8	4.0				.7	7	4.9	1	.7						
-.6-.8	-.7			2	1.4	7	4.9	8	5.6	1	.7			1	.9	2	1.8						
-.8-1.0	-.9					6	5.4	3	2.7	2	1.8			2	2.2	4	4.4						
-1.0-1.2	-1.1					1	1.1							1	1.3								
-1.2-1.4	-1.3							2	2.6					1	1.5	1	1.5						
-1.4-1.6	-1.5					1	1.5	5	7.5					1	1.7								
-1.6-1.8	-1.7					1	1.7	3	5.1							1	1.9						
-1.8-2.0	-1.9							1	1.9														
-2-2.5	-2.2							1	2.2				43.8		-1.4		4.1				62.6		71.3
-2.5-3	-2.7																						
<-3	-3.2							1	3.2				.33		-.01		.03				.47		.54
Total			43.9		38.6		-19.0		-29.3		44.6												
Mean			.33		.29		-.14		-.22		.34												

Table VI

continued

Class	Center $\bar{V}_H + \bar{V}_C$	11		12		13		14		15		16		17		18		19		20	
		$f_i$	$f_i C_i$																		
>3	3.2																				
2.5-3	2.7									1	2.8										
2-2.5	2.2								1	2.2											
1.8-2.0	1.9	1	1.9						2	3.8	1	1.9			3	5.7					
1.6-1.8	1.7	2	3.4			2	3.4	1	1.7			1	1.7	1	1.7	3	5.1	2	3.4	1	1.7
1.4-1.6	1.5	1	1.5			4	6.0	1	1.5			1	1.5	1	1.5						
1.2-1.4	1.3	5	6.5	3	3.9	10	13.0	5	6.5	2	2.6	2	2.6	5	6.5	4	5.2	1	1.3		
1.0-1.2	1.1	8	8.8	3	3.3	10	11.0	11	12.1	7	7.7	1	1.1	6	6.6	4	4.4	1	1.1	1	1.1
.8-1.0	.9	6	5.4	7	6.3	19	17.1	20	18.0	6	5.4			18	16.2	6	5.4	3	2.7	5	4.5
.6-.8	.7	14	9.8	12	8.4	22	15.4	18	12.6	10	7.0	16	11.2	20	14.0	19	13.3	10	7.0	6	4.2
.4-.6	.5	21	10.5	27	13.5	19	9.5	23	11.5	30	15.0	25	12.5	21	10.5	26	13.0	19	9.5	20	10.0
.2-.4	.3	21	6.3	26	7.8	29	8.7	30	9.0	39	11.7	29	8.7	26	7.8	27	8.1	35	10.5	32	9.6
0-.2	.1	25	2.5	26	2.6	14	11.4	14	1.4	21	2.1	37	3.7	25	2.5	34	3.4	41	4.1	37	3.7
-0-.2	-.1	19	1.9	19	1.9	4	.4	5	.5	11	1.1	16	1.6	7	.7	6	.6	16	1.6	27	2.7
-.2-.4	-.3	4	1.2	7	2.1			2	.6	3	.9	4	1.2			4	1.2	5	1.5	4	1.2
-.4-.6	-.5	3	1.5	3	1.5					2	1.0	1	.5								
-.6-.8	-.7	3	2.1																		
-.8-1.0	-.9																				
-1.0-1.2	-1.1																				
-1.2-1.4	-1.3																				
-1.4-1.6	-1.5																				
-1.6-1.8	-1.7																				
-1.8-2.0	-1.9																				
-2-2.5	-2.2																				
-2.5-3	-2.7																				
<-3	-3.2																				
<b>Total</b>			49.9		40.3		85.1		79.2		53.2		39.7		72.3		56.1		36.5		30.9
<b>Mean</b>			.38		.30		.64		.6		.4		.3		.54		.42		.27		.23

Table VII  
The Frequency of COH Advection,  $V_h$ -VC, During N-NE Flow

Class $V_h$ -VC	Center $C_1$	Square																			
		1		2		3		4		5		6		7		8		9		10	
		$f_1$	$f_1/C_1$	$f_1$	$f_1/C_1$	$f_1$	$f_1/C_1$	$f_1$	$f_1/C_1$	$f_1$	$f_1/C_1$	$f_1$	$f_1/C_1$	$f_1$	$f_1/C_1$	$f_1$	$f_1/C_1$	$f_1$	$f_1/C_1$	$f_1$	$f_1/C_1$
>3	3.2																				
2.5-3	2.7																				
2-2.5	2.2																				
1.5-2.0	1.9					1	1.9														
1.0-1.5	1.7					1	1.7														
1.4-1.6	1.5			1	1.5			1	1.5												
1.2-1.4	1.3	3	2.9	2	2.4	1	1.3	2	2.6			1	1.3								
1.0-1.2	1.1	1	1.1	3	2.3	4	4.4	2	2.2					2	2.2						
.8-1.0	.9	5	4.5	6	5.4	5	4.5	2	1.8	1	.9	3	2.7	3	2.7	3	2.7	1	.9	1	.9
.6-.8	.7	2	1.4	3	2.1	5	2.5	6	2.5	5	2.5	6	4.2	7	4.9	6	4.2	3	2.7	1	.7
.4-.6	.5	9	4.5	9	4.5	7	3.5	14	7.0	8	4.0	19	5.0	12	6.0	14	7.0	6	2.0	6	4.0
.2-.4	.3	15	4.5	12	3.6	13	2.9	13	2.9	13	2.6	17	3.1	12	2.6	11	2.3	12	2.6	11	2.3
0-.2	.1	17	1.7	16	1.6	17	1.7	13	1.3	10	1.0	15	1.5	10	1.0	17	1.7	12	2.2	21	2.1
-0-.2	-.1	10	1.0	10	1.0	10	1.0	7	.7	10	1.0	9	.9	7	.7	8	.8	13	1.3	11	1.1
-.2-.4	-.3	2	.6	3	.9			3	.9	3	.9	4	1.2	4	1.2	4	1.2	5	1.5	11	2.3
-.4-.6	-.5							3	1.5	1	.5					2	1.0	2	1.0	1	.5
-.6-.8	-.7					1	.7			1	.7							1	.7		
-.8-1.0	-.9																				
-1.0-1.2	-1.1																				
-1.2-1.4	-1.3																				
-1.4-1.6	-1.5																				
-1.6-1.8	-1.7																				
-1.8-2.0	-1.9																				
-2-2.5	-2.2																				
-2.5-3	-2.7																				
<-3	-3.2																				
Total			20.0		22.5		24.7		20.7		9.1		17.7		19.3		15.9		7.9		6.1
Mean			.21		.25		.26		.22		.16		.27		.20		.24		.12		.20

Table VII

continued

Class	Center	11		12		13		14		15		16		17		18		19		20		
		$C_i$	$f_i$	$f_i C_i$																		
>3	3.2																					
2.5-3	2.7																					
2-2.5	2.2																					
1.8-2.0	1.9																					
1.6-1.8	1.7																					
1.4-1.6	1.5																					
1.2-1.4	1.3																					
1.0-1.2	1.1																				1	1.1
.8-1.0	.9																				1	.9
.6-.8	.7	2	1.4	3	2.1	3	2.1			1	.7	2	1.4									
.4-.6	.5	12	6.0	7	3.5	8	4.0	3	1.5	6	3.0	5	2.5	5	2.5	3	1.5	1	.5	2	1.0	
.2-.4	.3	9	2.7	10	3.0	9	2.7	8	2.4	8	2.4	6	1.8	9	2.7	4	1.2	3	.9	6	1.8	
0-.2	.1	17	1.7	26	2.6	11	1.1	13	1.3	15	1.5	21	2.1	18	1.8	21	2.1	23	2.3	16	1.6	
-0-.2	-.1	10	1.0	10	1.0	16	1.6	17	1.7	15	1.5	16	1.6	9	.9	18	1.8	23	2.3	21	2.1	
-.2-.4	-.3	8	2.4	3	.9	14	4.2	17	5.1	14	4.2	11	3.3	16	4.8	14	4.2	9	2.7	15	4.5	
-.4-.6	-.5	5	2.5	4	2.0	3	1.5	4	2.0	4	2.0	3	1.5	3	1.5	2	1.0	4	2.0	3	1.5	
-.6-.8	-.7	2	1.4	1	.7	1	.7	1	.7	2	1.4			3	2.1	1	.7	1	.7	1	.7	
-.8-1.0	-.9																					
-1.0-1.2	-1.1			1	1.1			2	2.2					1	1.1							
-1.2-1.4	-1.3													1	1.3							
-1.4-1.6	-1.5																					
-1.6-1.8	-1.7																					
-1.8-2.0	-1.9																					
-2-2.5	-2.2																					
-2.5-3	-2.7																					
<-3	-3.2																					
Total			4.5		5.5		1.9		-6.5		-1.5		.5		-4.7		-2.9		-3.1		-3.3	
Mean			.07		.09		.03		-.1		-.02		.01		.01		-.07		-.05		-.05	

Table VIII

The Frequencies of COH Advection,  $\bar{V}_h$  VC, in the Northern Part of Denver During N-NE Flow in the Afternoon Hours

Hours $\bar{V}_h$ VC	Square																			
	1					2					3					4				
	11-13	13-15	15-17	17-19	19-21	11-13	13-15	15-17	17-19	19-21	11-13	13-15	15-17	17-19	19-21	11-13	13-15	15-17	17-19	19-21
1.8-2.0												1						1		
1.6-1.8												1						1	1	
1.4-1.6							1					1		1				1	1	
1.2-1.4				1	2			1				1		1				1	1	
1.0-1.2			1				1	1	1			1		2			1	3		
.8-1.0		2	1	1		1	1	2		2		3	2		1	2	1	4	4	
.6-.8		1	1				1	2				2	2	5		1	2	3	3	1
.4-.6	1	2	3	1	1	2	3	1	1	1	2	1	4	5		2	1	3	2	3
.2-.4	3	4	3	1		1	3	1	2		2	1								
0-.2	2	1	4	2	1	2	1	5	3		1	1	13	11	1	6	11	13	9	4
$E_+$	6	10	13	6	6	6	11	13	7	3	6	11	1	1	4		1	1	1	1
-.2-0		1	1	5			1	1	4	2				1			1		1	1
-.4-.2		1		1			1		1	1			2							
-.6-.4																				
-.8-.6		1											1	1	5		2	1	3	2
$E_-$		3	1	6			2	1	5	3		2								

Table VIII  
continued

Hours $\bar{V}_h - VC$	5					6					7					8				
	11-13	13-15	15-17	17-19	19-21	11-13	13-15	15-17	17-19	19-21	11-13	13-15	15-17	17-19	19-21	11-13	13-15	15-17	17-19	19-21
1.8-2.0																				
1.6-1.8																				
1.4-1.6																				
1.2-1.4																				
1.0-1.2																				
.8-1.0				1				2	1				1	2				3		
.6-.8		1	2		2	1	1	4					5	1				3	1	2
.4-.6		3	2	1		1	3	3		1	3	2	4	2		2	1	6	4	
.2-.4	2	2	1	3	1	2	2	2	5	2	1	1	2	6	1			4	3	
0-.2	2	2	5	4		1	4	3	2		1	2	5	2	2	2	1	3	1	3
$E_+$	4	8	10	9	3	4	9	14	8	5	5	12	14	10	3	4	9	14	10	3
-.20	1	3	3	2	3	1	4		3		1	1		1	2	2	3		1	2
-.4-.2	1		1	1		1			1	1				1	1				1	1
-.6-.4		1															1			
-.8-.6		1																		
$E_-$	2	5	4	3	3	2	4		4	1	1	1		2	3	2	4		2	3

REFERENCES

- Colorado State Department of Health, 1961: Denver metropolitan area air sampling survey, 19 pp.
- Conrad, V., and L. W. Pollak, 1950: Methods in Climatology. Harvard University Press, Cambridge, 459 pp.
- Defant, F., 1951: Local winds. Compendium of Meteorology, AMS, Boston, Massachusetts, 655-672.
- Gifford, F., Jr., 1953: A study of low level air trajectories at Oak Ridge, Tennessee. Monthly Weather Review, Vol. 81, No. 7, 179-192.
- Gosline, C. A., L. L. Falk, and E. N. Helmers, 1956: Evaluation of weather effects . . . . in: Air Pollution Handbook by Magill et al., Section 5, McGraw-Hill Book Co., Inc., New York.
- Hess, S. L., 1966: Introduction to Theoretical Meteorology. Holt, Rinehart and Winston, New York, 362 pp.
- Hewson, W. E., 1951: Atmospheric pollution. Compendium of Meteorology, AMS, Boston, Massachusetts, 1139-1157.
- Katz, M., H. D. Sanderson, and M. B. Ferguson, 1958: Evaluation of airborne particulates in atmospheric pollution studies. Analytical Chemistry, Vol. 30, No. 6, 1172-1180.
- Minnesota Department of Health, 1961: An appraisal of air pollution in Minnesota, 69 pp.
- Neiberger, M., 1961: The dispersion and deposition of air pollutants over cities. Air over Cities, R. A. Taft Sanitary Engineering Center, Cincinnati, Ohio, 155-171.
- Neimeyer, L. E., 1960: Forecasting air pollution potential. Monthly Weather Review, Vol. 88, No. 3, 88-96.
- Neuberger, H., H. Panofsky, and Z. Sekera, 1956: Physics of the atmosphere . . . . in: Air Pollution Handbook by Magill et al., Section 4, McGraw-Hill Book Co., Inc., New York.
- New Jersey State Department of Health, 1958: State wide air pollution survey--smoke index. Public Health News, No. 39, 227-242.

- Panofsky, H. A. , and G. W. Brier, 1958: Some Application of Statistics to Meteorology. Pennsylvania State University, University Park, 224 pp.
- Pasquill, F. , 1962: Atmospheric Diffusion. D. Van Nostard Company LTD, London, 297 pp.
- Petterssen, S. , 1956: Weather Analysis and Forecasting (2nd Ed.) McGraw-Hill Book Co. , Inc. , New York, 428 pp.
- Riehl, H. , and L. W. Crow, 1962: A study of Denver air pollution. Atmospheric Science Technical Report No. 33, Colorado State University, 15 pp.
- Sanderson, H. P. , and M. Katz, 1963: The optical evaluation of smoke or particulate matter collected on filter paper. Journal of the Air Pollution Control Association, Vol. 13, No. 10, 470-482.
- Schneeman, J. J. , 1957: The Denver area air pollution problem. U. S. Department of Health, Education and Welfare, Division of Sanitary Engineering Service, R. A. Taft Sanitary Engineering Center, Cincinnati, Ohio, 47 pp.
- Stalber, W. W. , and R. C. Dickerson, 1962: Sampling station and time requirements for urban air pollution surveys. Journal of the Air Pollution Control Association, Vol. 12, No. 4, 170-200.
- Summers, P. W. , 1961: Smoke concentration in Montreal related to local meteorological factors. Air over Cities, R. A. Taft Sanitary Engineering Center, Cincinnati, Ohio, 89-113.
- Thomson, P. D. , 1961: Numerical Weather Analysis and Prediction. The Macmillan Company, New York, 170 pp.
- U. S. Atomic Energy Commission, 1955: Meteorology and Atomic Energy. U. S. Government Printing Office, Washington, D. C. , 163 pp.
- U. S. Department of Health, Education and Welfare, 1962: In quest of clean air for Berlin, New Hampshire. Technical Report A62-9, The Robert A. Taft Sanitary Engineering Center, Cincinnati, Ohio, 47 pp.

DATA PROCESSING TECHNIQUES EMPLOYED  
WITH DENVER AIR POLLUTION  
WIND DATA

by  
William D. Ehrman

ABSTRACT

Machine procedures used in this study are explained in detail, including possible applications of these developed techniques to real time data acquisition and presentation installations.

For all of the Denver pollution periods analyzed in detail in this study, wind direction and velocity strip chart records were available from at least ten metropolitan stations. These charts were reduced to punched cards by an analogue-to-digital converter which digitalized a voltage output from a hand retracing of the original strip chart. The strip chart recorder was set to run at 150 times the original recording speed and five-minute instantaneous wind direction and velocity values were punched on cards.

A computer program mated the separate velocity and direction card decks, took trigonometric meridional and zonal components, and averaged these to output 30, 60, and 120-minute mean directions and velocities. The first year of data was then hand plotted on contour maps of Denver; but as the data reduction procedure became more efficient, a machine plotting capability was developed.

The basic contour map of Denver was traced on Cartesian coordinate paper, and point coordinates of straight line segments approximating the height contour lines were obtained by hand. These coordinates along with coordinates of the recording stations were fed into the National Center for Atmospheric Research Control Data 6600 computer and a series of instructions for a peripheral cathode ray tube plotter were generated to reproduce the original base map along with all permanent headings, such as the map scale, etc. Intermediate output of averaged wind directions and velocities then served as input to this program for all stations operating during a specified time period. Simultaneous sets of readings were then plotted at the station coordinates with an arrow indicating the wind direction. The permanent grid instructions were again sent to the plotter and another set of wind readings were plotted. The cathode ray image was continuously photographed on 35 mm microfilm; and thus, a permanent

record was obtained with microfilm prints being entirely adequate for the further analysis employed in this study (Fig. 1).

The cathode ray plotter produced finished data maps at more than 10 per second of central processor time (including the internal manipulations required to array the data from many stations in corresponding time sequence). An analysis program was also available to draw isoclines, but it was felt that the weak wind fields required human analysis and interpretation. The basic contour program was later used to plot a base map for divergence and vertical motion fields.

With the increasing availability of high speed computers equipped with analogue input channels, a real time data processing center could be established. Simultaneous analogue data from a large network of recording stations could be channeled directly to a computer and gridded. Analyzed output would be immediately available.

DENVER AIR POLLUTION WIND DIRECTIONS AND VELOCITIES

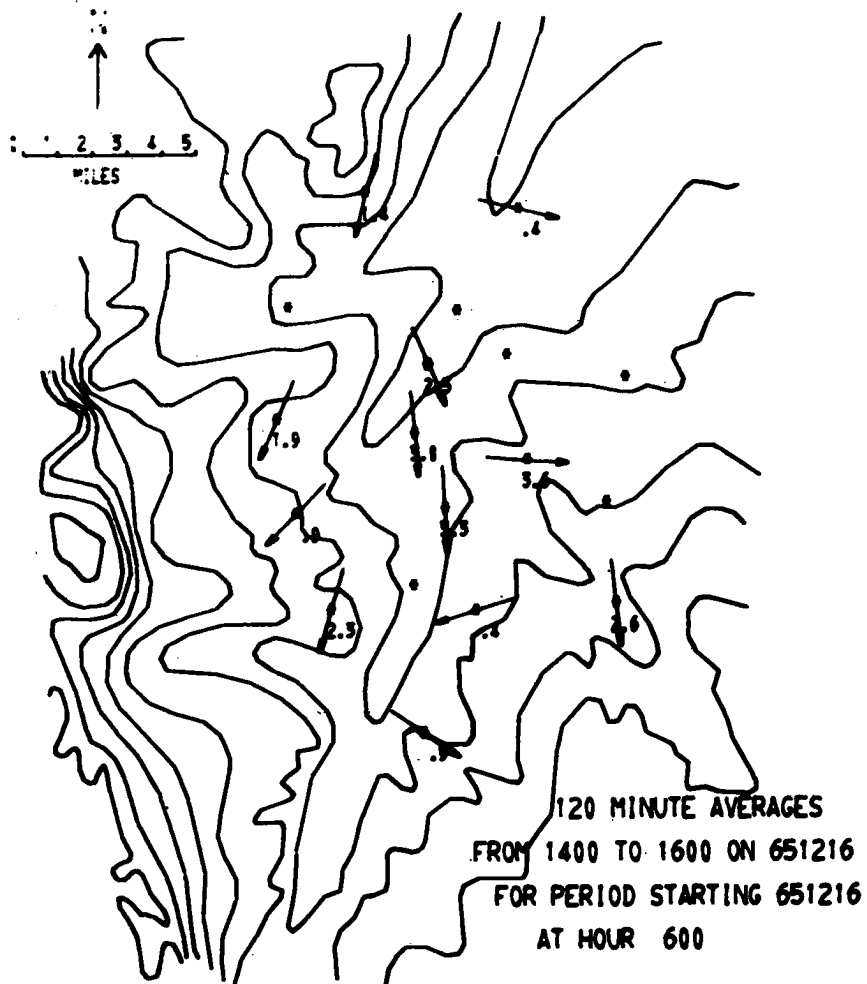


FIG. 1. Topographic contours and other permanent features are plotted from a re-used set of machine instructions. The lower right-hand legend identifies each wind field and its associated direction (arrows) and rounded velocity (digits) plotted at the station coordinate (asterisks).

MICROSCOPICAL ANALYSIS OF SUSPENDED  
PARTICULATES IN DENVER  
AIR POLLUTION

by  
Glenda Swanson

ABSTRACT

Results of microscopical analysis of suspended particulates in the Denver air are discussed. The study was a preliminary one in which to evaluate the feasibility of identification of suspended particulates in situ. The analysis relied on morphological identification and simple chemical microscopical techniques. It was found that wind changes and inversion conditions affect the composition of the sample as well as the size distribution.

## CHAPTER I

### INTRODUCTION

The study of Denver air pollution by Riehl and Crow (1962) clarified the wind patterns governing the pollution mass movement and/or build-up. The question of source contribution, however, remained unanswered. A new study was initiated which included a network of paper tape samplers. The tape sampler is described by Jacobs (1960). A difference in color on the sample spots led the investigators to question the composition of the particulate pollution mass.

A chemical analytical study was initiated for the 1965-1966 pollution season. A simple and direct method of chemical investigation by the use of chemical microscopy (Ferguson and Sheridan, 1966) was adopted. The study was a preliminary one established to check the feasibility of identifying particulates individually as well as pin-pointing source contribution as the pollution mass is built up and moved by meteorological conditions.

## CHAPTER II

### METHODOLOGY

Suspended atmospheric particulates were collected on a 47 mm (960 mm<sup>2</sup> effective area, Millipore ADM-30, 1966) membrane filter, pore size 0.45 micron. The filter was retained in a stainless steel "open-type" filter holder containing a 10 liter per minute limiting orifice. Air flow was provided by a small vacuum pump. The sampling time was varied in the hope of finding a minimum-optimum (in other words, an even distribution without an overlay of particles) distribution on the filter. The first several samples were "over-sampled" or too heavily deposited. As the mounting liquid was applied, the over-layed particles migrated with the flow to the edge of the filter. The geographic location of the sampling sites are shown in Fig. 1.

A polarizing microscope with transmitted illumination was used for analysis and photography. The photographic procedure is described by McCrone (1965). Two exceptions to this procedure were the lack of a tilting stage and the fact that the mounting medium consisted of a refractive index liquid of 1.510. An additional exception is that, although top lighting was used for analysis, the limit of the working distance of the objective would not permit the permanent set-up of top lighting. Ideally, the reflected light should arrive at about a 45° angle; in this case, the angle was changed to about 120°.

Morphological analysis was carried out with a 40X objective N. A. 0.85 (working distance 0.18 mm). The 20X eyepiece contained a Fairs globe and circle reticle (May, 1945) initially. A Whipple Disc was substituted later so that a larger area was analyzed per field, and a more accurate aliquot method was available. Size distribution analysis was performed with a 100X N. A. 1.25 oil immersion

objective and a 12.5X eyepiece. The eyepiece contained a calibrated eyepiece micrometer in which 1 division equaled 1 micron.

A sample slide box of 50 known atmospheric particulates was used for study and comparison (McCrone Associates, 1966).

The membrane filter on which the sample was collected was cut into fourths. Three-fourths of the filter was retained in a plastic Petri dish for future reference. A drop of Cargille refractive index liquid of 1.510 which renders the filter transparent was added to one-fourth of the filter (on a microscope slide), and the preparation completed with a cover slip. As was mentioned previously, the heavily deposited filters had a particle migration problem. A technique of inverting the filter and then adding the liquid was tried but although the particle migration problem was alleviated the distribution still changed. Dr. James P. Lodge of NCAR (Boulder, Colorado) was consulted. He stated that in past work with membrane filters he had noticed an adhesion between particles and the filter which occurs after a brief period of storage. It was his feeling that although the distribution of the over-layed particles changed, those particles in initial contact with the filter would probably remain evenly distributed. The decision was made, therefore, to let the particles migrate as freely as possible as in the first technique.

## CHAPTER III

### ANALYSIS

Martin's diameter of particles was measured for size distribution analysis and about 500 particles were sized (Jacobs, 1960). One of the major interests of particle size distribution has been the effect of aerosols on health. Fig. 2 demonstrates the deposition in lungs by particles of unit density.

Particles greater than 10, or possibly 12, microns diameter are completely retained in the nose or, if the subject is mouth breathing, they do not penetrate below the upper bronchi. Very few particles below  $5\mu$  diameter are retained in the nose, but above this size few are exhaled. Particles of about this size are trapped by sedimentation in the bronchioles and only a very small proportion reach the alveoli. Of the less than  $5\mu$  fraction of the cloud, maximal deposition of particles between  $0.8$  and  $1.6\mu$  diameter occurs in the fine bronchioles and alveoli. About 80% of particles diameter  $0.2\mu$  to  $0.3\mu$  are breathed out again. Below  $0.2\mu$  retention increases again with diminishing size as the effect of Brownian motion becomes predominant (Green and Lane, 1964).

An excellent discussion of systemic effects by aerosols is given by Cadle (1965).

Morphological analysis is based on recognition of characteristic forms, colors, and surface texture of the particles under study (Salzenstein, 1960). The particles were categorized into three classes of probable origin which are as follows:

#### A. Industrial Dusts

1. enamel dust
2. starch grains
3. inorganic fertilizer
4. fiberglass and mineral wool
5. cement dust
6. catalyst dust

7. rubber
  8. calcium carbonate
  9. detergent
- B. Combustion Products
1. coal
  2. cenospheres
  3. cloudy and glassy spheres
  4. iron oxide
  5. oil soot
  6. incinerator fly-ash
- C. Wind Erosion Products
1. quartz
  2. limestone
  3. gypsum
  4. glass
  5. cotton fibers
  6. olivine

The above particulates are only a small fraction of those encountered on a nationwide scale, but they are the main ones present in the Denver air.

As would be expected, the preceding classifications are not rigid. A few examples of the interplay of the particles are as follows:

- 1) Rubber can be from a manufacturer or from automobile tire wear;
- 2) Inorganic fertilizer could be a "wind erosion" product if blown off a lawn;
- 3) Detergent and/or starch grains could be from an incinerator operation;
- 4) Iron oxide could be blown off a rusted object;
- 5) Gypsum is used in the grinding stage of cement manufacture;

- 6) Limestone is a raw material of cement manufacture;
- 7) Olivine is used as a molding sand; however, the crystal habit is different from olivine of natural origin.

Another factor of uncertainty as Salzenstein (1960) states is: "The efficiency of the analyst is proportional to the number of particles seen and retained by the analyst".

Before particle characteristics are discussed, some definitions will be introduced. Almost all particles in air pollution are crystalline in nature; therefore, some of the more basic concepts of crystallography will be presented. Chamot and Mason (1958) explain a crystal form as that which "possesses the internal arrangement throughout its entire extent. Along any random direction through its structure, the atomic arrangement is repeated periodically". The crystal faces are the outer appearance of the inner structure.

There are six crystal systems:

- 1) cubic - one refractive index (n)
- 2) tetragonal - two refractive indices (2n)
- 3) hexagonal and trigonal - two refractive indices (2n)
- 4) orthorhombic - three refractive indices (3n)
- 5) monoclinic - three refractive indices (3n)
- 6) triclinic - three refractive indices (3n)

Extinction (the particle disappears or becomes black against the black background of the crossed polars) occurs when the polarized light vibrates parallel to one of the vibration axes of the crystal.

TABLE I  
CROSSED POLARS

Isotropic, extinguishes (1n)	Anisotropic, extinguishes only certain orientations	
cubic system	Uniaxial (2n)	Biaxial (3n)
glass	tetragonal	orthorhombic
amorphous substances	hexagonal and trigonal	monoclinic triclinic

Fig. 3 shows the approximate per cent of natural occurrence of the crystal systems.

Refractive index ( $n$ ) is the ratio of the velocity of light in a vacuum to the velocity of light in the medium under consideration

$$n_s = c_o / c_s$$

where  $c_o$  is the velocity of light in a vacuum and  $c_s$  is the velocity of light in a substance whose refractive index is  $n_s$ .

The refractive index ( $n$ ) was measured in this study by the application of the Becke method. Usually the substance to be identified is successively immersed in a known refractive index liquid until the substance is no longer visible. In other words, the velocity of light does not change in either medium. Other methods are also available (Allen, 1962).

The Becke line test is the most accurate in the immersion method but it can also be utilized in the case of a single immersion. For instance, the filter is immersed in  $n = 1.51$  liquid to render the filter itself transparent and a change in the  $n$  of the mounting liquid would render the filter only translucent or opaque.

To apply the Becke line test the sub-stage iris diaphragm is stopped down for central illumination (only parallel light rays are used), and the microscope is brought slightly above focus until a halo appears around the particle. The focus is raised slightly from this position. If the halo moves toward the medium, the  $n$  of the liquid is higher than that of the particle. If the halo moves into the particle periphery, the  $n$  of the particle is higher than that of the liquid. The degree of contrast of the particle indicates the amount of difference between the particle and the liquid. This, of course, is only a rough measure of refractive index but few pollution particulates have a definite  $n$  because of the variation in elemental composition. They have a range of refractive indices as a framework for identification along with morphology.

Doubly refractive substances are measured with plane polarized light. The analyzer is inserted (crossed polars) and the stage is rotated until the particle is at extinction (the light is vibrating parallel to one of the mutually perpendicular planes in the crystal or particle). The analyzer is removed and the refractive indices of medium and particle are compared. The stage is then rotated  $90^{\circ}$  and the indices are compared again (Allen, 1962).

More sophisticated tests such as density separations, dispersion staining and microchemistry are available but could not be used for this preliminary study.

Specific descriptions for the particles analyzed in this study of the Denver air are as follows:

A. Industrial Dusts

\*1. Enamel dust is very much like ground glass. It is isotropic and has a refractive index near 1.570. The particulate differs from glass in so far as it has a large percentage by volume of air bubbles and occasionally incorporates some anisotropic material. An example is shown in Fig. 11 at the intersection 7.5 D-E.

2. Starch grains vary in size and shape according to type such as corn, wheat, potato, tapioca, etc. They are recognizable as starch because they display, in an unmistakable fashion, a black cross under crossed polars. Starch from a feed grinding plant often contains spikey fiber-like particles which are the silica cells of the husk. An example of starch grains is seen in Fig. 6 at intersection 7.5 D-E.

\*3. Inorganic fertilizer is white and shows fairly high anisotropy or birefringence. It is an aggregate of many

---

\* Descriptions from the data sheet accompanying the slide box sample set, McCrone Associates, Chicago, Illinois.

small crystals. Potassium chloride (cubic) and ammonium sulfate (orthorhombic, columnar rod-like habit) may be present. An example is in Fig. 9 at intersections 7.5 D-E and 8.5 B. A comment to be added here is that the original photography was done with color film. The black and white renditions do not show good contrast in comparison with color.

\*4. Fiberglass or mineral wool is isotropic with a refractive index of about 1.51 - 1.56. The fiberglass is a smooth, cylindrical fiber whereas mineral wool is less carefully formed. No examples are included in the photographs. The occurrence of these constituents was infrequent when compared to enamel dust and starch.

\*5. Cement particles are an aggregate of small polygonal grains, very highly birefringent and with a high refractive index of about 1.73. An example is seen in Fig. 13 at the intersection mid-point 8.2 C-D.

\*6. Catalyst dust is isotropic. The particles are spherical, ranging in size from 10 - 50  $\mu$ . The particles are yellowish and brown to black after use. Because of the size limitation, it would not be expected to see these particles in the samples from the #3 sampling site. Catalyst dust originates from a refinery operation. Refractive index is about 1.56. An example is seen in Fig. 12 at intersection 2.2 D-E.

7. Rubber is opaque, usually black, when encountered in air pollution work. It exhibits a shape similar to that of eraser waste. It is tested for elasticity by pressing on the coverslip or the particle with a dissecting needle. A probable example is Fig. 15 at intersection 4 B-C.

8. Calcium carbonate is very highly birefringent and has refractive indices of  $\epsilon = 1.53$ ,  $\omega = 1.66$ . The source

can be a paint pigment user or a paper-coating operation (McCrone, private communication, 1966). An example is found in Fig. 5 at intersection 5.5 D.

\*9. Detergent is white by reflected light, black by transmitted light. It is an aggregate of small soap crystals. A strong light source will show the birefringence of the particle. Irregular extinction occurs. In other words, not all of the crystals in the aggregate extinguish at the same time. An example is found in Fig. 17 at intersection 2.2 D. The occurrence of detergent particles was rare because of wind speed and direction, which will be discussed later.

10. Resin or glue is yellowish to gold in color and is transparent. The refractive index is about 1.53. An example is seen in Fig. 14 at intersection 2.5 F.

#### B. Combustion Products

Coal combustion has four main constituents which, when found together, may be used effectively in the identification of industrial pollution by coal combustion processes.

\*1. Bituminous coal fragments are opaque with reddish edges and display conchoidal fracture. An example is shown in Fig. 17 at intersection 3.5 D-E.

2. Cenospheres are formed in the combustion process at the temperature of about  $350^{\circ}$  -  $550^{\circ}$ C. An example is shown in Fig. 15 at intersection 4 D. This is a cenosphere of oil soot; however, the appearance is alike.

3. Cloudy spheres occur when the temperature of combustion reaches about  $1000^{\circ}$ C. Glassy spheres are formed at about  $1100$  -  $1200^{\circ}$ C and are an indication of an efficient burning operation. An example of a glassy sphere is shown in Fig. 16 at mid-point C-D7.

\*4. Iron oxide is red by transmitted light and is a characteristic of pulverized fuel combustion. An example is shown in Fig. 12 at intersection 2.5 B. The particle is elongated and appears black in this photograph.

\*5. Oil soot is highly reflective. At about 200°C the oil droplet darkens to a brown color (example in Fig. 13 at intersections 6.5 C and 3.5 B). Between about 300 - 500°C, the droplet forms a crusty exterior and becomes extremely shiny. Cenospheres are formed at about 400 - 500°C and are hollow spheres (Fig. 15, intersection 4 D). If the particles remain in the stack, they become open and leaf-like with a lacy appearance (Fig. 11, intersections 4 D, 5 C, 9 F, etc.).

\*6. Incinerator fly-ash is difficult to pin-point because of the multitude of combusted constituents. However, paper ash is usually present and is a fibrous particulate. An example of incinerator fly-ash is shown in Fig. 6. At intersection 3 B a particle of unburned paper is shown. The black particles could be oil soot but seem to be of a more greasy nature. Also present in the sample was a wool fiber (not shown) with the same greasy particles adhering to it. As previously stated, incinerator fly-ash is difficult to analyze definitely. The total of the particulates, however, indicates an incinerator operation.

### C. Wind Erosion Products

\*1. Quartz is the most common mineral in the world. It is a hexagonal crystal which shows conchoidal fracture. Under crossed polars it displays low order polarization colors. The refractive indices are  $\epsilon = 1.553$  and  $\omega = 1.544$  (Larsen and Berman, 1964). An example is shown in Fig. 16 at intersection 6 C-D and Fig. 12 at 5 B.

\*2. Limestone or calcite is the second most common mineral in the world. It is a rhombic (trigonal) crystal with twin bands bisecting the acute rhomb angle. It is very highly birefringent and has refractive indices of  $\epsilon = 1.486$  and  $\omega = 1.658$ . The refractive index in the plane of the rhomb face is about 1.53. An example is given in Fig. 8 at intersection 2 E. The crystal is almost at extinction or it would appear much brighter. Fig. 7 shows limestone in its position of brightness at intersection 7.5 B-C.

3. Gypsum is a monoclinic crystal usually displaying oblique extinction under crossed polars. It usually exhibits low order polarization colors. The refractive indices are  $\alpha = 1.520$ ,  $\gamma = 1.530$  and  $\beta = 1.523$ . Crystal habit is a monoclinic tablet with 010 cleavage (Larsen and Berman, 1964). Example in Fig. 12 at intersection 4 B-C.

\*4. Glass is isotropic and displays conchoidal fracture. Its refractive index is about 1.570.

5. Olivine is a pale green mineral of the orthorhombic system. The refractive indices are  $\alpha = 1.653$ ,  $\gamma = 1.689$  and  $\beta = 1.670$ . The crystal habit is equant with 010 cleavage (Larsen and Berman, 1964). An example is shown in Fig. 11 at intersection 5 E-F.

## CHAPTER IV

### DISCUSSION OF RESULTS

The major sampling site was located close to the center of the city of Denver (Fig. 1). The greatest density of potential sources lies in a northerly and northeasterly direction from the sampling site. Located in this area are pulverized-fuel users, refinery operations, ceramic tile manufacturers, feed processing operations, fertilizer plants, paint manufacturers, oil combusters, and paper processing plants.

Directly west of the site is located a detergent manufacturer. Fuel usage is low by comparison to the north. Brewery operations and bookbinders lie in a southwest direction.

The southern part of the area contains a larger proportion of ceramic tile manufacturers and feed processors. Some paint manufacture and oil usage are located here.

The easterly direction contains oil users. The proportions of industrial operations are small compared to the other directions (Fig. 1).

A report by Schueneman (1957) estimated about 433,000 tons of coal used in the greater Denver area in 1956. On the average, about 200 pounds of solids are emitted per ton of coal burned. From this estimate alone, one would expect a high proportion of coal fragments, glassy spheres, and iron oxide in the Denver air. Petroleum fuel usage was pro-rated to be 1,508,000 barrels in 1956. Particulate emissions are about 0.5 pounds per ton of fuel burned depending on the variable of combustion efficiency.

The results of particulate morphological analysis are shown in Table II.

The meteorological condition on 5 January 1966 over Stapleton Airfield indicates an inversion in the lower layer of the atmosphere ( $\gamma = -2.3^{\circ}\text{C}/100\text{ m}$  with the upper winds at 1 - 5 mph at 6,000 - 7,000

TABLE II

Wind influence during sample collection and percentages of combustion products, industrial dust, and wind erosion product constituents in samples

Location of Sample Collection	Sample Number	Date	Start Stop		Wind Speed		Wind Direction			% of Combustion Products		% of Industrial Dust		% of Wind Erosion Products		
					Mph Before Change	Time of Change	Mph After Change	Degrees Before Change	Time of Change	Degrees After Change	Certain	Uncertain	Certain	Uncertain	Certain	Uncertain
Site #3	1	1/5/66	0916	1012	1			340			80	0	0	18	2	0
Site #3	2	1/5/66	1019	1115	1	1105	3	340	1105	210	82	0	0	6	6	6
Site #3	3	1/5/66	1120	1220	1	1155	4	210	1155	320	75	0	21	0	2	2
Site #3	4	1/5/66	1225	1321	4			320			50	0	9	41	0	0
Site #3	5	1/6/66	0752	0848	2			180			62	0	28	0	10	0
Site #3	6	1/6/66	0850	0946	1			210			61	0	29	0	10	0
Site #3	7	1/6/66	0955	1052	2	1035	7	160	1035	275	89	0	0	5	0	5
Site #3	8	1/6/66	1055	1151	10			275			72	0	17	0	10	0
Site #3	9	1/18/66	0924	1020	2			170			58	0	25	3	0	13
Site #3	10	1/18/66	1030	1225	2			170			63	0	37	0	0	0
Site #3	11	1/18/66	1230	1326	1			180			48	0	48	0	0	4
Site #3	12	1/22/66	1245	1342	4			330			66	0	34	0	0	0
Site #3	13	1/22/66	1342	1438	4			330			64	0	32	0	4	0
Site #3	14	2/23/66	0910	1110	4			140			73	0	26	1	2	0
Site #3	15	2/23/66	1115	1710	5			160			24	42	29	0	5	0
Site #3	16	3/23/66	0900	1100	3	1030	5	130	1030	160	78	7	15	0	0	0
Site #3	17	3/23/66	1100	1300	5			100			84	8	5	0	3	0
Site #3	18	3/23/66	1300	1500	3			140			76	2	12	0	10	0
Site #3	19	3/25/66	0830	1030	1	0855	2	100	0855	330	45	37	14	0	5	0
Site #2	20	1/6/66	1104	1132	10			275			41	0	50	0	9	0
Site #1	21	1/6/66	1201	1229	10			275			24	0	55	0	21	0

feet). Under such conditions a fanning (Fig. 4) of the industrial plume is to be expected. A breaking of the inversion occurred in the afternoon hours. The abrupt change in the nature of the samples taken on this day, however, indicate that the break-up over the city occurred about noon.

Sample #1 is pictured in Figs. 5 and 6. The particulates are large agglomerates differing from those in succeeding samples. The particles at intersection 7 C (Fig. 6) exhibiting the black cross are starch grains. The black particles could be oil soot but the coating action they exhibit indicates that the particles were burned together in an incinerator. Located at intersections 5 G, 8.5 C, 7.5 E, and 5 A are limestone. Fig. 5 shows some long chain aggregates (4 D, 4 F, and 8 C). These chains of carbon particles are indicative of a low temperature combustion operation (Green and Lane, 1964) such as an incinerator.

The column of industrial dust for Sample #1 indicates the problem of classification of starch grains. It is most likely that the starch grains were from the incinerator operation, thereby making the combustion product a total of 98%. Size distribution (Fig. 19) for this sample differs from succeeding samples collected at Site #3, although it is still within the limits found by other investigators: "The size of particles in outdoor air is below  $2\mu$  with nearly all particles below  $1.6\mu$ . Most particles are in the 0.3 to 1.1 range with the median being 0.5 (Bloomfield), 0.6 (Ives, et al.), and 0.7 (Siegal and Feiner)" (Jacobs, 1960). No attempt was made in this study to differentiate between 0.5, 0.6, and 0.7 particles. The sizing was based on a distinction between those particles that were approximately one-half a division and those that were one division as measured with the eyepiece micrometer. The remaining particles were sized by one division increments; i. e., 2, 3, 4, and 5.

Sample #2 was collected at a time when the wind reversed direction. Little change in the sample is expected because only the

last ten minutes of sampling was affected. A photograph of Sample #2 is seen in Fig. 7. The large particle at intersection 3 E is similar to those seen in Sample #1. The sample is very much like Sample #1 in that it is largely constituted of incinerator fly-ash. The uncertainty columns of Industrial Dusts and Wind Erosion Products result from the problems of starch and limestone classifications, respectively. A plot of size distribution for Sample #2 is shown in Fig. 19.

Sample #3 was collected while wind speed and direction were changing. Present still is resin (intersection 5.5 A, barely discernible), starch grains (1.5 B), oil soot (8 D-E and 9 B-E). A cotton fiber is located at intersection 4.5 E-F. The particle at intersection 6 D-E seems to be of a biological nature (insect parts, 40% certainty). Located at intersection 4 C is a particle of weathered enamel dust. The increase in industrial dust is probably due to the duration of the SSW wind which had traveled about one mile during the sampling time. The industries are located at about one mile from the site. The increased wind speed of the NW wind carried in the industrial dust from the NW direction (enamel dust, starch, oil soot). Iron oxide was present in the sample as well as glassy spheres and coal fragments (not pictured). The size distribution shown in Fig. 19 is very similar to Sample #2.

Sample #4 exhibits a large change in distribution of constituents. An explanation for this change could well be that the inversion is beginning to break. A looping condition of the plume is to be expected as the instability of the atmosphere increases. The sample is not pictured here. The filter was almost clean. The sample contained starch grains, enamel dust, and pulverized fuel constituents (coal, glassy spheres and iron oxide). The size distribution is shown in Fig. 19. One would expect an increase in the larger sizes because of the looping condition of the plume and this does occur as indicated by the graph.

An inversion condition ( $\gamma = -4.3^{\circ}\text{C}/100\text{ m}$ ) existed in the morning of 6 January 1966. The COH (coefficient of haze) value during the time period 0800 - 1000 was 2.8 at site number 3. During the preceding night, the average wind along the river valley was south at two mph. Sample #5 is pictured in Fig. 9. The particles at intersections 3.5 B-C, 5.5 E are calcium carbonate. An iron oxide particle is located at intersection 3 E-F. Located at intersection 1.5 C-D is a glassy sphere. The black particles are for the most part oil soot except at intersections 6.5 B-C and 6 D which are coal fragments. Starch grains are located at intersections 2.5 E-F and 5.5 C-D. Enamel dust and quartz are also present. Sized distribution is shown in Fig. 20. The wind pattern change at the collection time of Sample #6 seems to have had little effect on the constituent distribution of the sample. (Most probably because of the similarity of industry.)

A photograph of Sample #6 is pictured in Fig. 10. Particles of calcium carbonate are located at intersections 5.5 F, 2 A, 2 D, 2 E, and 4 F. A particle of detergent is located at 6 E-F. At intersections 3.5 D-E, 5 D, and 3.5 C-D are quartz particles. The black particles are again largely oil soot. At intersection 2.5 F is a fairly large glass sphere which is most probably a dust of a ceramic industry (70% certainty). Size distribution is shown in Fig. 20.

Sample #7 is pictured in Fig. 11. The most probable explanation of the increased size and change in constituent distribution is the wind speed. The particles were probably a settled dust and were re-entrained by the wind. The black particles in Fig. 11 are oil soot except at intersection 7 B where two coal fragments are located. Calcium carbonate is found at intersections 6 E, 5.5 C-D, and 4.5 E-F. Located at the intersections 6 F, 3 C, 3 E, and 6 D are enamel dust. One cement particle is located at intersection 8 C-D. Quartz particles are located at 4.5 F, 8 D-E, and 3 D. A plot of size distribution is shown in Fig. 20.

The influence of the west wind begins to level off in Sample #8 (Fig. 15). The percentage of combustion products has decreased with an increase of industrial dust and wind erosion products. Starch grains (black cross) are present in Fig. 12. A particle of resin is located at intersection 4.5 D (barely discernible). The spherical particle at 2.5 D-E is brown in color and could be a particle of catalyst dust. Limestone or calcium carbonate is located at intersections 8 D, 3.5E, 5.5 B-C, and 1.5 B-C. Gypsum is located at intersections 3 B and 2 D. A particle of iron oxide is located at intersection 2.5 B-C. The black particles are mainly coal fragments except at intersections 5 B-C and 2.5 E which are probably oil soot. Detergent particles are located at intersections 3.5 D-E and 6.5 F. The COH value at this time has decreased to 1.3. Size distribution is shown in Fig. 20.

The relatively weak inversion ( $\gamma = -1.7^{\circ}\text{C}/100\text{ m}$ ) which existed in the early morning hours of 18 January 1966 was broken at 1100 with a super adiabatic lapse rate of  $\gamma = 2.9^{\circ}\text{C}/100\text{ m}$ . The relatively fast change from inversion to super adiabatic condition indicates that heating was pronounced in the morning hours. Atmospheric instability in the lower layer increased steadily as the samples were collected. A looping condition of the plume is expected under the condition of atmospheric instability. It is expected that the denser particles settled in greater proportions with the looping condition. The light winds prevailing at this time would inhibit transport of the particulates as well. Little change is noticed in the combustion product distribution but the industrial dusts increase by 10% in each succeeding sample.

Figs. 13 and 14 are photographs of Sample #9. The particles present in Fig. 14 are as follows: At intersection 2.5 mid-point E and F and 7 mid-point D and E are resin or glue (75% certainty). They are barely discernible in the black and white rendition but appear as yellow spheres in color. Intersections 2 mid-point B and C,

9 A, 5 mid-point D and E, 8 mid-point A and B are particles of limestone. Located at intersections 2 F, 7 E-F, and 1 B are oil soot particles (90% certainty). Intersections 9 C-D and 9 D-E are coal fragments. A starch grain is located at 8 B-C.

Also present in the sample (Fig. 13) are oil spheres burned to about 200°C and emitted from the stack. Samples collected on this day were the only ones in which this particular phase of oil combustion was found; the reason for this is probably because the particles are relatively dense and usually settled out sooner in a fanning or fumigation condition. The uncertainty column for wind erosion products is a result of the problem of limestone or calcium carbonate classification. It is most likely that the limestone is an industrial dust. Particle size distribution is shown in Fig. 21.

Sample #10 is shown in Fig. 15. The cenosphere and sphere located at intersection 4 D are oil soot. The elongated particle at intersection 4 B could be rubber or oil soot. The particle could not be tested for elasticity with a dissecting needle because the membrane filter had a cushioning effect. A micro-manipulator was needed for confirmatory tests. The particle located at intersection 3.5 F is cement (75% certainty). A particle of resin is partially covered by the elongated particle at intersection 3.5 D. Particle size distribution is shown in Fig. 21.

The constituents of Sample #11 were largely enamel dust and pulverized fuel fly-ash. The particles shown in Fig. 16 are as follows:

Starch	7.5 E, 7.5 A-B
Glassy spheres	7 C-D
Resin	6 F
Coal fragments	4.5 D, 7.5 C, 7.5 C-D
Oil soot	6.5 A-B
Rubber (50% certainty)	3 D-E

Calcium carbonate	5.5 E-F
Quartz	6 D
Olivine	5 E-F

The transparent, low contrast, particles are, for the most part, enamel dust. Size distribution is shown in Fig. 21.

Atmospheric stability data for 22 January 1966 were not immediately available. Sample #12 is shown in Fig. 17. The particles shown in this figure are as follows:

Calcium carbonate	2 E, 2.5 C-D
Coal	3.5 D-E, 2 D-E
Oil soot	2 C-D, 2 D, 3 D
Starch	2 D-E
Enamel dust	2 F, 2 A-B, 2.5 D, 3 C-D

Glassy spheres were also present but are not included in the photograph. Size distribution is shown in Fig. 22.

The photograph (Fig. 18) of Sample #13 shows an unusual particle at intersection 5 E-F. It is probably a sphere of enamel dust which was coated with oil soot while still in the cooling process. A particle of limestone or calcium carbonate is located at intersection 3 D. Oil soot particles are located at intersection 4 D. Again glassy spheres and coal fragments were present but not included in the photograph. Size distribution of Sample #13 is shown in Fig. 22. The major constituents of Sample #14 (not shown) were pulverized fuel fly-ash, especially glassy spheres and enamel dust.

No example is given of Sample #15. The sample was very similar to Sample #14 except that quartz particles began to appear.

An inversion condition with a depth of 120 meters and  $\gamma = -3.3^{\circ}\text{C}/100\text{ m}$  existed on 23 March 1966. At 1100 a super adiabatic lapse rate of  $\gamma = 1.8^{\circ}\text{C}/100\text{ m}$  was present. This situation again, as on 18 January 1966, caused instability of the atmosphere

(looping of the plume). The high occurrence of combustion products as opposed to industrial dust cannot be explained. The samples contained some calcium carbonate and enamel dust, but the greatest proportion of constituents were tiny black particles whose characteristics were difficult to resolve. The sample collected on 25 March resembled closely the 23 March samples. Size distribution for Sample #19 is shown in Fig. 23.

Samples # 20 and 21 were collected at different sampling sites from previously discussed samples. Sample #20 was collected at site #1 and Sample #21 at site #2. Site locations are shown in Fig. 1. The sample constituents changed quite drastically from site #3 samples. The two factors of change are the influence of wind and a change of sampling location. As can be seen from the map, the combustion processes in these locations are few. The combustion particles were very small but glassy spheres were present which indicate some pulverized fuel usage. The major constituents were enamel dust and catalyst dust (60% certainty) in the industrial classification. Quartz and gypsum were present in wind erosion products. A sharp change in particle size distribution is demonstrated by Sample #21 (Fig. 24). The sampling personnel related the information that a street cleaning truck had preceded the sampling unit. Because of this similarity in location and wind factors of Samples # 20 and 21, the change in size distribution is most likely due to the street cleaner.

## CHAPTER V

### CONCLUSIONS

The differentiation of particulates on a morphological basis was surprisingly successful. Generalized source contribution was identified; i. e. , combustion product as opposed to industrial dust or wind erosion products. The microscope has fulfilled its role as a survey tool but for the pin-pointing of source contribution, it must be converted to an analytical tool by the use of accessories such as a hot stage and a micro-manipulator. The single most useful process to be used would be the removal of the particulates from the filter media. The problem of the refractive index range (the most common substances show low contrast) would be alleviated. Also, more sophisticated tests, such as density separations, could be used.

In order to establish the contribution of various sources to the air pollution problem in Denver, it would also be valuable if sampling sites and meteorological stations could be moved more easily and could be deployed along the periphery of suspected pollution sources.

### ACKNOWLEDGEMENTS

The author wishes to thank the personnel of the training section of the Robert A. Taft Sanitary Engineering Center, Cincinnati, Ohio, and Dr. Walter McCrone of McCrone Associates, Chicago, Illinois, who sponsored and taught the course on Microscopic Analysis of Atmospheric Particulates.

Grateful acknowledgement is also given to Dr. James P. Lodge, NCAR, Boulder, Colorado, for many helpful suggestions on microscopic technique.

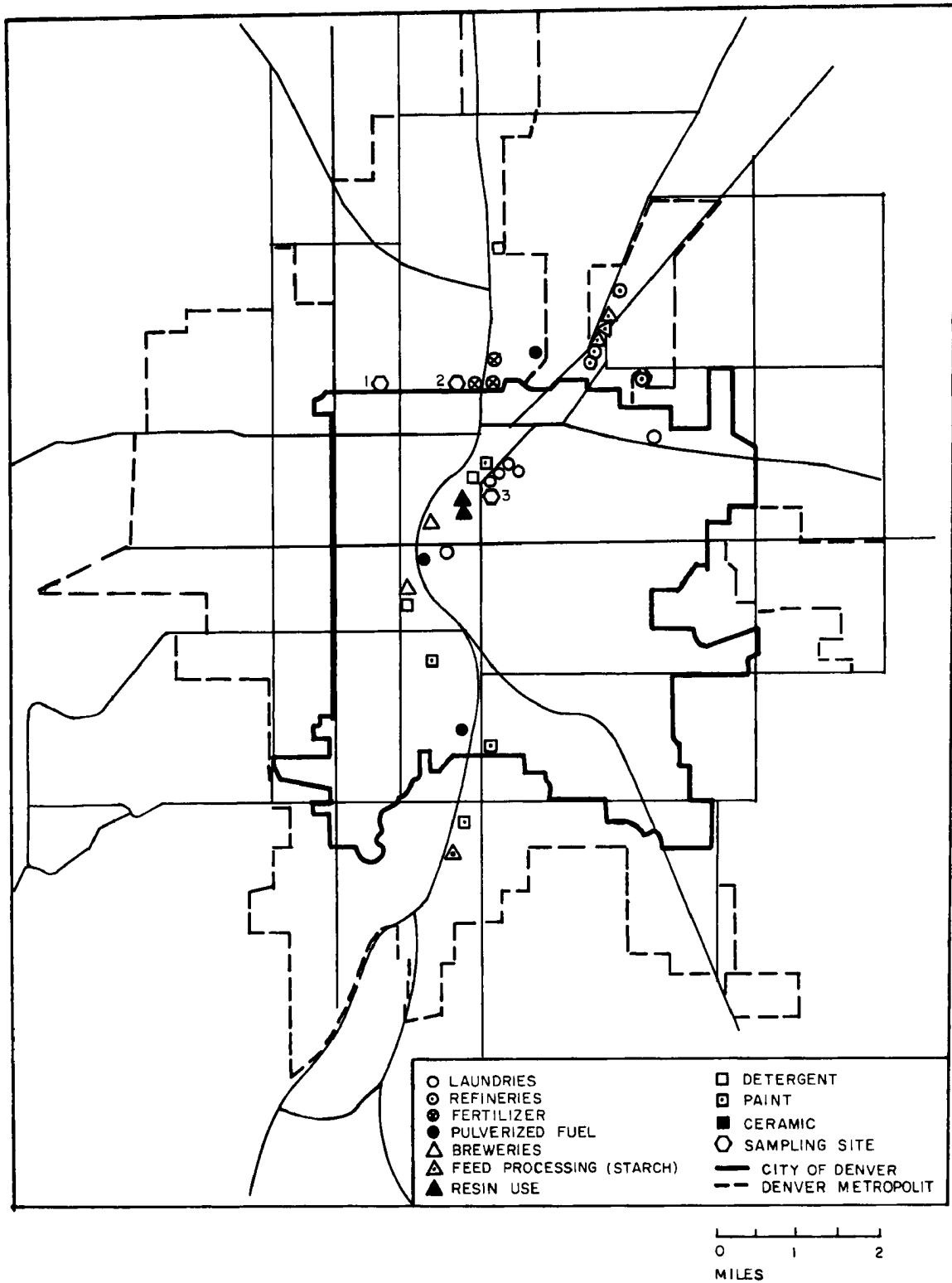


FIG. 1. Map of the Denver metropolitan area. Approximate locations of industries are given. The data of industrial location was incomplete; therefore, the map is only an indication of industrial type differences according to wind direction.

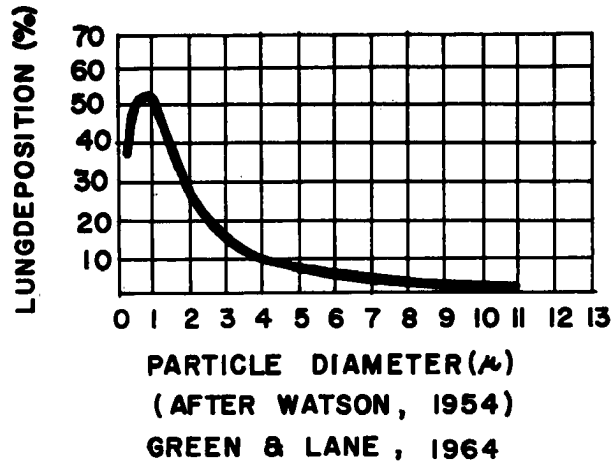


FIG. 2. Curve for deposition in the lungs of particles of unit density.

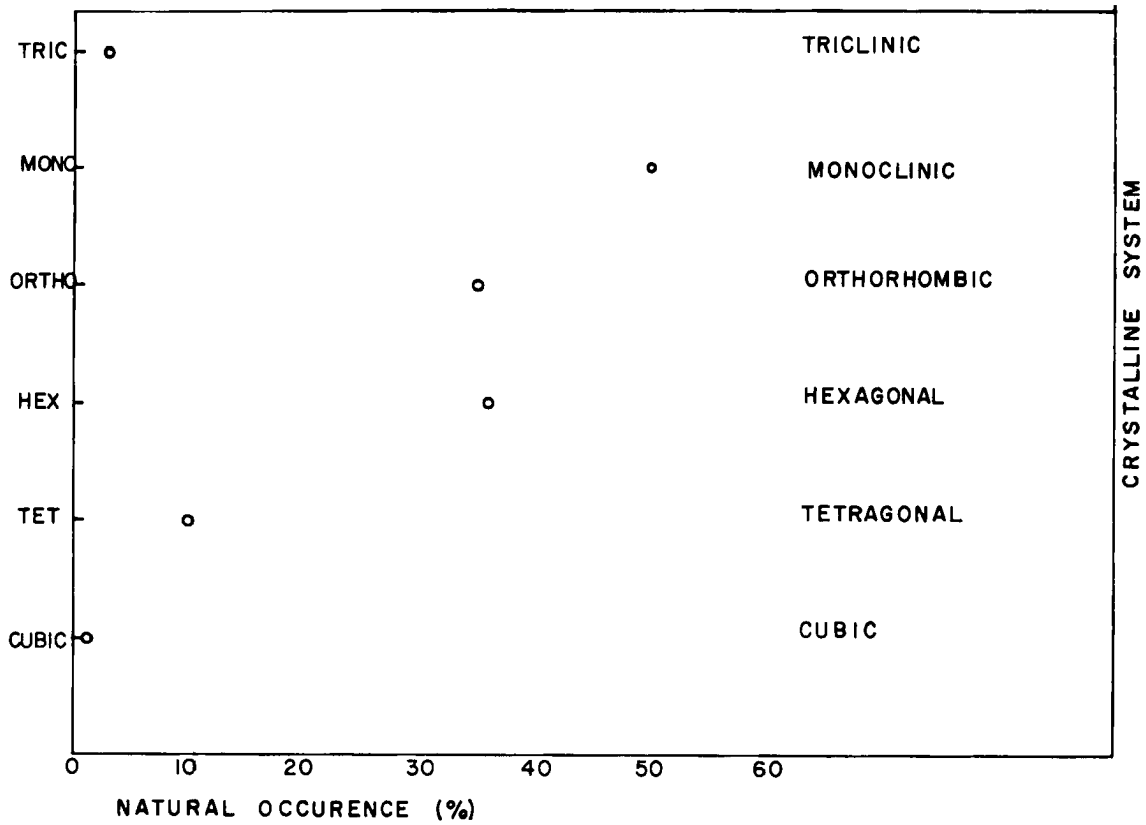


FIG. 3. Approximate percentage of natural occurrence of the crystal systems.

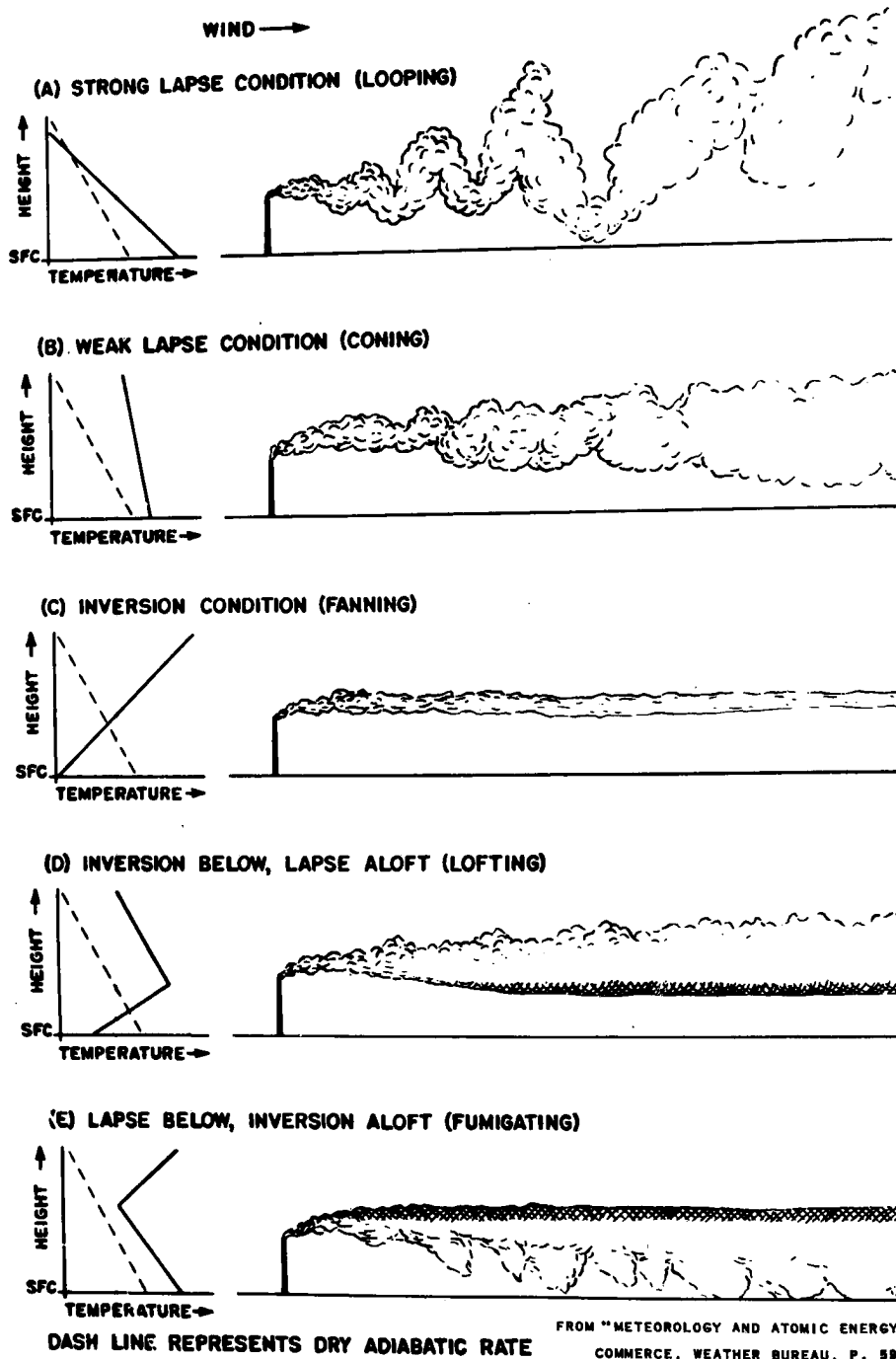


FIG. 4. Schematic representation of stack gas behavior under various conditions of vertical stability.

Photomicrographs of samples collected on membrane filters during the day of 5 January 1966. Location of individual particulates by intersections of alphabet and numerals.

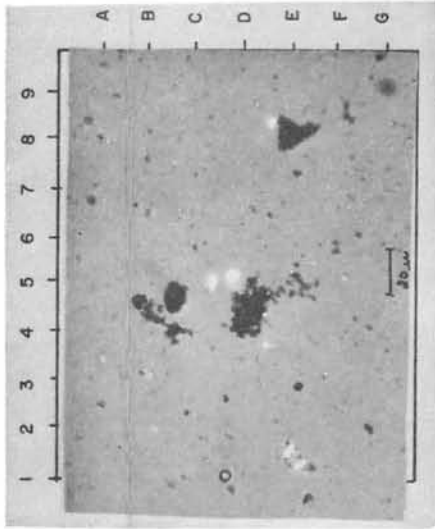


FIG. 5. Sample No. 1,  
Collected from 0916-1012.

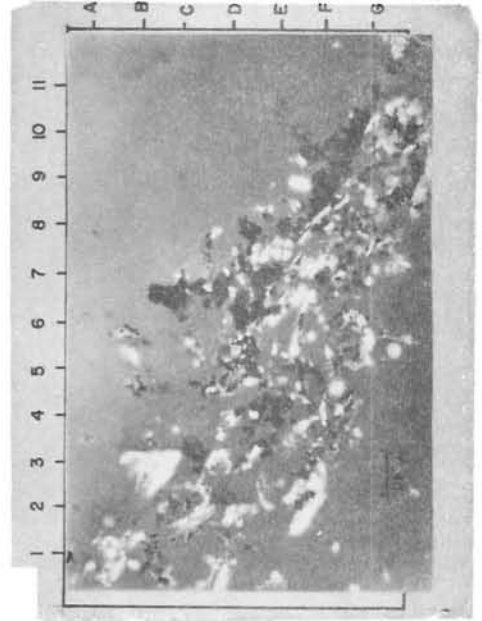


FIG. 6. Sample No. 1.  
Different field of view.

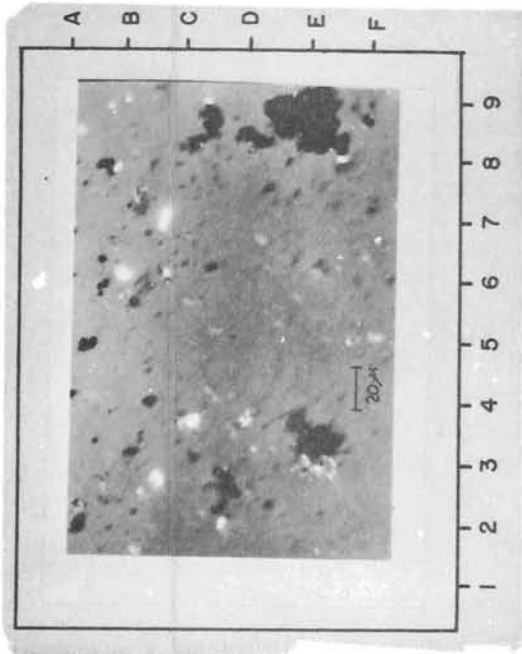


FIG. 7. Sample No. 2.  
Collected from 1019-1115.

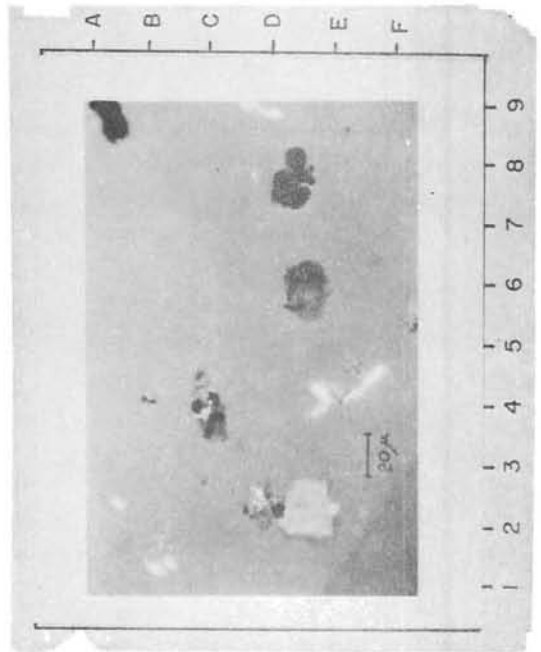


FIG. 8. Sample No. 3.  
Collected from 1120-1220.

Photomicrographs of samples collected on membrane filters during the day of 6 January 1966 at Site #3.

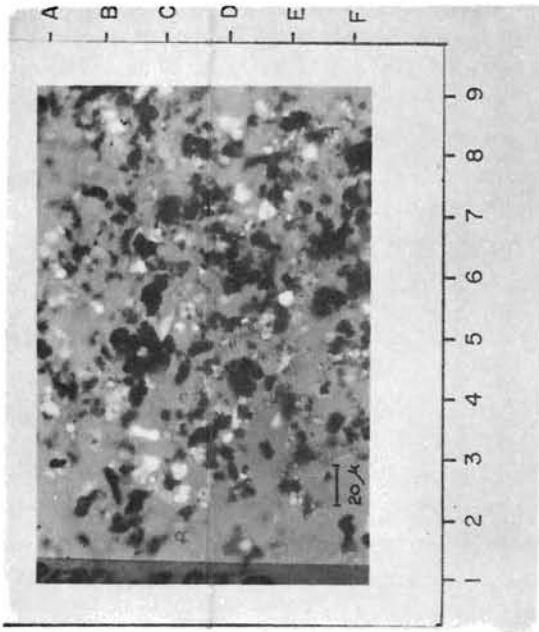


FIG. 9. Sample No. 5.  
Collected from 0752-0848.

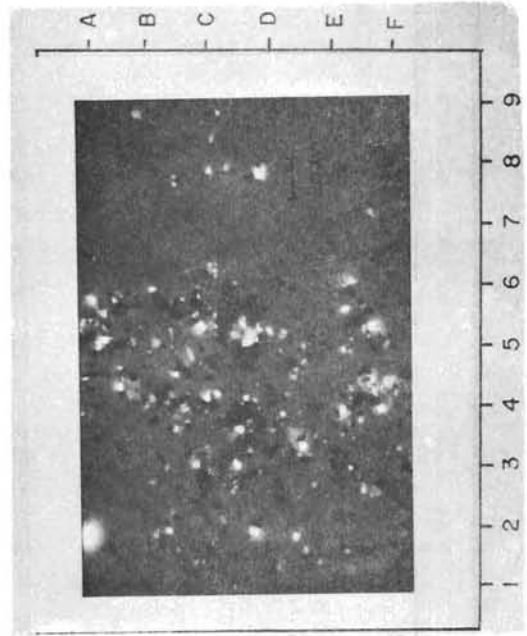


FIG. 10. Sample No. 6.  
Collected from 0850-0946.

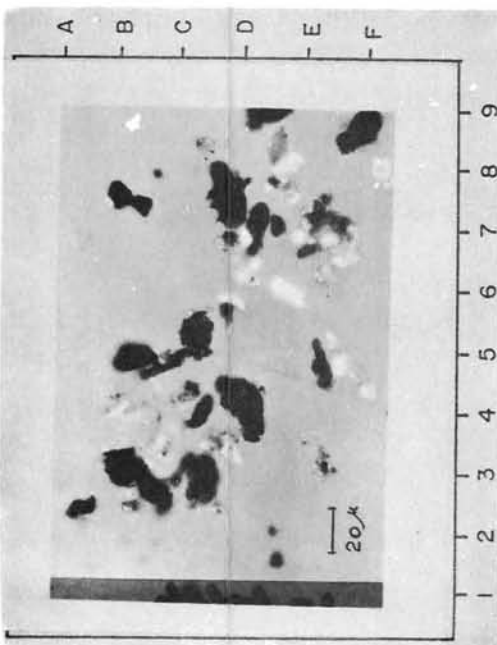


FIG. 11. Sample No. 7.  
Collected from 0955-1052.

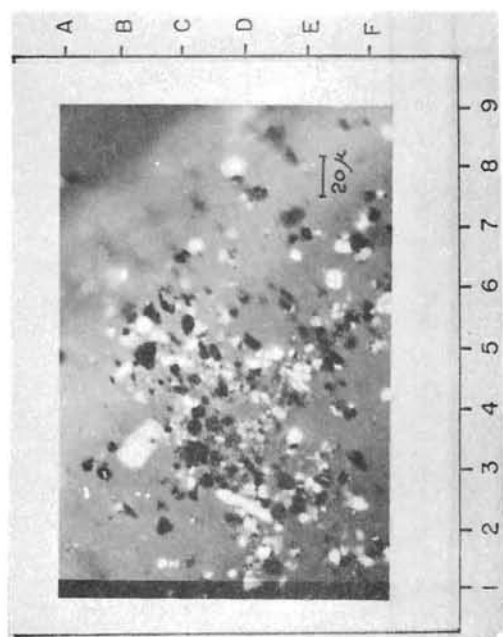


FIG. 12. Sample No. 8.  
Collected from 1055-1151.

Photomicrographs of samples collected on membrane filters during the day of 18 January 1966 at Site #3.

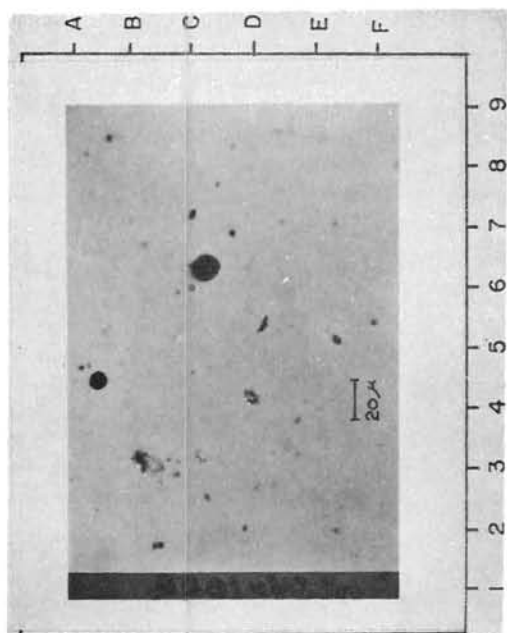


FIG. 13. Sample No. 9.  
Collected from 0924-1020.

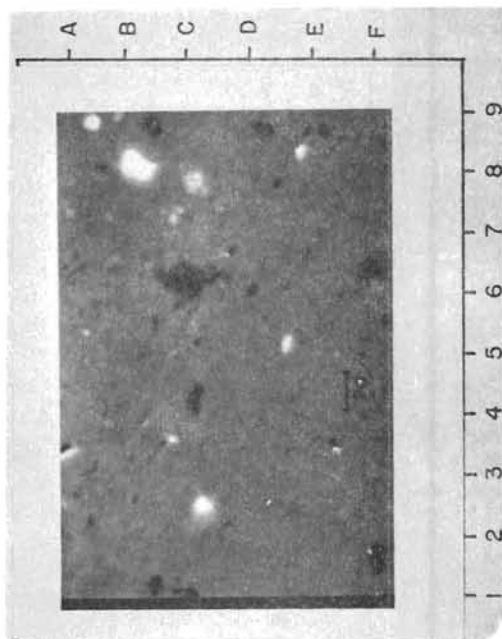


FIG. 14. Sample No. 9.  
Different field of view.

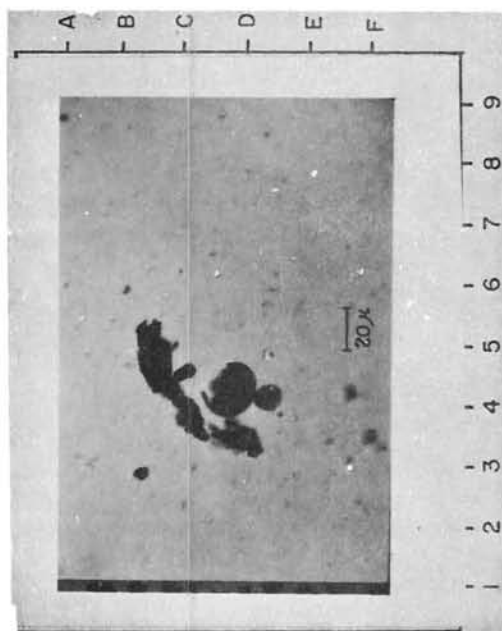


FIG. 15. Sample No. 10.  
Collected from 1030-1225.

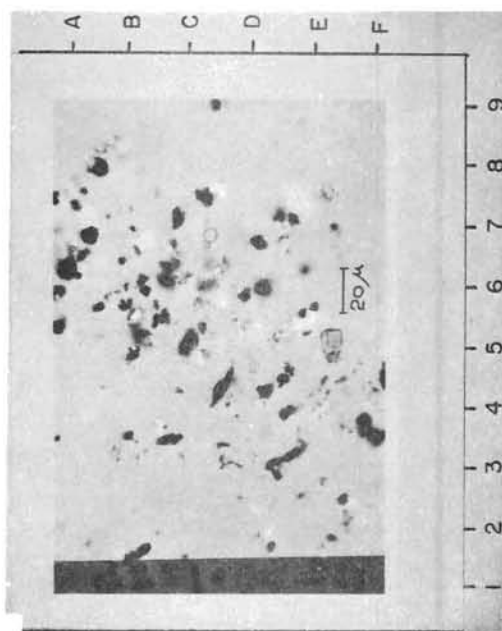


FIG. 16. Sample No. 11.  
Collected from 1230-1326.

Photomicrographs of samples collected on membrane filters during the day of 22 January 1966 at Site #3.

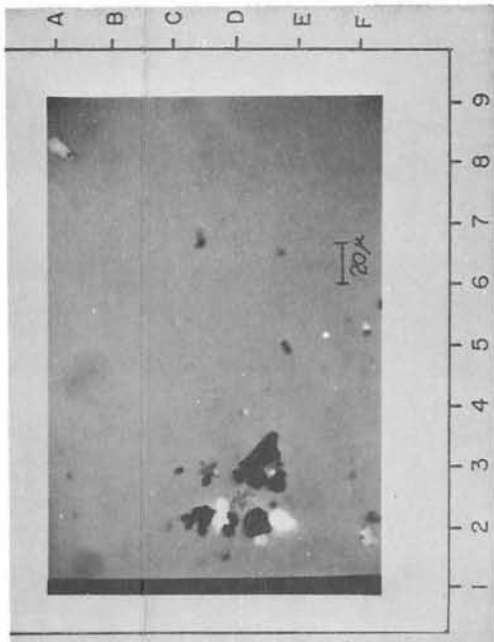


FIG. 17. Sample No. 12.  
Collected from 1245-1342.

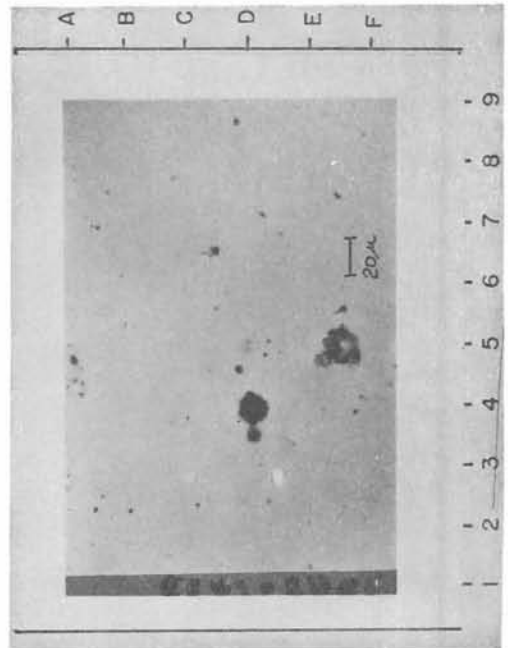


FIG. 18. Sample No. 13.  
Collected from 1342-1438.

JAN 5, 1966

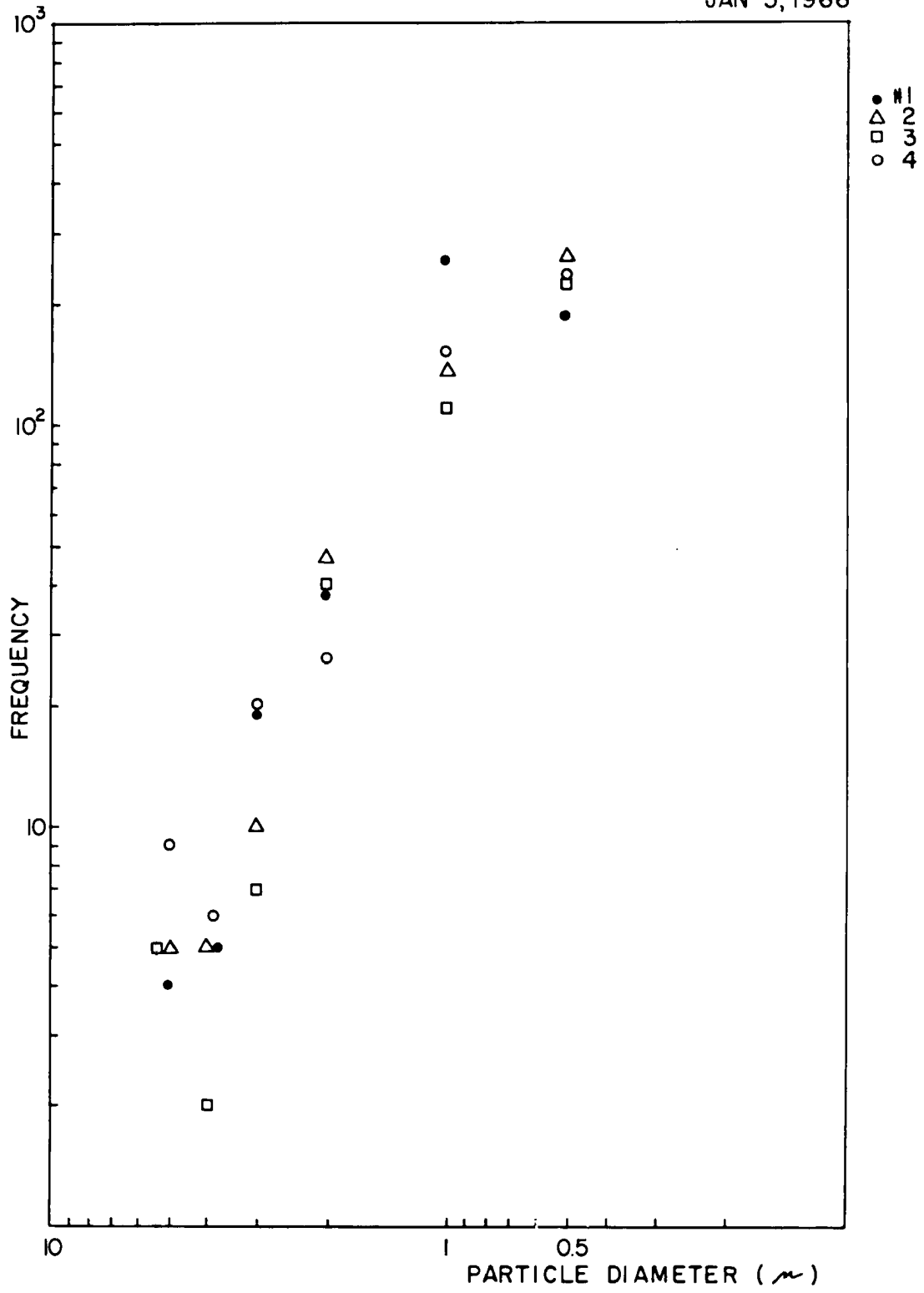


FIG. 19. Log-log plot of particle size distribution for samples collected on 5 January 1966.

JAN 6, 1966

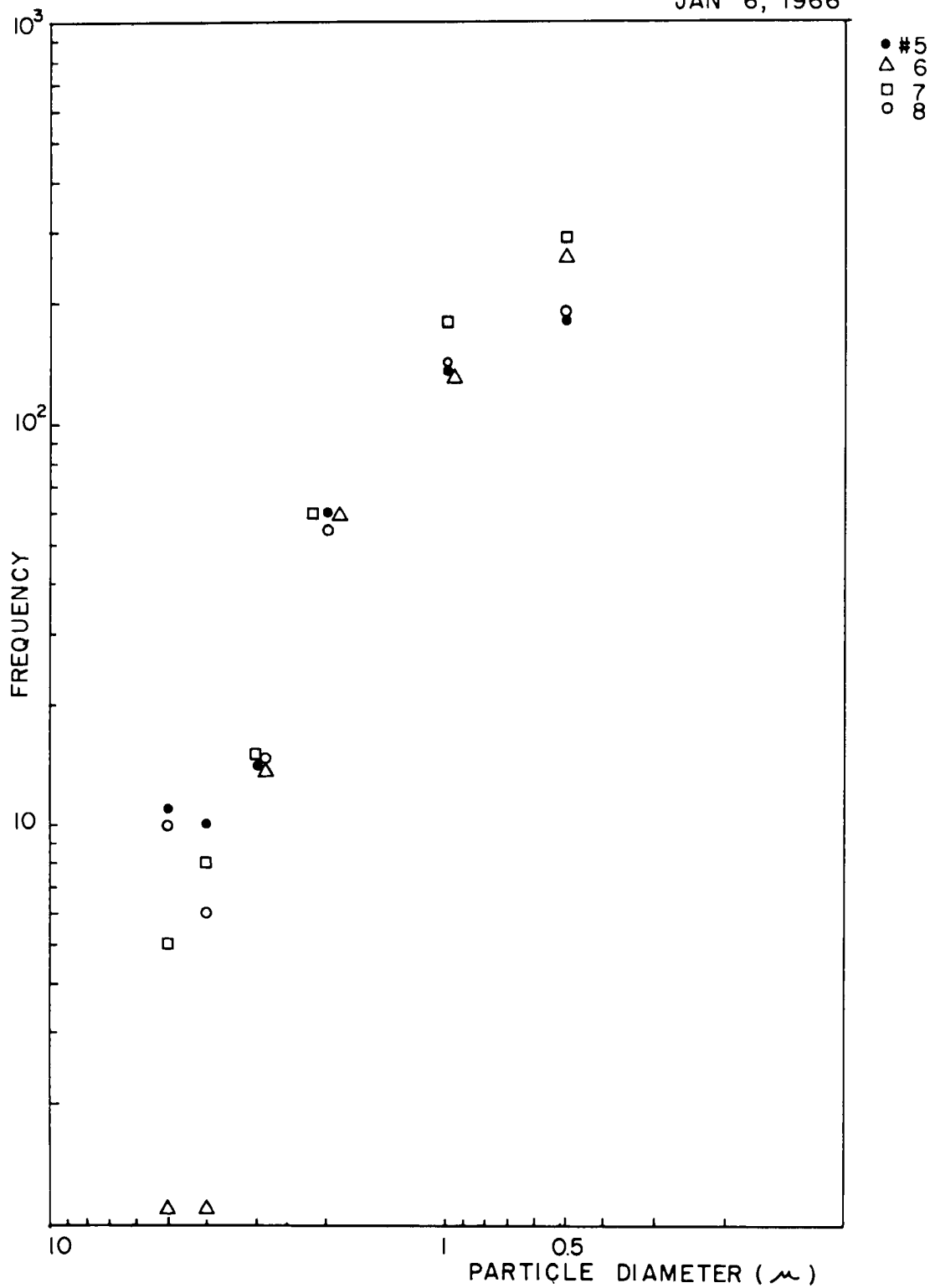


FIG. 20. Log-log plot of particle size distribution for samples collected on 6 January 1966.

JAN 18, 1966

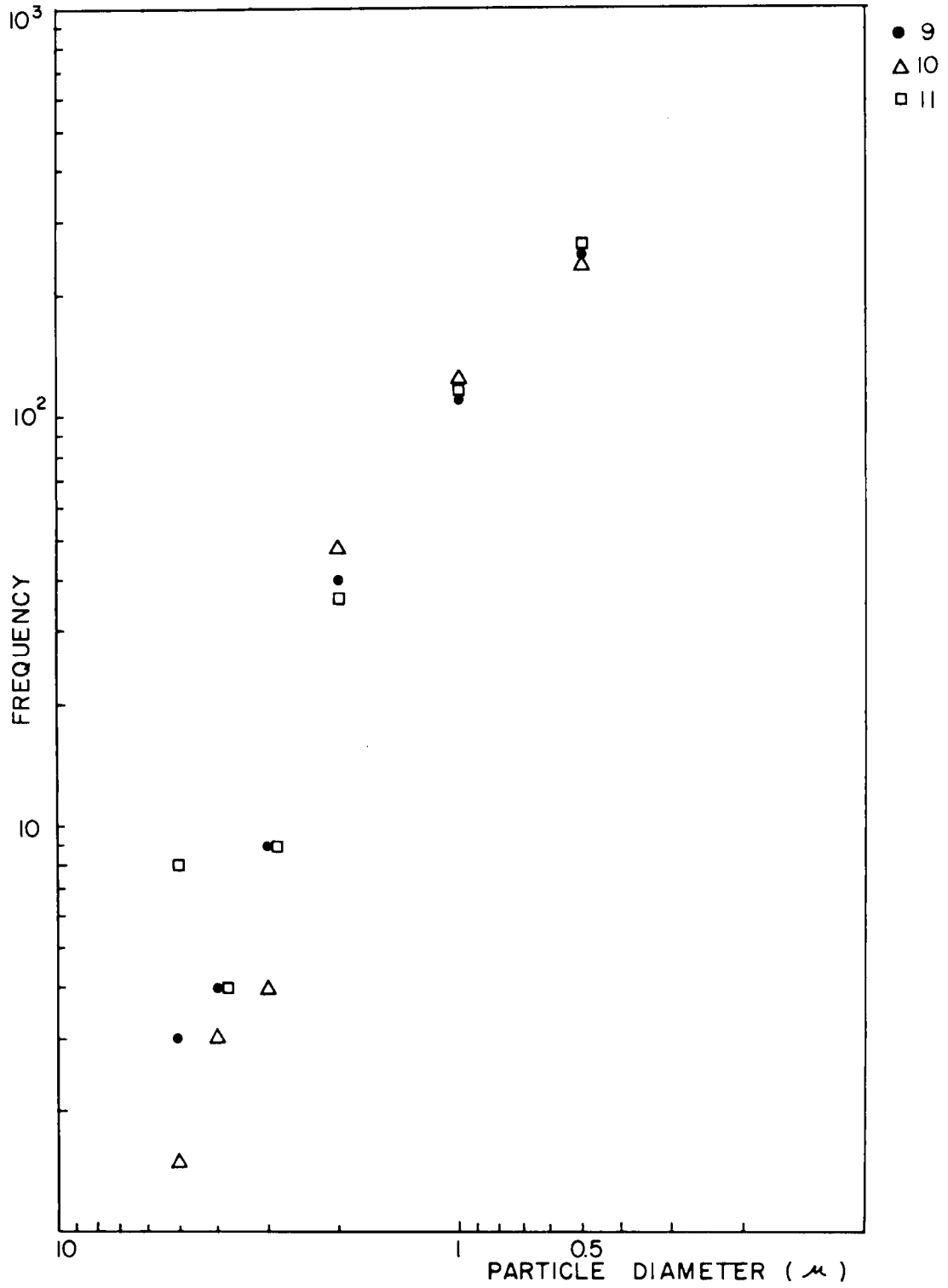


FIG. 21. Log-log plot of particle size distribution for samples collected on 18 January 1966.

JAN 22, 1966

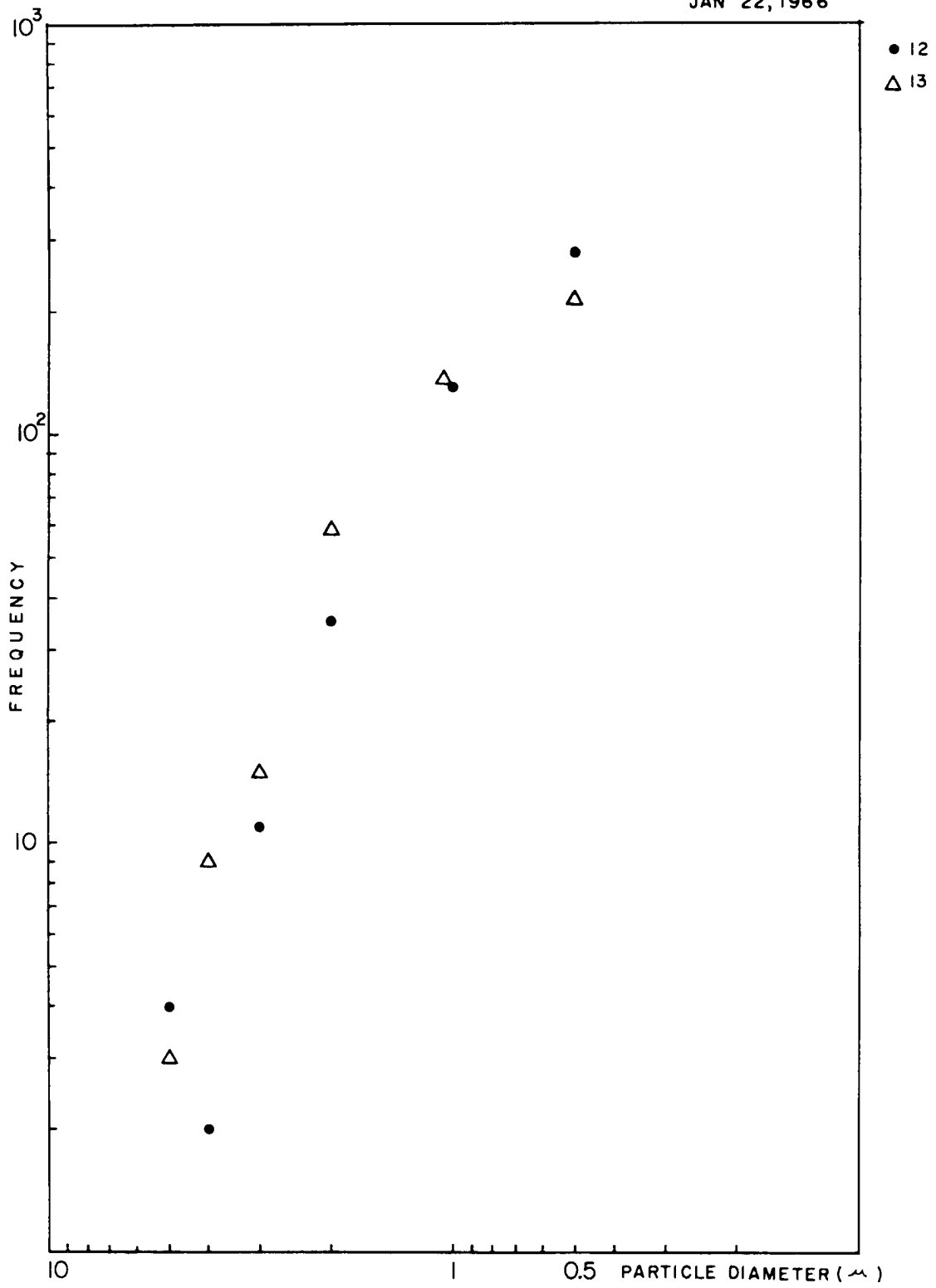


FIG. 22. Log-log plot of particle size distribution for samples collected on 22 January 1966.

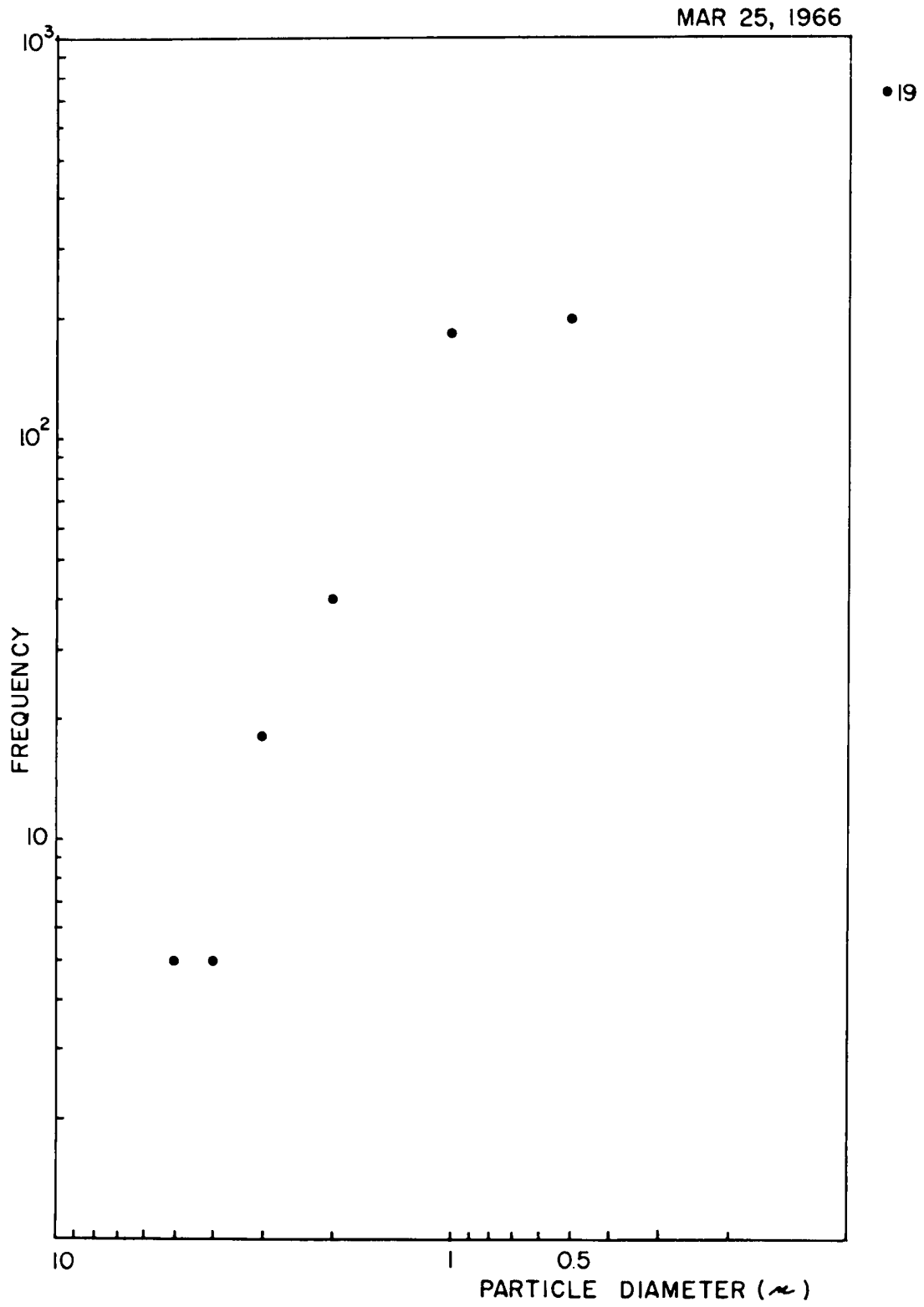


FIG. 23. Log-log plot of particle size distribution for samples collected on 25 March 1966.

JAN 6, 1966

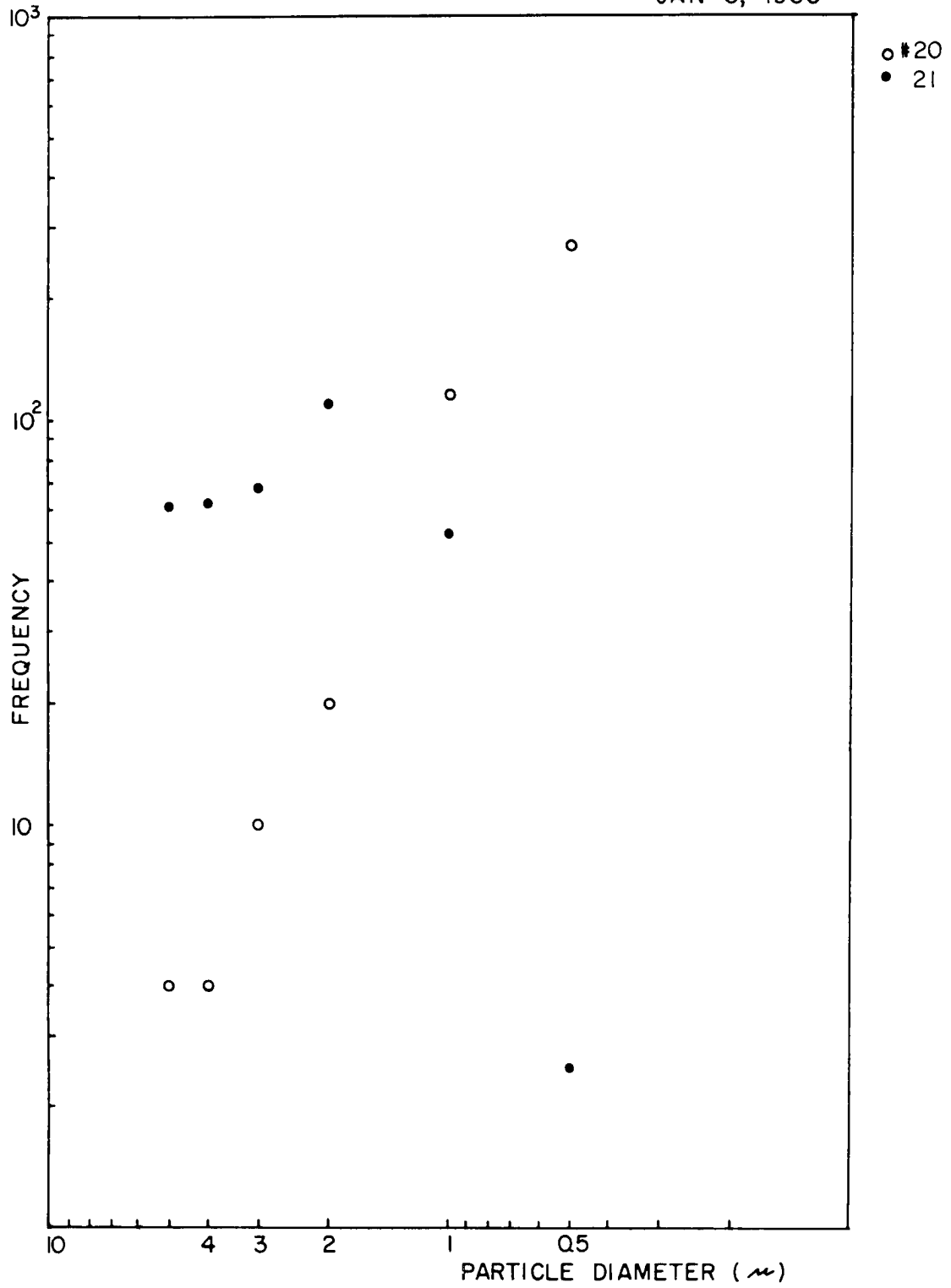


FIG. 24. Log-log plot of particle size distribution for samples collected on 6 January 1966 at Sites #1 and #2: ○, Site #1; ●, Site #2.

## REFERENCES

- Allen, R. M. , 1962: Practical Refractometry (2nd Ed.). R. P. Cargille Laboratories, Cedar Grove, New Jersey, 43 pp.
- Cadle, R. D. , 1965: Particle Size. Reinhold Publishing Corporation, New York, 390 pp.
- Chamot, E. M. , and C.W. Mason, 1958: Handbook of Chemical Microscopy (3rd Ed.). John Wiley and Sons, Vol. I, New York, 502 pp.
- Ferguson, J. S. , and E.G. Sheridan, 1966: Some applications of microscopy to air pollution. Presented at the 59th Annual Meeting of the Air Pollution Control Association, San Francisco, California, June 22, 43 pp.
- Green, H. L. , and W.R. Lane, 1964: Particulate Clouds: Dusts, Smokes, and Mists (2nd Ed.). D. Van Nostrand Co. , Inc. , Princeton, New Jersey, 471 pp.
- Jacobs, M. B. , 1960: The Chemical Analysis of Air Pollutants. Interscience Publishers, Inc. , New York, 430 pp.
- Larsen, E. S. , and H. Berman, 1964: The Microscopic Determination of the Non-Opaque Minerals (2nd Ed.). U. S. Government Printing Office, Washington, D. C. , 266 pp.
- May, K. R. , 1945: The cascade impactor: An instrument for sampling aerosols. Journal of Scientific Instruments, Vol. 22, pp. 187-195.
- Millipore Filter Corporation, 1966: Detection and Analysis of Particulate Contamination, ADM-30. Millipore Filter Corporation, Bedford, Massachusetts, 44 pp.
- McCrone, W. C. , 1965: Stereophotomicrography using the tilting stage. The Microscope and Crystal Front, Vol. 14, No. 11, pp. 429-439.
- McCrone Associates, 1966: Slide samples of atmospheric particulates. 493 East 31st Street, Chicago, Illinois.
- Riehl, H. , and L.W. Crow, 1962: A study of Denver air pollution. Atmospheric Science Technical Report No. 33, Colorado State University, 15 pp.

Salzenstein, M. A., 1960: How dust particles are identified. Air Engineering, Vol. 2, January, pp. 31-34.

Schueneman, J. J., 1957: The Denver area air pollution problem. U. S. Department of Health, Education and Welfare, Division of Sanitary Engineering Service, R. A. Taft Sanitary Engineering Center, Cincinnati, Ohio, 47 pp.

Authors: N. Djordjevic, W. Ehrman, and G. Swanson  
Project Leader: E. R. Reiter  
FURTHER STUDIES OF DENVER AIR POLLUTION

551.510.42  
Subject Headings:  
Air Pollution  
Air Trajectory Studies

Colorado State University  
Atmospheric Science Paper No. 105

Report under Contract 5 ROI AP 00216-03  
with the Department of Health, Education  
and Welfare

In the first part of this report meteorological conditions were investigated during which air pollution in the Denver metropolitan area was abnormally high during the winter seasons of 1964-1965 and 1965-1966. Advection patterns of pollution under the influence of diurnal wind changes were studied by means of detailed air trajectories. The "coefficient of haze" (COH) was used in determining the degree of air pollution. The second part of the report deals with automatic data reduction used in preparing meteorological data. The third part contains preliminary results of microscopic analyses of filter samples of pollutants. Size distributions of pollutants, as well as classification into types according to their probable origin, were considered.

Authors: N. Djordjevic, W. Ehrman, and G. Swanson  
Project Leader: E. R. Reiter  
FURTHER STUDIES OF DENVER AIR POLLUTION

551.510.42  
Subject Headings:  
Air Pollution  
Air Trajectory Studies

Colorado State University  
Atmospheric Science Paper No. 105

Report under Contract 5 ROI AP 00216-03  
with the Department of Health, Education  
and Welfare

In the first part of this report meteorological conditions were investigated during which air pollution in the Denver metropolitan area was abnormally high during the winter seasons of 1964-1965 and 1965-1966. Advection patterns of pollution under the influence of diurnal wind changes were studied by means of detailed air trajectories. The "coefficient of haze" (COH) was used in determining the degree of air pollution. The second part of the report deals with automatic data reduction used in preparing meteorological data. The third part contains preliminary results of microscopic analyses of filter samples of pollutants. Size distributions of pollutants, as well as classification into types according to their probable origin, were considered.

Authors: N. Djordjevic, W. Ehrman, and G. Swanson  
Project Leader: E. R. Reiter  
FURTHER STUDIES OF DENVER AIR POLLUTION

551.510.42  
Subject Headings:  
Air Pollution  
Air Trajectory Studies

Colorado State University  
Atmospheric Science Paper No. 105

Report under Contract 5 ROI AP 00216-03  
with the Department of Health, Education  
and Welfare

In the first part of this report meteorological conditions were investigated during which air pollution in the Denver metropolitan area was abnormally high during the winter seasons of 1964-1965 and 1965-1966. Advection patterns of pollution under the influence of diurnal wind changes were studied by means of detailed air trajectories. The "coefficient of haze" (COH) was used in determining the degree of air pollution. The second part of the report deals with automatic data reduction used in preparing meteorological data. The third part contains preliminary results of microscopic analyses of filter samples of pollutants. Size distributions of pollutants, as well as classification into types according to their probable origin, were considered.

Authors: N. Djordjevic, W. Ehrman, and G. Swanson  
Project Leader: E. R. Reiter  
FURTHER STUDIES OF DENVER AIR POLLUTION

551.510.42  
Subject Headings:  
Air Pollution  
Air Trajectory Studies

Colorado State University  
Atmospheric Science Paper No. 105

Report under Contract 5 ROI AP 00216-03  
with the Department of Health, Education  
and Welfare

In the first part of this report meteorological conditions were investigated during which air pollution in the Denver metropolitan area was abnormally high during the winter seasons of 1964-1965 and 1965-1966. Advection patterns of pollution under the influence of diurnal wind changes were studied by means of detailed air trajectories. The "coefficient of haze" (COH) was used in determining the degree of air pollution. The second part of the report deals with automatic data reduction used in preparing meteorological data. The third part contains preliminary results of microscopic analyses of filter samples of pollutants. Size distributions of pollutants, as well as classification into types according to their probable origin, were considered.

## ATMOSPHERIC SCIENCE PAPERS

(Beginning May 1966)

(Previous Numbers Refer to "Atmospheric Science  
Technical Papers")

101. On the Mechanics and Thermodynamics of a Low-Level Wave on the Easterlies by Russell Elsberry. Report prepared with support under Grant No. WBG-61, Environmental Science Services Administration. May 1966.
102. An Appraisal of TIROS III Radiation Data for Southeast Asia by U. Radok. Report prepared with support under Grant No. WBG-61, Environmental Science Services Administration. August 1966.
103. Atmospheric General Circulation and Transport of Radioactive Debris by J. D. Mahlman. Report prepared with support under Contract No. AT(11-1)-1340, U. S. Atomic Energy Commission. September 1966.
104. The Mutual Variation of Wind, Shear and Baroclinicity in the Cumulus Convective Atmosphere of the Hurricane by Wm. M. Gray. Report prepared with support under Grant No. GF-177, National Science Foundation. October 1966.

The "Atmospheric Science Papers" are intended to communicate without delay current research results to the scientific community. They usually contain more background information on data, methodology, and results than would normally be feasible to include in a professional journal. Shorter versions of these papers are usually published in standard scientific literature.

Editorial Office: Head, Department of Atmospheric Science  
Colorado State University  
Fort Collins, Colorado 80521